

Aus dem Institut für Funktionelle Anatomie  
der Medizinischen Fakultät Charité – Universitätsmedizin Berlin

DISSERTATION

Das Immunsuppressivum Cyclosporin A verursacht Stress im  
endoplasmatischen Retikulum und Apoptose in  
Nierenepithelzellen durch Hemmung der Cyclophilinaktivität

Immunosuppressant cyclosporine A induces  
endoplasmic reticulum stress and apoptosis in kidney epithelial  
cells due to suppression of cyclophilin activity

zur Erlangung des akademischen Grades  
Doctor rerum medicinalium (Dr. rer. medic.)

vorgelegt der Medizinischen Fakultät  
Charité – Universitätsmedizin Berlin

von

Duygu Elif Yilmaz  
aus Istanbul/Turkey

Datum der Promotion: 30 November 2023



## Table of contents

List of tables .....	iii
List of figures .....	iv
List of abbreviations.....	v
Abstract .....	1
1 Introduction.....	3
1.1 Calcineurin structure and function .....	3
1.2 Calcineurin inhibitors .....	3
1.3 Endoplasmic reticulum stress-induced unfolded protein response .....	5
1.4 Aim of this study .....	7
2 Methods.....	8
2.1 Cell culture and treatments .....	8
2.2 <i>Ex vivo</i> experiments .....	8
2.3 Cell viability .....	9
2.4 Immunofluorescence staining .....	9
2.5 Ultrastructural analysis.....	10
2.6 Western Blot (Immunoblotting).....	10
2.7 RNA Extraction and quantitative real-time PCR.....	12
2.8 siRNA Knockdown .....	12
2.9 Statistics.....	12
3. Results .....	14
4. Discussion.....	24
5. Conclusions.....	26
Reference list.....	27
Statutory Declaration .....	35
Declaration of individual contribution to the publication .....	36
Excerpt from Journal Summary List.....	37

---

Printing copy(s) of the publication(s) .....	42
Publication list.....	63
Acknowledgments .....	64

**List of tables**

Table 1: List of primary antibodies used for immunoblotting.....11

## List of figures

Figure 1: Calcineurin inhibition mechanism .....	4
Figure 2: Unfolded protein reponse (UPR) .....	6
Figure 3: Effects of cyclosporine A (CsA) and tacrolimus (Tac) on cell viability and morphology in HEK 293 cells.....	14
Figure 4: Effects of cyclosporine A (CsA) or tacrolimus (Tac) on unfolded protein response (UPR) markers in HEK 293 cells detected by real time PCR (RT PCR) analysis .....	15
Figure 5: Effects of cyclosporine A (CsA) or tacrolimus (Tac) on unfolded protein response (UPR) markers in HEK 293 cells detected by immunoblotting.....	16
Figure 6: Effects of cyclosporine A (CsA) or tacrolimus (Tac) on apoptosis markers in HEK 293 cells detected by immunoblotting .....	17
Figure 7: Effects of cyclosporine A (CsA) or tacrolimus (Tac) on apoptotic markers in HEK 293 cells detected by immunofluorescence staining.....	18
Figure 8: Effects of cyclosporine A (CsA) or tacrolimus (Tac) on unfolded protein response (UPR) markers in HRPTEpC cells by real time PCR (RT PCR) and im-munoblotting ...	19
Figure 9: Isolation of rat proximal tubules and effects of cyclosporine A (CsA) or tacrolimus (Tac) on unfolded protein response (UPR) markers detected by real time PCR (RT PCR).....	20
Figure 10: Knockdown of cyclophilins and its effects on CHOP and cCas-3 expression in HEK 293 cells detected by immunoblotting. ....	21
Figure 11: Effects of concomitant treatment of chemical chaperones, TUDCA or 4-PBA, on CHOP expression in cyclosporine A (CsA) treated HEK 293 cells detected by immunoblotting .....	22
Figure 12: Knockout of two unfolded protein response sensors, PERK or ATF6, and its effects of CHOP mRNA expression in HEK 293 cells detected by real time PCR (RT PCR) .....	23

## List of abbreviations

$\mu$ M	micromolar
4-PBA	4-phenylbutyric acid
ANOVA	analysis of variance
ATF4	activating transcription factor 4
ATF6	activating transcription factor 6
Bax	Bcl-2-associated X protein
BCL-2	B-cell lymphoma-2
BiP	binding immunoglobulin protein
<i>c.</i>	<i>circa</i>
cCas-3	cleaved caspase-3
CHOP	C/EBP homologous protein
CNI	calcineurin inhibitor
CRISPR/Cas9	Clustered regularly interspaced short palindromic repeats/ CRISPR-associated protein 9
CsA	cyclosporine A
CYPA	cyclophilin A
CYPB	cyclophilin B
DAPI	4',6-diamidino-2-phenylindole
FKBP12	FK506-binding protein
g	gravitational force
GAPDH	glyceraldehyde-3-phosphate dehydrogenase
h	hour
HEK 293	human embryonic kidney 293
HRP	horseradish peroxidase
HRPTEpC	human renal proximal tubular epithelial cells
IRE1 $\alpha$	inositol requiring enzyme-1
Kd	knockdown
KO	knockout
M	molar
MTT	3-(4,5-dimethylthiazol-2-yl)-2,5-diphenyltetrazolium bromide
nm	nanometer
NS	not significant

---

PBS	phosphate-buffered saline
PERK	protein kinase RNA-like ER kinase
PFA	paraformaldehyde
p-IRE1 $\alpha$	phosphorylated inositol requiring enzyme-1
PT	proximal tubule
RNA	ribonucleic acid
RQ	relative quantity
RT-PCR	real-time polymerase chain reaction
siRNA	small interfering RNA
sXBP1	spliced X-box binding protein 1
Tac	tacrolimus
TBS	tris-buffered saline
Tg	thapsigargin
TUDCA	tauroursodeoxycholic acid
UPR	unfolded protein response
XBP1	X-box binding protein 1

## Abstract

Calcineurin inhibitors (CNI) such as cyclosporine A (CsA) and tacrolimus (Tac), are widely-used as immunosuppressants after solid organ transplantations to prevent allograft rejection. However, their therapeutic benefits are limited by nephrotoxicity. In particular, CsA is associated with greater nephrotoxicity than Tac. CNI inhibit calcineurin indirectly by building complexes with different immunophilins: CsA binds to cyclophilins and Tac interacts with the FK506-binding protein (FKBP). These complexes then bind to and inhibit calcineurin. We hypothesized that the stronger nephrotoxicity of CsA may be associated with suppression of cyclophilins, whose chaperone function is crucial in proteostasis. Imbalanced proteostasis may lead to endoplasmic reticulum (ER) stress and maladaptive unfolded protein response (UPR) in kidney epithelia. To this end, the effects of CsA and Tac treatment (10  $\mu$ M, for 6 hours each) on UPR and apoptosis markers were evaluated in human embryonic kidney 293 (HEK 293) cells, primary human renal proximal tubular epithelial cells (HRPTEpC) and freshly isolated rat proximal tubules (PT). CsA treatment in cultured cells and isolated PTs induced significant increases to the levels of UPR and proapoptotic markers, whereas Tac treatment resulted in either mild or no effect. Knockdown of cyclophilin A (CYPA) or cyclophilin B (CYPB) via small interfering RNA (siRNA) stimulated proapoptotic UPR and apoptosis, similar to CsA treatment. Concomitant application of the chemical chaperones tauroursodeoxycholic acid (TUDCA) or 4-phenylbutyric acid (4-PBA) alleviated CsA-induced ER stress and UPR. Similarly, inactivation of critical UPR pathways by CRISPR/Cas9 mediated deletion of protein kinase RNA-like ER kinase (PERK) or activating transcription factor 6 (ATF6) in HEK 293 cells also blunted CsA-induced UPR.

In summary, CsA induces stronger expression of UPR and proapoptotic markers than Tac, which suggests that higher nephrotoxicity associated with CsA treatment may be, at least in part, derived from the suppression of cyclophilins rather than calcineurin inhibition. Indeed, concomitant treatment with chemical chaperones alleviated the CsA-induced UPR, and genetic suppression of the UPR also blunted the detrimental effects of CsA. Thus, modulation of the UPR may be an effective adjuvant approach to mitigate the nephrotoxicity associated with CsA.

## Zusammenfassung

Der Einsatz der Calcineurin-Inhibitoren (CNI), Cyclosporin A (CsA) oder Tacrolimus (Tac), gehört zu den Standards bei immunsuppressiver Therapie nach Organtransplantation. Die nephrotoxischen Nebenwirkungen von CNI stellen jedoch ein Problem für deren klinische Verwendung dar. Im Vergleich mit Tac hat CsA eine stärker toxische Wirkung. Calcineurin wird durch CNI indirekt über dessen Komplexbildung mit verschiedenen Immunophilinen gehemmt. Dabei bindet CsA an Cyclophiline und Tac an FK506-bindendes Protein (FKBP). Die dadurch entstehenden Komplexe binden dann an Calcineurin und hemmen es. Wir stellten die Hypothese auf, dass eine angenommene höhere Nephrotoxizität von CsA mit der Unterdrückung von Cyclophilinen in Verbindung steht, weil deren Chaperonfunktion für die Erhaltung der zellulären Proteostase entscheidend ist. Eine unausgeglichene Proteostase kann zu Stress des endoplasmatischen Retikulums (ER) und zu maladaptiver Unfolded protein response (UPR) in Nierenepithelien führen. Zur Überprüfung der Hypothese wurden Effekte von CsA und Tac (10  $\mu$ M, 6 Stunden, jeweils) auf UPR- und Apoptosemarker in humanen embryonalen Nierenzellen 293 (HEK 293), primären humanen proximalen tubulären Nierenepithelzellen (HRPTEpC) und frisch isolierten proximalen Tubuli (PT) von Ratten vergleichend untersucht. Die Behandlung mit CsA induzierte eine signifikant stärkere Expression von UPR- und Apoptosemarkern in kultivierten Zellen und isolierten PTs als mit Tac. Die Synthesehemmung (Knock-down) von Cyclophilin A (CYPA) oder Cyclophilin B (CYPB) mittels kleiner interferierender RNA (siRNA) stimulierte proapoptotische UPR und Apoptose in ähnlicher Weise wie die CsA-Behandlung. CsA-induzierte UPR und Apoptose wurden durch die gleichzeitige Anwendung der chemischen Chaperone, Tauroursodeoxycholsäure (TUDCA) oder 4-Phenylbuttersäure (4-PBA), gelindert. In ähnlicher Weise wurden die zelltoxischen Effekte von CsA durch Hemmung der kritischen UPR-Komponenten, Proteinkinase-RNA-ähnliche ER-Kinase (PERK) und Transkriptionsfaktor 6 (ATF6), in HEK 293 Zellen über CRISPR/Cas9-vermittelte Gen-Editon jeweils deutlich gemildert.

Zusammenfassend verursacht CsA ein höheres Ausmass an epithelialer UPR und Apoptose als Tac. Die mit CsA-Behandlung einhergehende höhere Nephrotoxizität kommt offenbar anteilig durch Unterdrückung der zugehörigen Cyclophiline zustande. Die Dämpfung der UPR durch chemische Chaperone oder Hemmung ihrer genetischen Komponenten sollte dazu beitragen können, die zelltoxischen Effekte von CsA zu vermindern.

# 1 Introduction

## 1.1 Calcineurin structure and function

Calcineurin is a calcium ( $\text{Ca}^{2+}$ ) and calmodulin dependent serine/threonine phosphatase (Rusnak & Mertz, 2000). Its heterodimeric structure consists of a catalytic subunit, calcineurin A, and a regulatory subunit, calcineurin B (Bandyopadhyay et al., 2004). Calcineurin A exists in three isoforms, namely  $\alpha$ ,  $\beta$  and  $\gamma$ . While calcineurin A $\alpha$  and  $\beta$  are broadly distributed, calcineurin A $\gamma$  is expressed primarily in the brain and testes (Williams & Gooch, 2012).

Increases in intracellular  $\text{Ca}^{2+}$  levels induce the formation of  $\text{Ca}^{2+}$ -calmodulin complexes that then bind to and activate calcineurin. Activated calcineurin dephosphorylates transcription factors of the nuclear factor of activated T cells (NFAT) family. Consequently, dephosphorylated and activated NFATs translocate into the nucleus and induce a variety of transcriptional programs including T cell activation (Creamer, 2020; Park et al., 2019).

## 1.2 Calcineurin inhibitors

Calcineurin inhibitors (CNI), cyclosporine A (CsA) and tacrolimus (Tac) are the most commonly-used drugs for immunosuppression to prevent allograft rejection after solid organ transplantation (Farouk & Rein, 2020; Kitamura, 2010). Since their introduction in 1980s, the use of CNIs after transplantation has dramatically improved graft and patient survival (Ume et al., 2021). However, nephrotoxic effects of CNI substantially limit their therapeutic benefits at long term (Farouk & Rein, 2020). In particular, CsA administration is associated with higher nephrotoxicity than Tac, alongside less favourable side-effects. For instance, comparative studies have shown long term Tac use is associated with a more favourable cardiovascular risk profile and better renal function, as determined by glomerular filtration rate or serum creatinine levels, than CsA (Jurewicz, 2003; Lucey et al., 2005). It is also reported that, CsA has more impact on dyslipidemia; CsA but not Tac significantly increases total cholesterol and low density lipoprotein cholesterol levels (Deleuze et al., 2006). It should be noted, however, that Tac use is strongly associated with post-transplant diabetes (Haddad et al., 2006; Martins et al., 2004). Interestingly, CsA and Tac have opposing effects on hair growth: CsA may trigger hypertrichosis whereas Tac use may lead to *alopecia areata* (Gafer-Gvili et al., 2003; Tricot et al., 2005).

Differences in toxicity profiles of the two CNIs may be related to their mechanism of calcineurin inhibition. CsA and Tac do not inhibit calcineurin directly. Instead, they build complexes with different immunophilins, so called for their action as receptors for immunosuppressive drugs (Calderón-Sánchez et al., 2011; Steiner & Haughey, 2010). While CsA builds complexes with cyclophilins (CYP), Tac (FK-506) interacts with FK-506 binding proteins (FKBP). Thus, immunosuppressant-immunophilin complexes bind to and inhibit calcineurin function (Figure 1; Dutz et al., 1993).

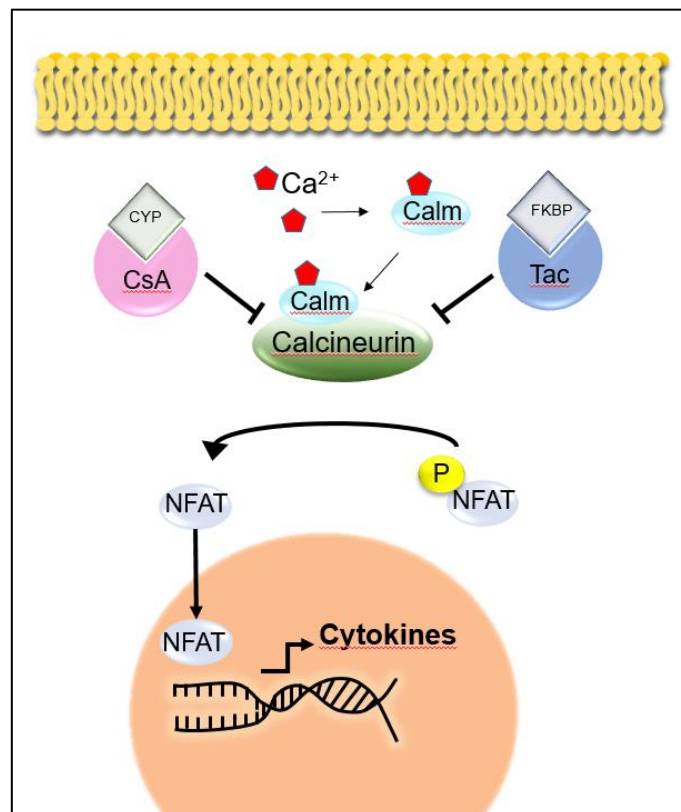


**Figure 1: Calcineurin inhibition mechanism:** Upon increase in intracellular calcium levels, calcium ions (Ca<sup>+</sup>) bind to calmodulin (Calm) that then in turn activates calcineurin. Consequently, calcineurin dephosphorylates and activates nuclear factor of activated T cells (NFAT) transcription factors. Dephosphorylated NFATs translocate to the nucleus and regulate the expression of genes responsible for T cell proliferation, differentiation and activation, such as interleukin-2. Calcineurin inhibitors cyclosporine A (CsA) and tacrolimus (Tac) build complexes with cyclophilins (CYP) and FK-binding proteins (FKBP), respectively, which then inhibit calcineurin activity and the T cell immune response. Source: Own elaboration.

Immunophilins are ubiquitous peptidylprolyl cis-trans isomerases (PPI) that are expressed in a variety of human organs such as brain, liver, heart and kidney (Calderón-Sánchez et al., 2011). Immunophilins, particularly cyclophilins, act as chaperons assisting

protein folding, for this reason deficiency of cyclophilins can give rise to endoplasmic reticulum (ER) stress induced unfolded protein response (UPR; Cho et al., 2014; Yilmaz et al., 2022).

### 1.3 Endoplasmic reticulum stress-induced unfolded protein response

The endoplasmic reticulum (ER) is one of the largest organelles in eukaryotic cells. It plays key roles in protein synthesis, folding and structural maturation (Oakes & Papa, 2015). ER homeostasis may be challenged by pathophysiological alterations that result in accumulation of unfolded or misfolded proteins within the ER lumen, causing ER stress (Hetz et al., 2020). ER stress triggers a compensatory intracellular signal transduction pathway known as the unfolded protein response (UPR), which acts to reduce protein synthesis, improve protein folding, and induce ER-associated degradation (ERAD) of misfolded proteins. However, should overwhelming or prolonged ER stress occur, the UPR can instead activate apoptotic pathways (Hetz et al., 2020; So, 2018; Walter & Ron, 2011).

The UPR comprises three major signaling pathways initiated by different ER resident transmembrane proteins: activating transcription factor 6 (ATF6), inositol-requiring protein 1  $\alpha$  (IRE1 $\alpha$ ) and protein kinase RNA-like ER kinase (PERK; Figure 2). Luminal domains within these proteins sense the accumulation of unfolded proteins via dissociation of the binding immunoglobulin protein (BiP, GRP78), initiating the UPR signaling cascade (Hetz, 2012; Hetz et al., 2020; Lemmer et al., 2021). After activation of the UPR, ATF6 is transported from the ER to the Golgi apparatus to be cleaved by site-1 protease (S1P) and site-2 protease (S2P), releasing the 50 kDa cytosolic domain of ATF6 (ATF6 p50; Hetz et al., 2020; Pachikov et al., 2021). As a soluble and active transcription factor, ATF6 p50 translocates to the nucleus to enhance the transcription of UPR-related genes (Nadanaka et al., 2007). In association with UPR activation, IRE1 $\alpha$  undergoes autotransphosphorylation and causes the splicing of unspliced X-box-binding protein-1 (uXBP1). Spliced XBP1 (sXBP1) is an active transcription factor that regulates the expression of genes involved in protein folding and ERAD (Pavlović & Heindryckx, 2021; Walczak et al., 2019). PERK, as the third branch of UPR, undergoes homodimerization and phosphorylation upon UPR induction, similar to IRE1 $\alpha$ . Activation of PERK leads to phosphorylation of eukaryotic translation initiation factor 2A (eIF2a), which causes a general down-

regulation of translation to decrease ER workload. However, under prolonged stress conditions, preferential translation of activating transcription factor 4 (ATF4) may lead to expression of proapoptotic factors such as C/EBP homologous protein (CHOP; Bergmann & Molinari, 2018; Metcalf et al., 2020; Sano & Reed, 2013).

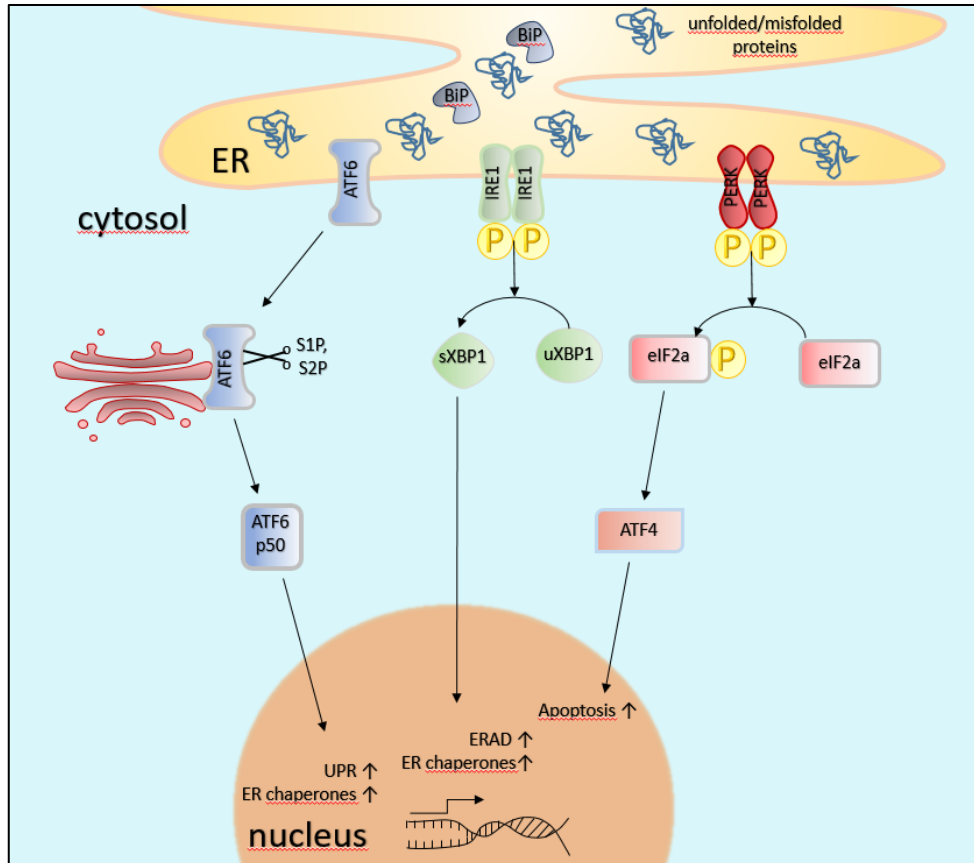


**Figure 2: Unfolded protein response (UPR):** Three UPR sensor proteins – activating transcription factor 6 (ATF6), inositol-requiring protein 1  $\alpha$  (IRE1 $\alpha$ ) and protein kinase RNA-like ER kinase (PERK) – sense the accumulation of unfolded or misfolded proteins and initiate UPR signaling. BiP, binding immunoglobulin protein; ER, endoplasmic reticulum; S1P, site-1 protease; S2P, site-2 protease; uXBP1, unspliced X-box-binding protein-1; sXBP1, spliced X-box-binding protein-1; ERAD, ER-associated degradation; eIF2a, eukaryotic translation initiation factor 2A; ATF4, activating transcription factor 4. Source: Own elaboration.

In summary, the ER is a crucial organelle that plays essential roles in protein folding and quality control. Accumulation of unfolded or misfolded proteins can cause stress in the ER that leads to the UPR (Chadwick & Lajoie, 2019; Lücke & Weiwad, 2011). Pharmacological inhibition of calcineurin via CsA or Tac is enacted through the inhibition of CYP or FKBP immunophilins, respectively. Cyclophilins function as chaperones and play a key role in the proteostasis. Thus, CsA-induced suppression of cyclophilin chaperone

activity may aggravate cell toxicity via impaired cellular proteostasis and ER stress (Yilmaz et al., 2022).

#### **1.4 Aim of this study**

The present study addresses the hypothesis that differential suppression of distinct immunophilins – cyclophilins or FKBP12 – may contribute to differences in the toxicity profiles of the clinically relevant calcineurin inhibitors, CsA and Tac. To this end, the effects of CsA and Tac on cellular proteostasis were compared in cultured kidney cells and freshly isolated rat proximal tubules, where a focus was placed on ER stress and UPR. The results demonstrated that CsA caused more pronounced cellular toxicity due to the suppression of cyclophilin chaperone function. This conclusion was corroborated by siRNA-mediated knockdown of cyclophilins, which recapitulated the effects of CsA with respect to the ER stress and proapoptotic UPR. In contrast, Tac induced only mild or no activation of the proapoptotic UPR pathways. Pharmacologic or genetic interventions that suppressed the proapoptotic UPR alleviated the CsA toxicity, making them promising therapeutic avenues (Yilmaz et al., 2022).

## 2 Methods

### 2.1 Cell culture and treatments

Human embryonic kidney 293 (HEK 293) cells were purchased from German Collection of Microorganisms and Cell Cultures (DSMZ, Catalog no: ACC 305) and cultured in Minimum Essential Medium Eagle (Sigma) supplemented with 5% FBS (Thermo Fisher Scientific) and 1% L-glutamine (Corning). Human renal proximal tubular epithelial cells (HRPTEpC, Catalog no: 93005A, Sigma-Aldrich) were cultured in RenaEpi Growth Medium (Sigma-Aldrich) supplemented with 10% FBS (Thermo Fisher Scientific). Cells were incubated at 37 °C, in a humidified atmosphere with 5% CO<sub>2</sub>. PERK knockout (PERK KO) and ATF6 knockout (ATF6 KO) HEK293 cells were generated using CRISPR/Cas9 mediated gene editing as previously described (Ran et al., 2013). Briefly, oligonucleotides (PERK: CACCGGGAAAATCTCTGACTACATA, AAACATATGTAGTCAGAGATTTTCCC; ATF6: CACCGTGAAATGGGGGAGCCGGCTG, AAAC-CAGCCGGCTCCCCATTTCAC) were cloned into pSpCas9(BB)-2A-GFP (catalog no: PX458, Addgene) vector. After transfection, cells were sorted into 96-well plates using a FACS Aria III (Becton Dickinson). Single-cell clones were expanded, and CRISPR/Cas9-mediated mutations verified by Sanger sequencing of the respective genomic loci. Cells were treated with the calcineurin inhibitors cyclosporine A (CsA, Sigma-Aldrich) or tacrolimus (Tac, Sigma-Aldrich) dissolved in DMSO (Roth); 0.1 μM thapsigargin (Tg, Sigma-Aldrich) treatment served as the positive control. To detect the effect of chemical chaperones, either 5 μM sodium 4-phenylbutyrate (4-PBA, Abcam) or 300 μM tauroursodeoxycholic acid (TUDCA, Calbiochem) was combined with CsA (Yilmaz et al., 2022).

### 2.2 *Ex vivo* experiments

Animal experiments were conducted in line with the German Animal Welfare Regulation Authorities for the protection of animals used for scientific purposes (T0351/11). Male Wistar rats (7-9 weeks old, N=4) were sacrificed via coadministration of ketamine (0.4 mg/g body weight) and xylazine (0.04 mg/g body weight) intraperitoneally. The kidneys of each animal were removed immediately, and dissected into thin cortical slices that were then digested by collagenase II (2 mg/mL) in a defined incubation solution (140 mM NaCl, 0.4 mM KH<sub>2</sub>PO<sub>4</sub>, 1.6 mM K<sub>2</sub>HPO<sub>4</sub>, 1 mM MgSO<sub>4</sub>, 10 mM sodium acetate, 1 mM α-ketoglutarate, 1.3 mM calcium gluconate, 5 mM glycine, 48 mg/L trypsin inhibitor, 25 mg/L

DNase I, pH 7.4) at 37°C under continuous agitation (850 rpm; Pohl et al., 2010; Yilmaz et al., 2022). Proximal tubules (PTs) were collected using a dissection microscope (+4°C). Subsequently, each sample was divided into four sets of c. 20-40 PTs, which were then transferred into vials containing 10 µM CsA, 10 µM Tac, 0.1 µM Tg, or 0.04% DMSO (v/v) in 150 µl of Dulbecco's modified Eagle's medium solution (low glucose; PAN Biotech) supplemented with 1% L-glutamine (200 mM), and 1% penicillin/streptomycin (PAA Laboratories). After 6 h incubation (37 °C, 8% CO<sub>2</sub>, open lid), PTs were harvested for RNA and protein isolation (Yilmaz et al., 2022).

### 2.3 Cell viability

Cell viability was assessed via 3-(4,5-dimethylthiazol-2-yl)-2,5-diphenyltetrazolium bromide (MTT, Biofrox GmbH) assay. Cells were inoculated at a concentration of  $1 \times 10^5$  cells/mL to a 96-well plate and incubated overnight at 37 °C with 5% CO<sub>2</sub>. Afterwards, the culture medium was replaced with CsA or Tac supplemented media at concentrations of 0, 5, 10, 20, 40 and 80 µM for 6 hours. Meanwhile, 5 mg/mL MTT was dissolved in phosphate-buffered saline (PBS) and sterile filtered (0.22 µm, Whatman). After 6 h, 5 µL MTT solution was added to each well and incubated at 37 °C for a further 90 minutes. Subsequently, the medium was discarded and intracellularly precipitated formazan crystals dissolved in DMSO (100 µL per well) followed by incubating at 37 °C for 15 minutes under gentle agitation. The light absorbance of the resulting solutions were then measured at 560 nm with a microplate reader (Biochrom ASYS Expert 96). Untreated cells were considered to be 100% viable and used to calculate relative viability of the treated cells (Yilmaz et al., 2022).

### 2.4 Immunofluorescence staining

Calcineurin inhibitor (CNI) treated cells were fixed in 4% paraformaldehyde for 10 minutes and permeabilized for 30 minutes in tris-buffered saline (TBS) supplemented with 0.5% Triton X-100 (v/v; Merck). Subsequently, the samples were blocked with 5% BSA in TBS for 30 minutes at room temperature. Primary antibodies (1:500 CHOP, Cell Signaling Technology, 2895; 1:500 Cleaved Caspase-3, Cell Signaling Technology, 9661) were incubated overnight at 4°C in a humidified chamber. After washing, the samples were incubated for a further hour with a TBS solution containing DAPI (0.1 µg/mL, 4',6-diamidino-2-phenylindole, Sigma-Aldrich), phalloidin (1:100, Alexa Fluor 488 phalloidin, Invitrogen)

and a Cy3-labelled secondary antibody (1:300, Dianova) at room temperature in a dark, humidified chamber. Coverslips were mounted (ProLong Glass Antifade Mountant, Invitrogen) on glass slides and fluorescent signals imaged using a confocal microscope (LSM 5 Exciter, Zeiss). Signal intensities were quantified using ImageJ software (version 1.48v, NIH; Yilmaz et al., 2022).

## 2.5 Ultrastructural analysis

CNI treated cells were fixed in 2.5% glutaraldehyde in cacodylate buffer. Later, cells were scraped and postfixed in 1% osmium tetroxide, 0.8% potassium hexacyanoferrate(II) in 0.1 M sodium cacodylate buffer for 90 minutes. Afterwards, cell suspension were firstly embedded to 2% agarose (Sigma) and incubated overnight at +4°C. The samples were then dehydrated in increasing concentrations of ethanol. Subsequently, the samples were immersed in propylene oxide for 1 h and in propylene oxide-EPON (SERVA) mixtures (2:1, 1:1 and 1:2 for 1 h each). Finally, the samples were infiltrated in pure EPON that was then polymerized through overnight incubation. Ultra-thin 70 nm thick sections were cut (Ultracut S, Leica) and imaged with an electron microscope (EM906, Zeiss; Yilmaz et al., 2022).

## 2.6 Western Blot (Immunoblotting)

After treatment, cells were harvested and homogenized in homogenization buffer (250 mM sucrose, 10 mM triethanolamin, protease inhibitor (cOmplete, Roche) and phosphatase inhibitor (PhosSTOP EASYpack, Roche)). Next, cells were sonicated for 1 second, 5 times. Cell debris were pelleted by 10 min centrifugation at 1000 × g (4 °C). Supernatant were collected and protein concentrations measured using a copper-based total protein quantification kit (Micro BCA Protein Assay Kit, Thermo Scientific). Equal amounts of protein were then placed into a sodium dodecyl sulfate polyacrylamide gel, separated by electrophoresis (SDS-PAGE), and transferred to a nitrocellulose membrane (Macherey-Nagel). Membranes were blocked with 5% BSA (SERVA) and subsequently incubated with a primary antibody of interest overnight (4 °C; Table 1).

Table 1: List of primary antibodies used for immunoblotting

Primary antibody	Company	Host species	Primary antibody dilution	Catalogue number
ATF-6 (D4Z8V)	Cell Signaling Technology	rabbit	1:500, 5% BSA in PBS	65880
Bax	Abcam	rabbit	1:1000, 5% BSA in TBST	ab32503
BCL-2	Santa Cruz Biotechnology	mouse	1:1000, 5% BSA in TBST	sc-7382
Calcineurin A $\beta$	Pineda Antikörper-Service	rabbit	1:1000, 5% BSA in PBS	-
Calcineurin A $\alpha$	Pineda Antikörper-Service	rabbit	1:1000, 5% BSA in PBS	-
CHOP (L63F7)	Cell Signaling Technology	mouse	1:500, 5% BSA in TBST	2895
Cleaved Caspase-3 (Asp175)	Cell Signaling Technology	rabbit	1:500, 5% BSA in TBS	9661
Cyclophilin A	Abcam	rabbit	1:1000, 5% BSA in PBS	ab41684
Cyclophilin B	Abcam	rabbit	1:1000, 5% BSA in PBS	ab41684
FKBP12	Abcam	rabbit	1:1000, 5% BSA in PBS	ab2918
GAPDH	Abcam	rabbit	1:2000, 5% BSA in TBS	ab181602
IRE1 $\alpha$	Cell Signaling Technology	rabbit	1:1000, 5% BSA in TBST	3294
NFAT4/NF-ATc3 (phospho S165)	Abcam	rabbit	1:500, 5% BSA in TBST	ab59204
PERK (C33E10)	Cell Signaling Technology	rabbit	1:1000, 5% BSA in PBS	3192
Phospho-IRE1 $\alpha$ (phospho S724)	Abcam	rabbit	1:1000, 5% BSA in TBST	ab48187
$\beta$ Actin	Sigma	mouse	1:2000, 5% BSA in TBST	A2228
sXBP1	Abcam	rabbit	1:1000, 5% BSA in PBS	ab220783

Table 1 was modified from Duygu Elif Yilmaz et al. 2022, J Biol Chem (Yilmaz et al., 2022).

After washing, membranes were incubated with horseradish peroxidase (HRP)-conjugated secondary antibodies (1:2000 dilution, Dako) for an hour under gentle agitation at room temperature. Amersham ECL Western Blotting detection reagent (GE Healthcare) was used to visualize the membrane via Intas ECL ChemoCam Imager (Intas Science

Imaging). Densitometry of the bands were evaluated via ImageJ software (version 1.48v, NIH; Yilmaz et al., 2022).

## 2.7 RNA Extraction and quantitative real-time PCR

Total RNA was isolated using PeqGOLD TriFast (VWR Life Science), according to the manufacturer's instructions. Reverse transcription was performed using 1 µg of RNA with Tetro Reverse Transkriptase kit (Bioline GmbH). The following sets of primers (Metabion) were used (Osowski & Urano, 2011): BiP (human): forward 5'-TGTTCAACCAATTATCAGCAAACCTC-3'; reverse 5'-TTCTGCTGTATCCTCTTACCAGT-3', sXBP1 (human): forward 5'-CTGAGTCCGAATCAGGTGCAG-3'; reverse 5'-ATCCATGGGGA-GATGTTCTGG-3', CHOP (human) forward 5'-AGAACCAGGAAACGGAAACAGA-3'; reverse 5'-TCTCCTTCATGCGCTGCTTT-3', BiP (rat): forward 5'-TGGGTACATTTGATCTGACTGGA-3'; reverse 5'-CTCAAAGGTGACTTCAATCTGGG-3', CHOP (rat) forward 5'-AGAGTGGTCAGTGCGCAGC-3'; reverse 5'-CTCATTCTCCTGCTCCTTCTCC-3'. Quantitative real-time PCR (RT PCR) was performed using HOT FIREPol EvaGreen qPCR Mix (Solis BioDyne) and the 7500 Fast Real-Time PCR system (Applied Biosystems). The relative quantity (RQ) of mRNA was normalized to a housekeeping gene, GAPDH, forward: 5'-GCACCACCAACTGCTTAGC-3', reverse: 5'-GGCATGGACTGTGGTCATGAG-3' (Yilmaz et al., 2022).

## 2.8 siRNA Knockdown

HEK 293 cells were transfected with siRNA (Ambion GmbH) at 40% confluency using INTERFERin (Polyplus Transfection) according to the manufacturer's instructions. The following siRNA target sequences were used; CYPA: sense 5'-AGGUCCCAAAGACAG-CAGAtt-3', antisense 5'-UCUGCUGUCUUUGGGACCUtg-3' and CYPB: sense 5'-CCGUCAAGGUGUAUUUUGAtt-3', antisense 5'-UCAAAAUACACCUUGACGGtg-3' (Yilmaz et al., 2022).

## 2.9 Statistics

The presented results were obtained from at least three biological replicates. Comparative analysis between two groups was performed by unpaired *t*-test via GraphPad Prism

---

8 (GraphPad Software Inc). A probability of  $p < 0.05$  was considered significant (Yilmaz et al., 2022).

### 3. Results

In order to identify suitable CNI doses, MTT assays were performed to evaluate the viability of HEK 293 cells in the presence of increasing concentrations of CsA or Tac (0 to 80  $\mu\text{M}$ ). CNI doses over 20  $\mu\text{M}$  caused substantial decreases in viability: 43% viability in CsA and 60% in Tac. Thus, 10  $\mu\text{M}$  CsA and Tac treatments were chosen for further experiments in which the treatment duration was determined (Figure 3A; Yilmaz et al., 2022).

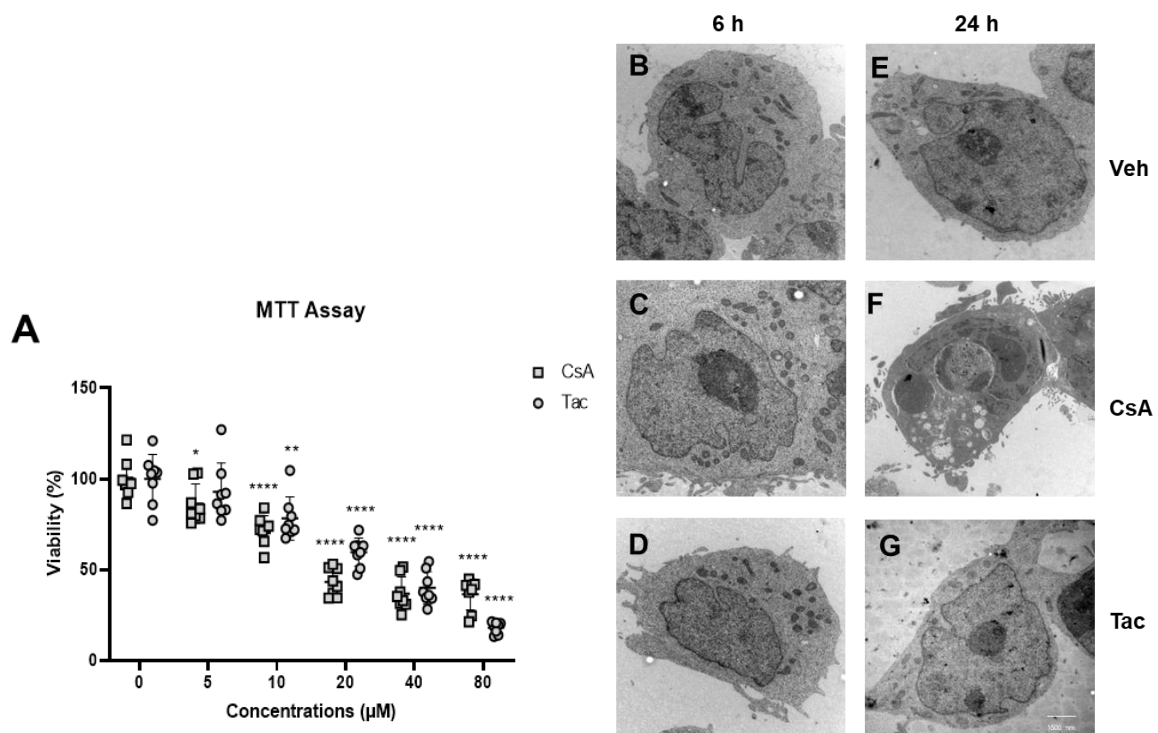


**Figure 3: Effects of cyclosporine A (CsA) and tacrolimus (Tac) on cell viability and morphology in HEK 293 cells:** **A** Cell viability assay of HEK 293 cells after 6 hours of CsA or Tac treatment (0-80  $\mu\text{M}$ ). N = three independent experiments. Data are the means  $\pm$  SD, \* $p < 0.05$ , \*\* $p < 0.01$ , \*\*\*\* $p < 0.0001$ . **B-D** Electron microscopy images showing 10  $\mu\text{M}$  CsA or 10  $\mu\text{M}$  Tac treatment do not alter the cellular morphology after 6 hours of treatment. **E-G** Treatment with 10  $\mu\text{M}$  of CsA but not Tac for 24 hours causes cytoplasmic vacuolization. Figure 3 was modified from Duygu Elif Yilmaz et al. 2022, J Biol Chem (Yilmaz et al., 2022).

Following 6 or 24 h CsA and Tac treatments were done and cell ultrastructural analyses were performed on transmission micrographs. While no obvious morphological differences were seen between the treatment groups after 6 h of treatment, 24 h treatment caused apparent vacuolization in CsA-treated but not in Tac-treated HEK 293 cells (Figure 3B-G). Therefore, the doses of 10  $\mu\text{M}$  CsA or Tac and the time duration for 6 h were

chosen for the treatment protocol to study ER stress and UPR in response to CNI (Yilmaz et al., 2022).

Next, we evaluated the effects of CsA vs. Tac on UPR related genes in HEK 293 cells using quantitative real-time PCR (RT PCR). Thapsigargin (Tg, 0.1  $\mu$ M) treatment, an established ER stress-inducer, was also included as a positive control (Osowski & Urano, 2011). The results revealed that CsA, but not Tac, induces UPR in HEK 293 cells, as evident by increased BiP, sXBP1 and CHOP expression levels (BiP: +231%,  $p < 0.01$ ; sXBP1: +2142%,  $p < 0.05$ ; CHOP: +751%,  $p < 0.05$ ), similar to those induced by Tg (Figure 4A-C; Yilmaz et al., 2022).

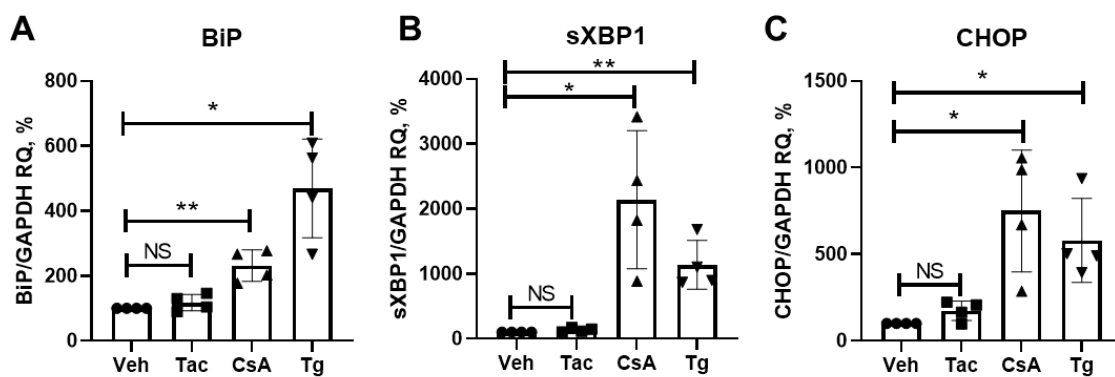


**Figure 4: Effects of cyclosporine A (CsA) or tacrolimus (Tac) on unfolded protein response (UPR) markers in HEK 293 cells detected by real time PCR (RT PCR) analysis: A-C** Graphs show the mRNA expression levels of BiP (A), sXBP1 (B) and CHOP (C) in HEK 293 cells after 10  $\mu$ M CsA or 10  $\mu$ M Tac treatment for 6 hours. Vehicle (Veh) is DMSO and thapsigargin (Tg, 0.1  $\mu$ M) served as positive control. N = four independent experiments. Data are the means  $\pm$  SD, \* $p < 0.05$ , \*\* $p < 0.01$ , NS – not significant. Figure 4 was modified from Duygu Elif Yilmaz et al. 2022, J Biol Chem (Yilmaz et al., 2022).

Immunoblotting results also showed that UPR marker proteins were increased after CsA, but not Tac treatment (Figure 5 A-E). CsA increased the phosphorylation of IRE1 $\alpha$  (+230%,  $p < 0.01$  for p-IRE1 $\alpha$ ) while total IRE1 $\alpha$  amount remained the same (Figure 5A-C). On the other hand, sXBP1 and CHOP were significantly increased by CsA treatment (sXBP1: +223%,  $p < 0.001$ ; CHOP: +227%,  $p < 0.01$ ; Figure 5A, D-E (Yilmaz et al., 2022).

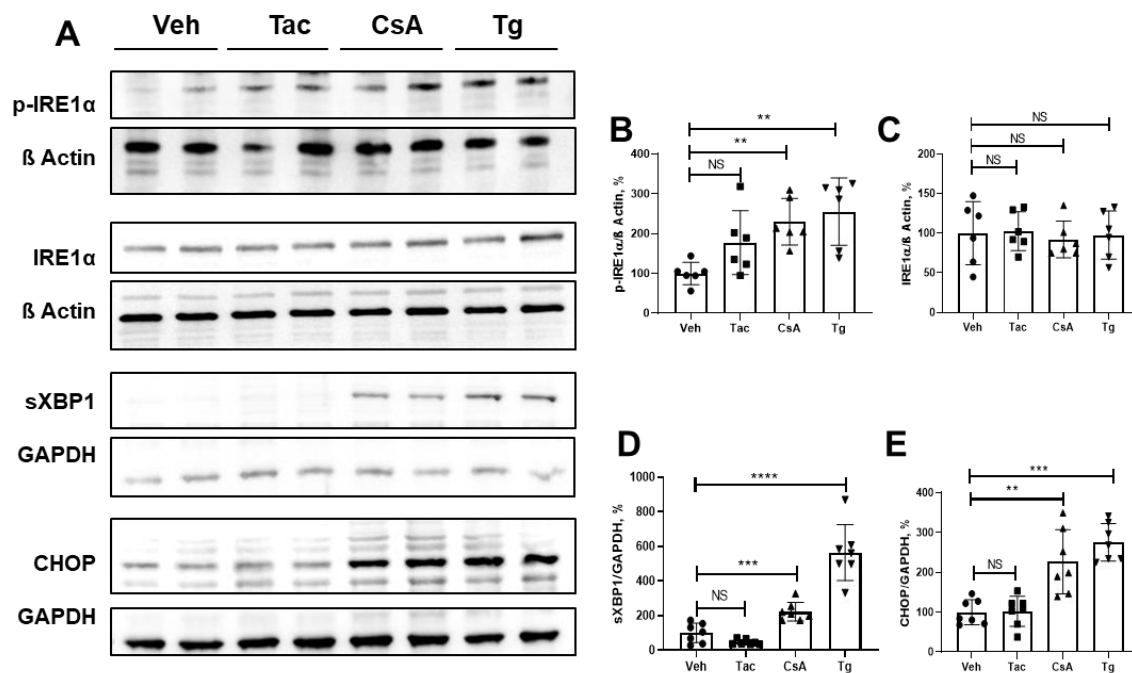


**Figure 5: Effects of cyclosporine A (CsA) or tacrolimus (Tac) on unfolded protein response (UPR) markers in HEK 293 cells detected by immunoblotting: A** Representative immunoblots show the protein expression levels of p-IRE1α (110 kDa), total IRE1α (110 kDa), sXBP1 (56 kDa) and CHOP (27 kDa) in HEK 293 cells after 10 μM CsA or 10 μM Tac treatment for 6 hours. Vehicle (Veh) is DMSO, thapsigargin (Tg, 0.1 μM, 6 h) served as positive control, β actin (42 kDa) or GAPDH (37 kDa) served as loading controls. **B-E** Graphs represent the densitometric evaluation of p-IRE1α (B), total IRE1α (C), sXBP1 (D) and CHOP (E) expressions. Protein expressions were normalized to β actin or GAPDH expressions. N = three independent experiments. Data are the means ± SD, \*\*p < 0.01, \*\*\*p < 0.001, \*\*\*\*p < 0.0001, NS – not significant. Figure 5 was modified from Duygu Elif Yilmaz et al. 2022, J Biol Chem (Yilmaz et al., 2022).

Next, we evaluated the anti- and proapoptotic markers B-cell lymphoma 2 (BCL-2) and Bcl-2-associated X protein (Bax), respectively (Szegezdi et al., 2009). Immunoblots show that CsA and Tg treatments resulted in diminished expression of anti-apoptotic BCL-2 (CsA: -76%, p < 0.05; Tg: -58%, p < 0.01) and increased Bax levels (CsA: +218%, p < 0.0001; Tg: +234, p < 0.01) in HEK 293 cells (Figure 6A-B). Tac treatment did not affect the BCL-2 expression, but did cause a slight increase in the expression of Bax protein (Tac: +168%, p < 0.05; Figure 6A-B; Yilmaz et al., 2022).

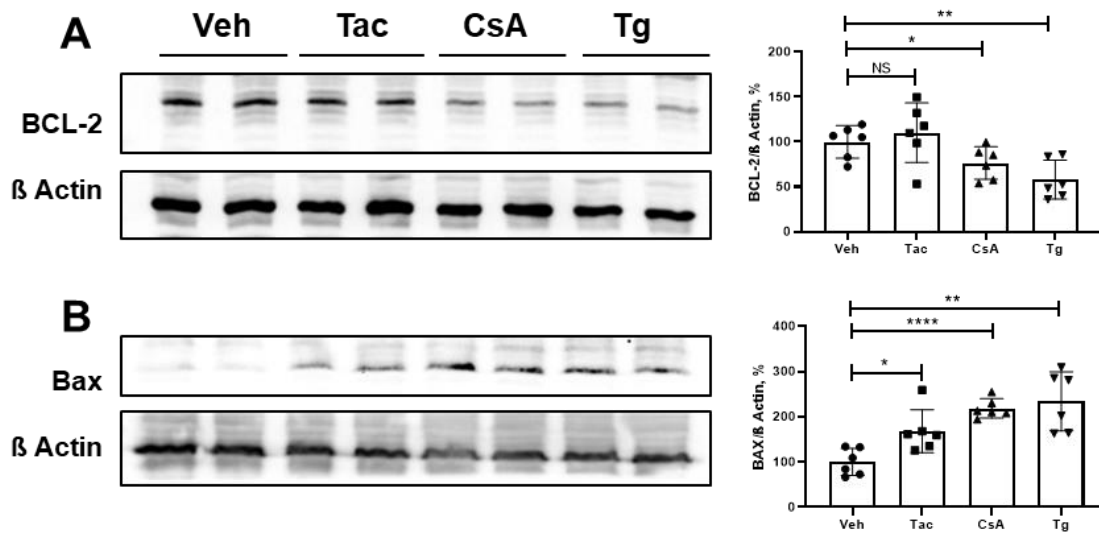


**Figure 6: Effects of cyclosporine A (CsA) or tacrolimus (Tac) on apoptosis markers in HEK 293 cells detected by immunoblotting: A-B** Representative immunoblots show the protein expression levels of BCL-2 (26 kDa; A) and Bax (21 kDa; B) in HEK 293 cells after 10  $\mu$ M CsA or 10  $\mu$ M Tac treatment for 6 hours. Vehicle (Veh) is DMSO, thapsigargin (Tg, 0.1  $\mu$ M) served as positive control and  $\beta$  actin (42 kDa) served as loading control. Graphs represent the densitometric evaluation of BCL-2 (A) and Bax (B) expressions. Protein expressions were normalized to  $\beta$  actin. N = three independent experiments. Data are the means  $\pm$  SD, \* $p$  < 0.05, \*\* $p$  < 0.01, \*\*\*\* $p$  < 0.0001, NS – not significant. Figure 6 was modified from Duygu Elif Yilmaz et al. 2022, J Biol Chem (Yilmaz et al., 2022).

Apoptotic parameters were also evaluated via immunofluorescence staining. Confocal microscopy images revealed that CHOP signal intensity was significantly higher after CsA and Tg treatments (CsA: +235%,  $p$  < 0.0001; Tg: +137%,  $p$  < 0.001). Tac and Veh treatments, by comparison, did not cause a significant change to CHOP expression (Figure 7A-B; Yilmaz et al., 2022). cCas-3 positive cells were counted as another apoptotic marker (Sharma et al., 2021). cCas-3 positive cell number was explicitly higher only in CsA and Tg treated cells (CsA: +422%,  $p$  < 0.01; Tg: +448,  $p$  < 0.01; Figure 7A, C). Tac induced no increase compared to vehicle (Yilmaz et al., 2022).

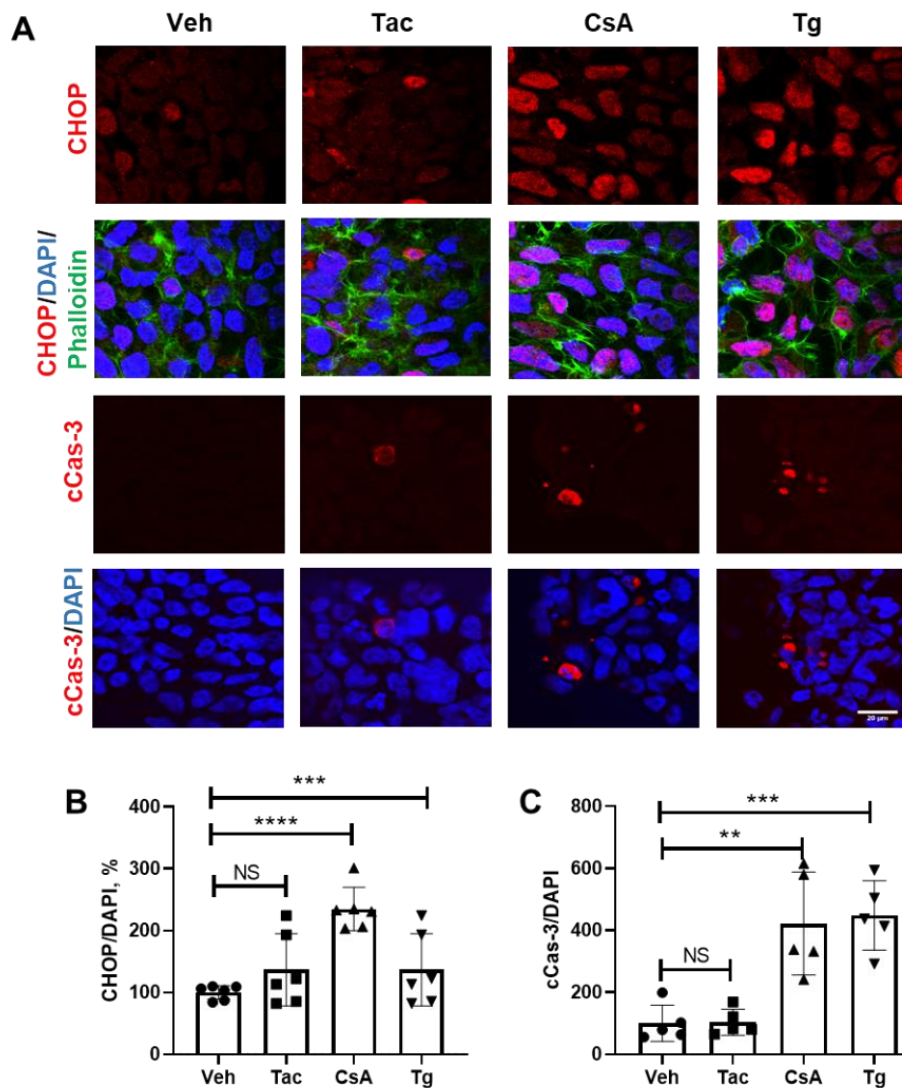


**Figure 7: Effects of cyclosporine A (CsA) or tacrolimus (Tac) on apoptotic markers in HEK 293 cells detected by immunofluorescence staining:** **A** Representative confocal microscopy images show the protein expression levels of CHOP (red signal) or cCas-3 (red signal) in HEK 293 cells treated with 10  $\mu$ M CsA or 10  $\mu$ M Tac for 6 hours. Vehicle (Veh) is DMSO and thapsigargin (Tg, 0.1  $\mu$ M) served as positive control. To detect the cellular localization of proteins, nuclei were labeled with DAPI (blue signal) and cytoskeleton with phalloidin, a phallotoxin that binds to F-actin (green signal). **B-C** Graphs represent the evaluation of CHOP (B) or cCas-3 (C) expressions. Protein signals were normalized to DAPI. Data are the means  $\pm$  SD, \*\* $p$  < 0.01, \*\*\* $p$  < 0.001, \*\*\*\* $p$  < 0.0001, NS – not significant. Figure 7 was modified from Duygu Elif Yilmaz et al. 2022, J Biol Chem (Yilmaz et al., 2022).

We have then corroborated the data obtained from HEK 293 cells with primary human renal proximal tubular epithelial cells (HRPTEpC). RT PCR results showed that CsA induced an increase of UPR related genes including BiP, CHOP and sXBP1 (BiP: +233%,  $p$  < 0.0001; sXBP1: +288%,  $p$  < 0.0001; CHOP: +278%,  $p$  < 0.01) compared to vehicle

treated cells (Figure 8A-C). Tac induced only a moderate increase in BiP mRNA (+135%,  $p < 0.01$ ; Figure 8A). Analysis of sXBP1 abundance by immunoblotting revealed significant increases in CsA or Tg treated cells compared to Tac or Veh treated cells (CsA: +188%,  $p < 0.01$ ; Tg: +309  $p < 0.0001$ ; Figure 8D; Yilmaz et al., 2022).

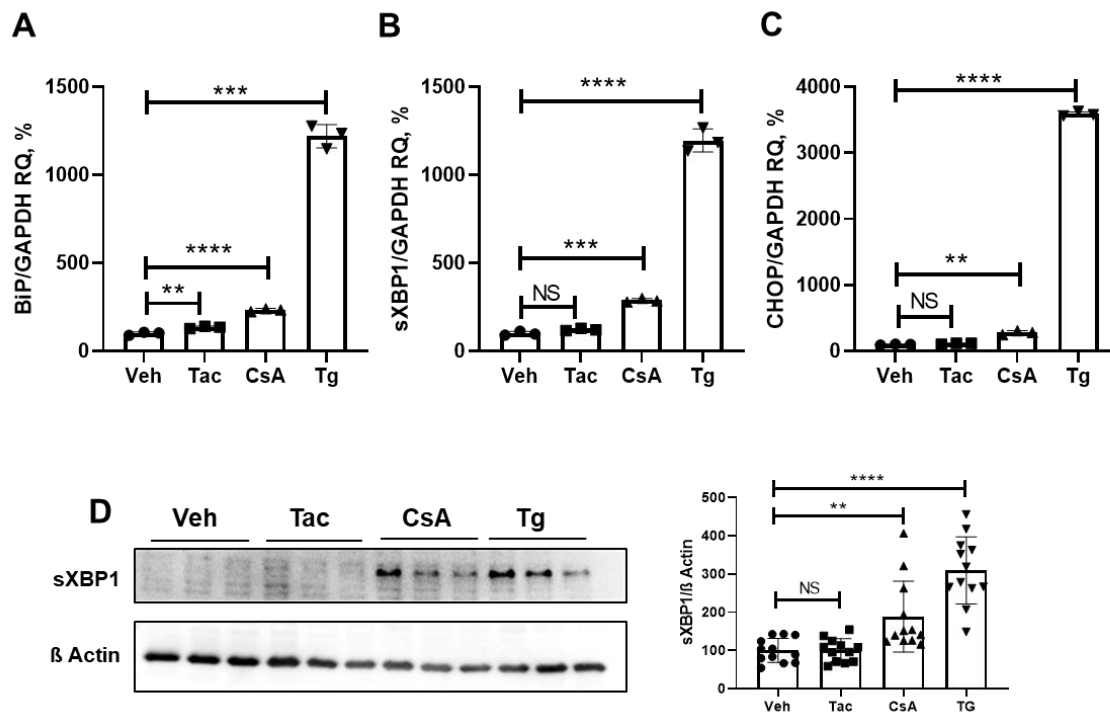


**Figure 8: Effects of cyclosporine A (CsA) or tacrolimus (Tac) on unfolded protein response (UPR) markers in HRPTEpC cells by real time PCR (RT PCR) and immunoblotting: A-C** Graphs show the mRNA expression levels of BiP (A), sXBP1 (B) and CHOP (C) in HRPTEpC cells after 10  $\mu\text{M}$  CsA or 10  $\mu\text{M}$  Tac treatment for 6 hours. Vehicle is DMSO and thapsigargin (Tg, 0.1  $\mu\text{M}$ ) served as positive control. N = three independent experiments. Data are the means  $\pm$  SD,  $**p < 0.01$ ,  $***p < 0.001$ ,  $****p < 0.0001$ , NS – not significant. **D** Representative immunoblot shows the expression of sXBP1 (56 kDa) in HRPTEpC cells after 10  $\mu\text{M}$  CsA or 10  $\mu\text{M}$  Tac treatment for 6 hours. Vehicle (Veh) is DMSO, thapsigargin (Tg, 0.1  $\mu\text{M}$ ) served as positive control and  $\beta$  actin (42 kDa) as loading control. Graph represents the densitometric evaluation of sXBP1 expression. Protein expressions were normalized to  $\beta$  actin. N = three independent experiments. Data are the means  $\pm$  SD,  $**p < 0.01$ ,  $****p < 0.0001$ , NS – not significant. Figure 8 was modified from Duygu Elif Yilmaz et al. 2022, J Biol Chem (Yilmaz et al., 2022).

Supporting experiments were performed in freshly isolated proximal tubules obtained from 7-9 weeks old male Wistar rats. Each set of tubules was divided into four subsets (Figure 9A), which were incubated with Veh, Tac, CsA or Tg in 2 mL reaction tubes (Figure 9B). Subsequent RT PCR analyses revealed that CsA induced BiP and CHOP mRNA

levels (BiP: +234%,  $p < 0.05$ ; CHOP: +366%,  $p < 0.05$ ) while Tac did not, in line with previous results (Figure 9C-D; Yilmaz et al., 2022).

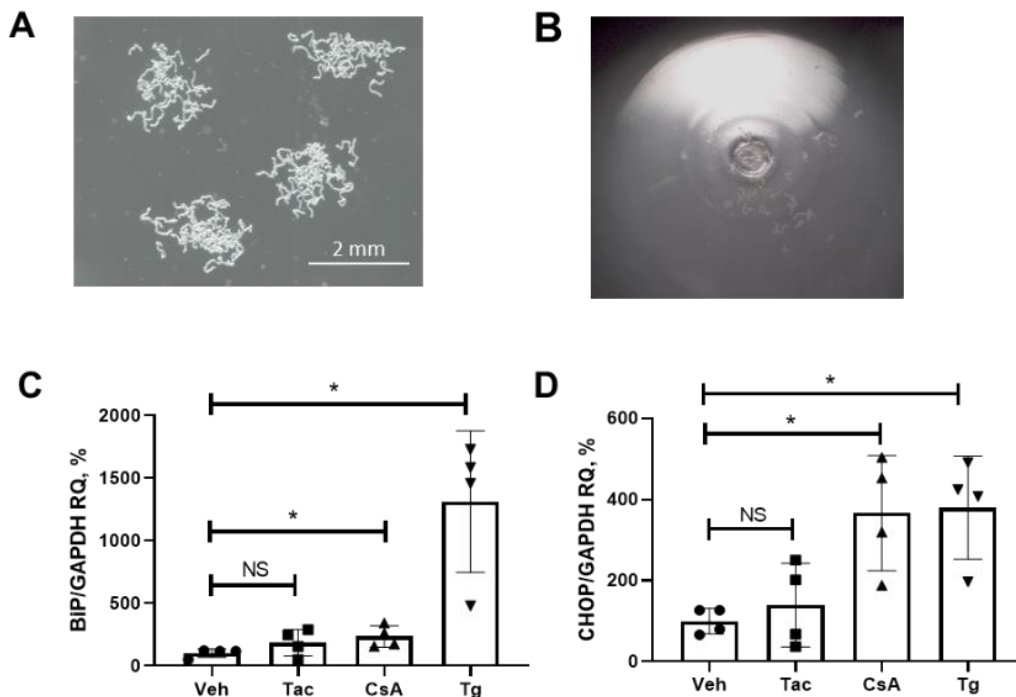


**Figure 9: Isolation of rat proximal tubules and effects of cyclosporine A (CsA) or tacrolimus (Tac) on unfolded protein response (UPR) markers detected by real time PCR (RT PCR):** **A** A set of proximal tubules divided in 4 subsets. **B** Tubule subsets were then separated into individual 2 mL reaction tubes and treated with 10  $\mu$ M CsA or 10  $\mu$ M Tac, for 6 hours. Vehicle is DMSO and thapsigargin (Tg, 0.1  $\mu$ M) served as positive control. **C-D** Graphs show the mRNA expression levels of BiP (C) and CHOP (D) in proximal tubules. N = four independent experiments. Data are the means  $\pm$  SD, \* $p < 0.05$ , NS – not significant. Figure 9 was modified from Duygu Elif Yilmaz et al. 2022, J Biol Chem (Yilmaz et al., 2022).

To test the role of cyclophilin activity in CsA mediated cell toxicity, CYPA or CYPB were suppressed by siRNA-mediated knockdown in HEK 293 cells. The knockdown experiments resulted in decreased protein expression levels of CYPA (-53%,  $p < 0.001$ ) and CYPB (-57%,  $p < 0.0001$ ; Figure 10A-D) in HEK 293 cells. Immunoblotting analysis of CHOP and cCas-3 revealed that knockdown of either cyclophilin increased CHOP and cCas3 levels (CYPA knockdown: CHOP: +247%,  $p < 0.0001$ ; cCas-3: +284%,  $p < 0.001$  and CYPB knockdown: CHOP: +364%,  $p < 0.0001$ ; cCas-3: +327%,  $p < 0.001$ ) similar to CsA treatment (CHOP: +343%,  $p < 0.0001$ ; cCas-3: +214%,  $p < 0.01$ ; Figure 10E-G). These results suggested that CsA induced UPR depends, at least in part, on the suppression of cyclophilin activity (Yilmaz et al., 2022).

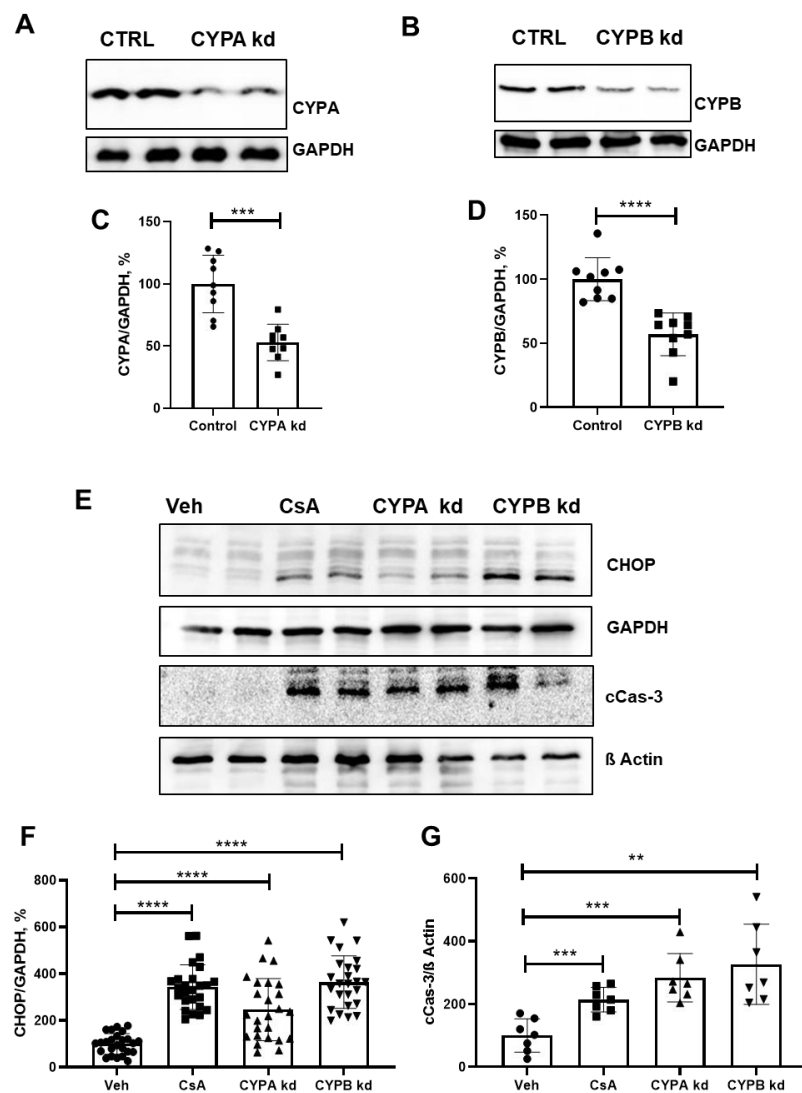


**Figure 10: Knockdown of cyclophilins and its effects on CHOP and cCas-3 expression in HEK 293 cells detected by immunoblotting:** **A-B** Representative immunoblots verify the siRNA mediated knockdown of cyclophilin A (18 kDa; **A**) and B (21 kDa; **B**) in HEK 293 cells. **C-D** Graphs represent the densitometric evaluation of CYPA (**C**) or CYPB (**D**) expression. Protein expressions were normalized to GAPDH. Data are the means  $\pm$  SD, \*\*\* $p$  < 0.001, \*\*\*\* $p$  < 0.0001. **E** Representative immunoblots show the expression of CHOP (27 kDa) or cCas-3 (19 kDa) in CsA (10  $\mu$ M) treated or CYPB knockdown HEK 293 cells. GAPDH (37 kDa) or  $\beta$  actin (42 kDa) served as loading controls. **F-G** Graphs represent the densitometric evaluation of CHOP (**F**) or cCas-3 (**G**) expression. Protein expressions were normalized to loading controls, GAPDH or  $\beta$  actin. N = three independent experiments. Data are the means  $\pm$  SD, \*\* $p$  < 0.01, \*\*\* $p$  < 0.001, \*\*\*\* $p$  < 0.0001. Figure 10 was modified from Duygu Elif Yilmaz et al. 2022, J Biol Chem (Yilmaz et al., 2022).

Next, we tested whether concomitant use of chemical chaperones may alleviate the CsA induced UPR. The results showed that use of chemical chaperones such as TUDCA or 4-PBA diminished the expression of proapoptotic UPR marker, CHOP. Immunoblots show that, CsA alone induced an expression of CHOP (+625%,  $p < 0.0001$ ) which was blunted by concomitant application of TUDCA (+274%,  $p < 0.001$ ; Figure 11A). Similar results were seen with concomitant application of 4-PBA (from +712%,  $p < 0.0001$  to +238%,  $p < 0.0001$ ; Figure 11B; Yilmaz et al., 2022).

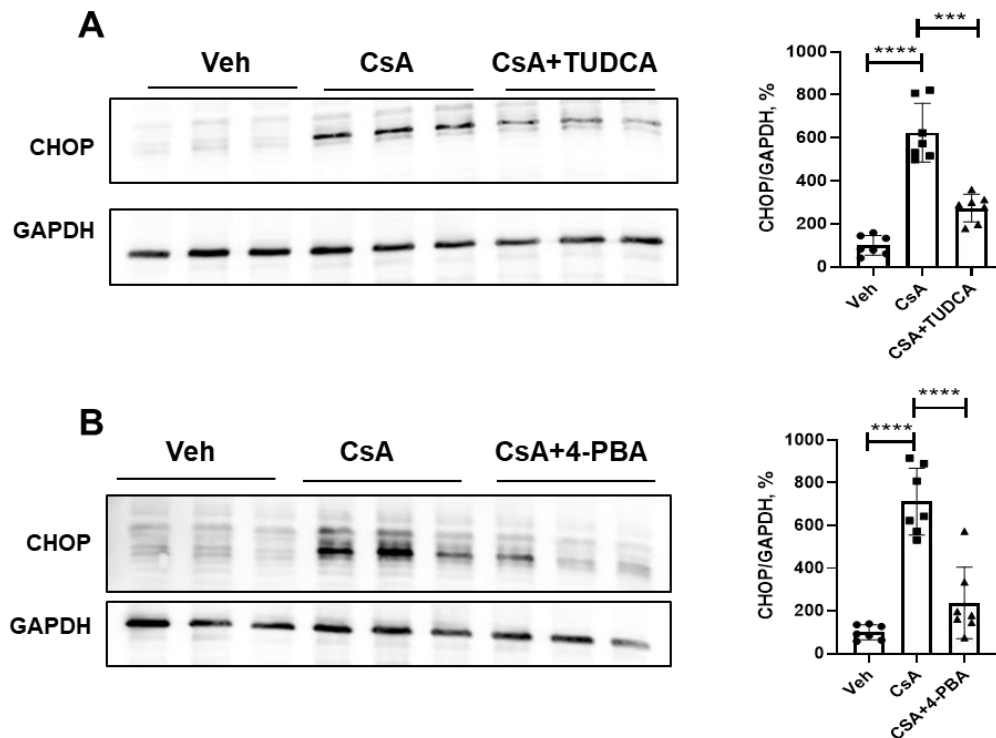


**Figure 11: Effects of concomitant treatment of chemical chaperones, TUDCA or 4-PBA, on CHOP expression in cyclosporine A (CsA) treated HEK 293 cells detected by immunoblotting: A-B** Representative immunoblots show the expression of CHOP (27 kDa) in HEK cells treated with CsA (10  $\mu$ M), CsA+TUDCA (300  $\mu$ M; A) or CsA+4-PBA (5  $\mu$ M; B). GAPDH (37 kDa) served as loading control. Graphs represent the densitometric evaluation of CHOP expression. Protein expressions were normalized to loading control, GAPDH. Data are the means  $\pm$  SD, \*\*\* $p < 0.001$ , \*\*\*\* $p < 0.0001$ . Figure 11 was modified from Duygu Elif Yilmaz et al. 2022, J Biol Chem (Yilmaz et al., 2022).

In order to genetically suppress CsA-induced UPR in HEK 293 cells, two of the key UPR sensors, PERK and ATF6, were deleted via CRISPR/Cas9 mediated gene knockout (Figure 12A-C). Next, unmodified (control), PERK knockout, and ATF6 knockout HEK 293 cells were treated with vehicle, Tac or CsA. RT PCR results showed that expression of CHOP mRNA levels were decreased in modified HEK 293 cells. CsA treatment caused

a strong increase in CHOP expression in unmodified HEK 293 cells (+905%,  $p < 0.05$ ), while PERK knockout and ATF6 knockout HEK 293 cells showed comparatively blunted CHOP increases (+486%,  $p < 0.05$  and +343%,  $p < 0.05$ , respectively; Figure 12D). These RT PCR results suggest that genetic modulation of UPR sensors has a promising potential for alleviating CsA-induced UPR (Yilmaz et al., 2022).

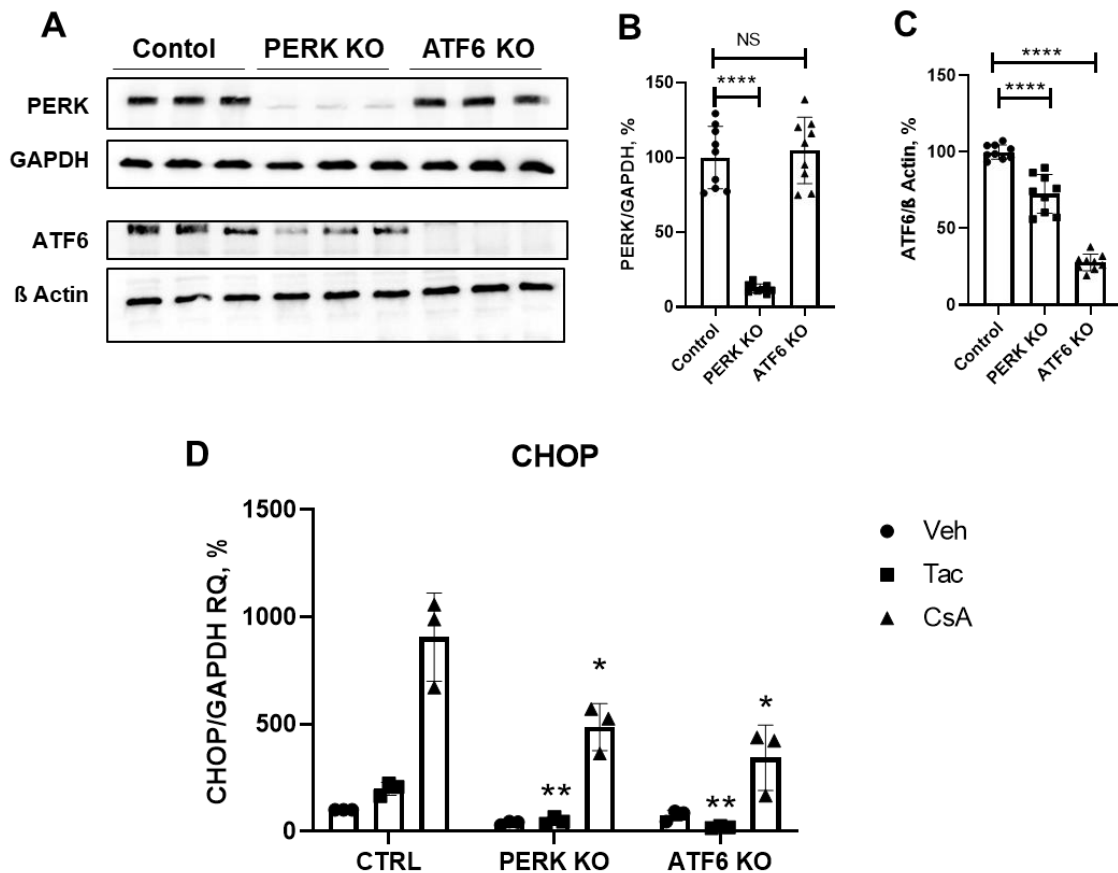


**Figure 12: Knockout of two unfolded protein response sensors, PERK or ATF6, and its effects of CHOP mRNA expression in HEK 293 cells detected by real time PCR (RT PCR):**

**A** Representative immunoblots verify the knock out of PERK (125 kDa) or ATF6 (75 kDa) proteins in HEK 293 cells. GAPDH (37 kDa) or  $\beta$  actin (42 kDa) serves as loading controls. **B-C** Graphs represent the densitometric evaluation of PERK (B) or ATF6 (C) expression. Protein expressions were normalized to loading controls. Data are the means  $\pm$  SD, \*\*\*\* $p < 0.0001$ , NS – not significant. **D** Graph shows mRNA expression levels of CHOP in native (CTRL), PERK knockout (PERK KO) and ATF6 knockout (ATF6 KO) HEK 293 cells. N = three independent experiments. Data are the means  $\pm$  SD, \* $p < 0.05$ , \*\* $p < 0.001$ . Figure 11 was modified from Duygu Elif Yilmaz et al. 2022, J Biol Chem (Yilmaz et al., 2022).

## 4. Discussion

Currently, immunosuppressive regimens that prevent allograft rejection in organtransplanted patients typically include calcineurin inhibitors (Naesens et al., 2009). Retrospective analysis of CNI induced renal side effects suggested that Tac may exhibit a more favourable profile than CsA (Jurewicz, 2003). Several lines of evidence suggest that CsA-derived toxicity is associated with impaired proteostasis that causes a maladaptive unfolded protein response and eventual apoptotic induction as a consequence of this (Adams et al., 2019; Fedele et al., 2020; Ram & Ramakrishna, 2014). In line with this, the results of the present study revealed induction of a proapoptotic UPR after CsA application in cultured renal cells and freshly isolated rat tubules. CsA treatment caused increased expression of the UPR markers BiP, p-IRE1 $\alpha$ , sXBP1 and CHOP. CsA treatment also led to decreased levels of anti-apoptotic protein BCL-2, as well as upregulated levels of apoptotic proteins Bax and cCas-3, indicating the failure of the adaptive UPR branch and the activation of proapoptotic pathways (Hetz & Papa, 2018; Yilmaz et al., 2022). By contrast, Tac treatment showed no effect on the aforementioned UPR markers with the exception of a mild increase in BiP mRNA levels in cultured proximal tubular cells (HRPTEpC) and Bax in protein levels in HEK 293 cells (Yilmaz et al., 2022). These results corroborate and extend on previous work demonstrating that CsA induces ER stress (Han et al., 2008; Lhoták et al., 2012).

To gain mechanistic insights into CsA-driven cell toxicity, we tested for potential calcineurin-independent effects of the drug through siRNA-mediated knockdown of cyclophilin (CYP) A or B (Yilmaz et al., 2022). Cyclophilins are a subgroup of the immunophilin family exerting peptidyl-prolyl *cis-trans* isomerase (PPIase) activity. They exhibit a ubiquitous expression pattern and a high degree of evolutionary conservation from prokaryotes to eukaryotes (Kumari et al., 2013; P. Wang & Heitman, 2005). Cyclophilins play important roles in protein folding due to their PPIase activity. Previous studies have reported on the protective effects of CYP A and B activity in CsA-induced nephrotoxicity or aldosterone-induced proximal tubular cell injury models (Hong et al., 2004; B. Wang et al., 2016). In the present work, cyclophilin knockdown in HEK 293 cells produced significant increases in CHOP and cCas-3 levels, similar to CsA treatment. This suggests that CsA-induced inhibition of cyclophilin chaperone function may be responsible for ER stress and maladaptive UPR, rather than calcineurin inhibition. Since Tac treatment caused a comparatively mild effect on the UPR, it is conceivable that the roles of cyclophilins in maintaining

intact cellular proteostasis are more crucial than those of FKBP12, at least in relation to UPR induction (Yilmaz et al., 2022). Although Tac seems to have a more favorable drug profile than CsA in terms of renal side effects, Tac treatment *in vivo* has been shown to promote hypertension as subsequences of vasoconstriction and renal sodium retention (Hoorn et al., 2011). Moreover, Tac has been associated with new onset of diabetes mellitus, which may then aggravate cardiovascular disorders (Farouk & Rein, 2020; Heisel et al., 2004; Song, 2016).

Previous studies have shown that protein misfolding and ER stress occur in acute kidney injury, diabetic nephropathy, and chronic kidney disease leading to renal fibrosis. Chemical chaperones that improve protein folding may alleviate this ER stress and reduce kidney injury subsequently (Cybulsky, 2017; Liu et al., 2016). Concordantly, the present study demonstrates concomitant application of chemical chaperones such as TUDCA or 4-PBA reduced CSA-induced cellular toxicity in HEK 293 cells (Yilmaz et al., 2022).

In addition to pharmacological modulation of UPR, genetic approaches may also add to our understanding of CsA mediated nephrotoxicity. In the present study, CRISPR/Cas9 gene editing was performed to knockout two of the three UPR sensors: ATF6 and PERK (Yilmaz et al., 2022). While the knockout was also attempted for IRE1 $\alpha$ , the resulting cells were unviable highlighting the essential role of this gene in the cell survival (Raymundo et al., 2020; Yilmaz et al., 2022). Our results revealed that knockout of either PERK or ATF6 blunted the effects of CsA-induced UPR as demonstrated by the reduced expression of CHOP. (Yilmaz et al., 2022). A previous study also showed that liver-specific knockout of *PERK* caused a sharp reduction in UPR-related genes during ER stress (Teske et al., 2011). Similarly, another study reported that deletion of *ATF6 $\alpha$*  in mouse embryonic fibroblasts showed a decreased expression of CHOP and BiP in response to the ER stress-inducer, thapsigargin (Diedrichs et al., 2018). Although our results demonstrate that knockout of PERK or ATF6 in HEK 293 cells show promising outcomes to alleviate the proapoptotic UPR, animal experiments are mandatory for further interpretations (Yilmaz et al., 2022).

## 5. Conclusions

In conclusion, the present study describes a calcineurin-independent mechanism of CsA-induced cellular toxicity that can be explained by the suppression of cyclophilin activity, which results in uncompensated ER stress and proapoptotic UPR. This mechanism may be, at least in part, responsible for the more pronounced nephrotoxic effects of CsA as compared to Tac. Using chemical chaperones and genetic approaches to ameliorate the CsA-induced UPR may provide new avenues for rational therapeutic strategies.

## Reference list

- Adams, C. J., Kopp, M. C., Larburu, N., Nowak, P. R., & Ali, M. M. U. (2019). Structure and Molecular Mechanism of ER Stress Signaling by the Unfolded Protein Response Signal Activator IRE1. *Frontiers in Molecular Biosciences*, 6, 11. <https://doi.org/10.3389/fmolb.2019.00011>
- Bandyopadhyay, J., Lee, J., & Bandyopadhyay, A. (2004). Regulation of calcineurin, a calcium/calmodulin-dependent protein phosphatase, in *C. elegans*. *Molecules and Cells*, 18(1), 10–16.
- Bergmann, T. J., & Molinari, M. (2018). Three branches to rule them all? UPR signalling in response to chemically versus misfolded proteins-induced ER stress: Chemical ER stress versus misfolded protein-induced ER stress. *Biology of the Cell*, 110(9), 197–204. <https://doi.org/10.1111/boc.201800029>
- Calderón-Sánchez, E., Rodríguez-Moyano, M., & Smani, T. (2011). Immunophilins and cardiovascular complications. *Current Medicinal Chemistry*, 18(35), 5408–5413. <https://doi.org/10.2174/092986711798194379>
- Chadwick, S. R., & Lajoie, P. (2019). Endoplasmic Reticulum Stress Coping Mechanisms and Lifespan Regulation in Health and Diseases. *Frontiers in Cell and Developmental Biology*, 7, 84. <https://doi.org/10.3389/fcell.2019.00084>
- Cho, K., Patil, H., Senda, E., Wang, J., Yi, H., Qiu, S., Yoon, D., Yu, M., Orry, A., Peachey, N. S., & Ferreira, P. A. (2014). Differential Loss of Prolyl Isomerase or Chaperone Activity of Ran-binding Protein 2 (Ranbp2) Unveils Distinct Physiological Roles of Its Cyclophilin Domain in Proteostasis. *Journal of Biological Chemistry*, 289(8), 4600–4625. <https://doi.org/10.1074/jbc.M113.538215>
- Creamer, T. P. (2020). Calcineurin. *Cell Communication and Signaling*, 18(1), 137. <https://doi.org/10.1186/s12964-020-00636-4>
- Cybulsky, A. V. (2017). Endoplasmic reticulum stress, the unfolded protein response and autophagy in kidney diseases. *Nature Reviews Nephrology*, 13(11), 681–696. <https://doi.org/10.1038/nrneph.2017.129>

- Deleuze, S., Garrigue, V., Delmas, S., Chong, G., Swarcz, I., Cristol, J. P., & Mourad, G. (2006). New Onset Dyslipidemia After Renal Transplantation: Is There a Difference Between Tacrolimus and Cyclosporine? *Transplantation Proceedings*, *38*(7), 2311–2313. <https://doi.org/10.1016/j.transproceed.2006.06.125>
- Diedrichs, D. R., Gomez, J. A., Huang, C.-S., Rutkowski, D. T., & Curtu, R. (2018). A data-entrained computational model for testing the regulatory logic of the vertebrate unfolded protein response. *Molecular Biology of the Cell*, *29*(12), 1502–1517. <https://doi.org/10.1091/mbc.E17-09-0565>
- Dutz, J. P., Fruman, D. A., Burakoff, S. J., & Bierer, B. E. (1993). A role for calcineurin in degranulation of murine cytotoxic T lymphocytes. *Journal of Immunology (Baltimore, Md.: 1950)*, *150*(7), 2591–2598.
- Farouk, S. S., & Rein, J. L. (2020). The Many Faces of Calcineurin Inhibitor Toxicity-What the FK? *Advances in Chronic Kidney Disease*, *27*(1), 56–66. <https://doi.org/10.1053/j.ackd.2019.08.006>
- Fedele, A. O., Carraro, V., Xie, J., Averous, J., & Proud, C. G. (2020). Cyclosporin A but not FK506 activates the integrated stress response in human cells. *Journal of Biological Chemistry*, *295*(44), 15134–15143. <https://doi.org/10.1074/jbc.RA120.014531>
- Gafter-Gvili, A., Sredni, B., Gal, R., Gafter, U., & Kalechman, Y. (2003). Cyclosporin A-induced hair growth in mice is associated with inhibition of calcineurin-dependent activation of NFAT in follicular keratinocytes. *American Journal of Physiology-Cell Physiology*, *284*(6), C1593–C1603. <https://doi.org/10.1152/ajpcell.00537.2002>
- Haddad, E., McAlister, V., Renouf, E., Malthaner, R., Kjaer, M. S., & Gluud, L. L. (2006). Cyclosporin versus tacrolimus for liver transplanted patients. *Cochrane Database of Systematic Reviews*, *2010*(1). <https://doi.org/10.1002/14651858.CD005161.pub2>
- Han, S. W., Li, C., Ahn, K. O., Lim, S. W., Song, H. G., Jang, Y. S., Cho, Y. M., Jang, Y. M., Ghee, J. Y., Kim, J. Y., Kim, S. H., Kim, J., Kwon, O. J., & Yang, C. W. (2008). Prolonged Endoplasmic Reticulum Stress Induces Apoptotic Cell Death in an Experimental Model of Chronic Cyclosporine Nephropathy. *American Journal of Nephrology*, *28*(5), 707–714. <https://doi.org/10.1159/000127432>

- Heisel, O., Heisel, R., Balshaw, R., & Keown, P. (2004). New Onset Diabetes Mellitus in Patients Receiving Calcineurin Inhibitors: A Systematic Review and Meta-Analysis. *American Journal of Transplantation*, *4*(4), 583–595. <https://doi.org/10.1046/j.1600-6143.2003.00372.x>
- Hetz, C. (2012). The unfolded protein response: Controlling cell fate decisions under ER stress and beyond. *Nature Reviews. Molecular Cell Biology*, *13*(2), 89–102. <https://doi.org/10.1038/nrm3270>
- Hetz, C., & Papa, F. R. (2018). The Unfolded Protein Response and Cell Fate Control. *Molecular Cell*, *69*(2), 169–181. <https://doi.org/10.1016/j.molcel.2017.06.017>
- Hetz, C., Zhang, K., & Kaufman, R. J. (2020). Mechanisms, regulation and functions of the unfolded protein response. *Nature Reviews. Molecular Cell Biology*, *21*(8), 421–438. <https://doi.org/10.1038/s41580-020-0250-z>
- Hong, F., Lee, J., Piao, Y. J., Jae, Y. K., Kim, Y.-J., Oh, C., Seo, J.-S., Yun, Y. S., Yang, C. W., Ha, J., & Kim, S. S. (2004). Transgenic mice overexpressing cyclophilin A are resistant to cyclosporin A-induced nephrotoxicity via peptidyl-prolyl cis–trans isomerase activity. *Biochemical and Biophysical Research Communications*, *316*(4), 1073–1080. <https://doi.org/10.1016/j.bbrc.2004.02.160>
- Hoorn, E. J., Walsh, S. B., McCormick, J. A., Fürstenberg, A., Yang, C.-L., Roeschel, T., Paliege, A., Howie, A. J., Conley, J., Bachmann, S., Unwin, R. J., & Ellison, D. H. (2011). The calcineurin inhibitor tacrolimus activates the renal sodium chloride cotransporter to cause hypertension. *Nature Medicine*, *17*(10), 1304–1309. <https://doi.org/10.1038/nm.2497>
- Jurewicz, W. A. (2003). Tacrolimus versus ciclosporin immunosuppression: Long-term outcome in renal transplantation. *Nephrology Dialysis Transplantation*, *18*(90001), 7i–11. <https://doi.org/10.1093/ndt/gfg1028>
- Kitamura, M. (2010). Induction of the unfolded protein response by calcineurin inhibitors: A double-edged sword in renal transplantation. *Nephrology Dialysis Transplantation*, *25*(1), 6–9. <https://doi.org/10.1093/ndt/gfp516>
- Kumari, S., Roy, S., Singh, P., Singla-Pareek, S., & Pareek, A. (2013). Cyclophilins: Proteins in search of function. *Plant Signaling & Behavior*, *8*(1), e22734. <https://doi.org/10.4161/psb.22734>

- Lemmer, I. L., Willemsen, N., Hilal, N., & Bartelt, A. (2021). A guide to understanding endoplasmic reticulum stress in metabolic disorders. *Molecular Metabolism*, *47*, 101169.  
<https://doi.org/10.1016/j.molmet.2021.101169>
- Lhoták, Š., Sood, S., Brimble, E., Carlisle, R. E., Colgan, S. M., Mazzetti, A., Dickhout, J. G., Ingram, A. J., & Austin, R. C. (2012). ER stress contributes to renal proximal tubule injury by increasing SREBP-2-mediated lipid accumulation and apoptotic cell death. *American Journal of Physiology-Renal Physiology*, *303*(2), F266–F278. <https://doi.org/10.1152/ajprenal.00482.2011>
- Liu, S.-H., Yang, C.-C., Chan, D.-C., Wu, C.-T., Chen, L.-P., Huang, J.-W., Hung, K.-Y., & Chiang, C.-K. (2016). Chemical chaperon 4-phenylbutyrate protects against the endoplasmic reticulum stress-mediated renal fibrosis in vivo and in vitro. *Oncotarget*, *7*(16), 22116–22127.  
<https://doi.org/10.18632/oncotarget.7904>
- Lucey, M. R., Abdelmalek, M. F., Gagliardi, R., Granger, D., Holt, C., Kam, I., Klintmalm, G., Langnas, A., Shetty, K., Tzakis, A., & Woodle, E. S. (2005). A Comparison of Tacrolimus and Cyclosporine in Liver Transplantation: Effects on Renal Function and Cardiovascular Risk Status. *American Journal of Transplantation*, *5*(5), 1111–1119. <https://doi.org/10.1111/j.1600-6143.2005.00808.x>
- Lücke, C., & Weiwad, M. (2011). Insights into immunophilin structure and function. *Current Medicinal Chemistry*, *18*(35), 5333–5354. <https://doi.org/10.2174/092986711798194324>
- Martins, L., Ventura, A., Branco, A., Carvalho, M. J., Henriques, A. C., Dias, L., Sarmiento, A. M., & Amil, M. (2004). Cyclosporine versus tacrolimus in kidney transplantation: Are there differences in nephrotoxicity? *Transplantation Proceedings*, *36*(4), 877–879. <https://doi.org/10.1016/j.transproceed.2004.03.083>
- Metcalf, M. G., Higuchi-Sanabria, R., Garcia, G., Tsui, C. K., & Dillin, A. (2020). Beyond the cell factory: Homeostatic regulation of and by the UPR<sup>ER</sup>. *Science Advances*, *6*(29), eabb9614.  
<https://doi.org/10.1126/sciadv.abb9614>

- Nadanaka, S., Okada, T., Yoshida, H., & Mori, K. (2007). Role of disulfide bridges formed in the luminal domain of ATF6 in sensing endoplasmic reticulum stress. *Molecular and Cellular Biology*, *27*(3), 1027–1043. <https://doi.org/10.1128/MCB.00408-06>
- Naesens, M., Kuypers, D. R. J., & Sarwal, M. (2009). Calcineurin Inhibitor Nephrotoxicity. *Clinical Journal of the American Society of Nephrology*, *4*(2), 481–508. <https://doi.org/10.2215/CJN.04800908>
- Oakes, S. A., & Papa, F. R. (2015). The role of endoplasmic reticulum stress in human pathology. *Annual Review of Pathology*, *10*, 173–194. <https://doi.org/10.1146/annurev-pathol-012513-104649>
- Osowski, C. M., & Urano, F. (2011). Measuring ER Stress and the Unfolded Protein Response Using Mammalian Tissue Culture System. In *Methods in Enzymology* (Vol. 490, pp. 71–92). Elsevier. <https://doi.org/10.1016/B978-0-12-385114-7.00004-0>
- Pachikov, A. N., Gough, R. R., Christy, C. E., Morris, M. E., Casey, C. A., LaGrange, C. A., Bhat, G., Kubyshkin, A. V., Fomochkina, I. I., Zyablitskaya, E. Y., Makalish, T. P., Golubinskaya, E. P., Davydenko, K. A., Eremenko, S. N., Riethoven, J.-J. M., Maroli, A. S., Payne, T. S., Powers, R., Lushnikov, A. Y., ... Petrosyan, A. (2021). The non-canonical mechanism of ER stress-mediated progression of prostate cancer. *Journal of Experimental & Clinical Cancer Research*, *40*(1), 289. <https://doi.org/10.1186/s13046-021-02066-7>
- Park, H.-S., Lee, S. C., Cardenas, M. E., & Heitman, J. (2019). Calcium-Calmodulin-Calcineurin Signaling: A Globally Conserved Virulence Cascade in Eukaryotic Microbial Pathogens. *Cell Host & Microbe*, *26*(4), 453–462. <https://doi.org/10.1016/j.chom.2019.08.004>
- Pavlović, N., & Heindryckx, F. (2021). Targeting ER stress in the hepatic tumor microenvironment. *The FEBS Journal*, febs.16145. <https://doi.org/10.1111/febs.16145>
- Pohl, M., Kaminski, H., Castrop, H., Bader, M., Himmerkus, N., Bleich, M., Bachmann, S., & Theilig, F. (2010). Intrarenal Renin Angiotensin System Revisited. *Journal of Biological Chemistry*, *285*(53), 41935–41946. <https://doi.org/10.1074/jbc.M110.150284>

- Ram, B. M., & Ramakrishna, G. (2014). Endoplasmic reticulum vacuolation and unfolded protein response leading to paraptosis like cell death in cyclosporine A treated cancer cervix cells is mediated by cyclophilin B inhibition. *Biochimica et Biophysica Acta (BBA) - Molecular Cell Research*, *1843*(11), 2497–2512. <https://doi.org/10.1016/j.bbamcr.2014.06.020>
- Ran, F. A., Hsu, P. D., Wright, J., Agarwala, V., Scott, D. A., & Zhang, F. (2013). Genome engineering using the CRISPR-Cas9 system. *Nature Protocols*, *8*(11), 2281–2308. <https://doi.org/10.1038/nprot.2013.143>
- Raymundo, D. P., Doultinos, D., Guillory, X., Carlesso, A., Eriksson, L. A., & Chevet, E. (2020). Pharmacological Targeting of IRE1 in Cancer. *Trends in Cancer*, *6*(12), 1018–1030. <https://doi.org/10.1016/j.trecan.2020.07.006>
- Rusnak, F., & Mertz, P. (2000). Calcineurin: Form and Function. *Physiological Reviews*, *80*(4), 1483–1521. <https://doi.org/10.1152/physrev.2000.80.4.1483>
- Sano, R., & Reed, J. C. (2013). ER stress-induced cell death mechanisms. *Biochimica et Biophysica Acta (BBA) - Molecular Cell Research*, *1833*(12), 3460–3470. <https://doi.org/10.1016/j.bbamcr.2013.06.028>
- Sharma, P., Alizadeh, J., Juarez, M., Samali, A., Halayko, A. J., Kenyon, N. J., Ghavami, S., & Zeki, A. A. (2021). Autophagy, Apoptosis, the Unfolded Protein Response, and Lung Function in Idiopathic Pulmonary Fibrosis. *Cells*, *10*(7), 1642. <https://doi.org/10.3390/cells10071642>
- So, J.-S. (2018). Roles of Endoplasmic Reticulum Stress in Immune Responses. *Molecules and Cells*, *41*(8), 705–716. <https://doi.org/10.14348/molcells.2018.0241>
- Song, J.-L. (2016). Minimizing tacrolimus decreases the risk of new-onset diabetes mellitus after liver transplantation. *World Journal of Gastroenterology*, *22*(6), 2133. <https://doi.org/10.3748/wjg.v22.i6.2133>
- Steiner, J. P., & Haughey, N. J. (2010). Immunophilin Ligands. In *Encyclopedia of Movement Disorders* (pp. 66–68). Elsevier. <https://doi.org/10.1016/B978-0-12-374105-9.00254-9>

- Szegezdi, E., MacDonald, D. C., Ní Chonghaile, T., Gupta, S., & Samali, A. (2009). Bcl-2 family on guard at the ER. *American Journal of Physiology-Cell Physiology*, *296*(5), C941–C953.  
<https://doi.org/10.1152/ajpcell.00612.2008>
- Teske, B. F., Wek, S. A., Bunpo, P., Cundiff, J. K., McClintick, J. N., Anthony, T. G., & Wek, R. C. (2011). The eIF2 kinase PERK and the integrated stress response facilitate activation of ATF6 during endoplasmic reticulum stress. *Molecular Biology of the Cell*, *22*(22), 4390–4405.  
<https://doi.org/10.1091/mbc.e11-06-0510>
- Tricot, L., Lebb??, C., Pillebout, E., Martinez, F., Legendre, C., & Thervet, E. (2005). Tacrolimus-Induced Alopecia in Female Kidney-Pancreas Transplant Recipients: *Transplantation*, *80*(11), 1546–1549.  
<https://doi.org/10.1097/01.tp.0000181195.67084.94>
- Ume, A. C., Wenegieme, T.-Y., & Williams, C. R. (2021). Calcineurin inhibitors: A double-edged sword. *American Journal of Physiology-Renal Physiology*, *320*(3), F336–F341.  
<https://doi.org/10.1152/ajprenal.00262.2020>
- Walczak, A., Gradzik, K., Kabzinski, J., Przybylowska-Sygut, K., & Majsterek, I. (2019). The Role of the ER-Induced UPR Pathway and the Efficacy of Its Inhibitors and Inducers in the Inhibition of Tumor Progression. *Oxidative Medicine and Cellular Longevity*, *2019*, 1–15.  
<https://doi.org/10.1155/2019/5729710>
- Walter, P., & Ron, D. (2011). The unfolded protein response: From stress pathway to homeostatic regulation. *Science (New York, N.Y.)*, *334*(6059), 1081–1086. <https://doi.org/10.1126/science.1209038>
- Wang, B., Lin, L., Wang, H., Guo, H., Gu, Y., & Ding, W. (2016). Overexpressed cyclophilin B suppresses aldosterone-induced proximal tubular cell injury both *in vitro* and *in vivo*. *Oncotarget*, *7*(43), 69309–69320. <https://doi.org/10.18632/oncotarget.12503>
- Wang, P., & Heitman, J. (2005). The cyclophilins. *Genome Biology*, *6*(7), 226. <https://doi.org/10.1186/gb-2005-6-7-226>

- Williams, C. R., & Gooch, J. L. (2012). Calcineurin inhibitors and immunosuppression – a tale of two isoforms. *Expert Reviews in Molecular Medicine*, 14, e14. <https://doi.org/10.1017/erm.2012.8>
- Yilmaz, D. E., Kirschner, K., Demirci, H., Himmerkus, N., Bachmann, S., & Mutig, K. (2022). Immunosuppressive calcineurin inhibitor cyclosporine A induces proapoptotic endoplasmic reticulum stress in renal tubular cells. *Journal of Biological Chemistry*, 298(3), 101589. <https://doi.org/10.1016/j.jbc.2022.101589>

## Statutory Declaration

"I, Duygu Elif, Yilmaz, by personally signing this document in lieu of an oath, hereby affirm that I prepared the submitted dissertation on the topic 'Immunsuppressant cyclosporine A induces endoplasmic reticulum stress and apoptosis in kidney epithelial cells due to suppression of cyclophilin activity / Das Immunsuppressivum Cyclosporin A verursacht Stress im endoplasmatisches Retikulum und Apoptose in Nierenepithelzellen durch Hemmung der Cyclophilinaktivität' independently and without the support of third parties, and that I used no other sources and aids than those stated.

All parts which are based on the publications or presentations of other authors, either in letter or in spirit, are specified as such in accordance with the citing guidelines. The sections on methodology (in particular regarding practical work, laboratory regulations, statistical processing) and results (in particular regarding figures, charts and tables) are exclusively my responsibility.

Furthermore, I declare that I have correctly marked all of the data, the analyses, and the conclusions generated from data obtained in collaboration with other persons, and that I have correctly marked my own contribution and the contributions of other persons (cf. declaration of contribution). I have correctly marked all texts or parts of texts that were generated in collaboration with other persons.

My contributions to any publications to this dissertation correspond to those stated in the below joint declaration made together with the supervisor. All publications created within the scope of the dissertation comply with the guidelines of the ICMJE (International Committee of Medical Journal Editors; <http://www.icmje.org>) on authorship. In addition, I declare that I shall comply with the regulations of Charité – Universitätsmedizin Berlin on ensuring good scientific practice.

I declare that I have not yet submitted this dissertation in identical or similar form to another Faculty.

The significance of this statutory declaration and the consequences of a false statutory declaration under criminal law (Sections 156, 161 of the German Criminal Code) are known to me."

Date

Signature

---

## Declaration of individual contribution to the publication

Duygu Elif Yilmaz contributed the following to the below listed publication:

Publication 1: Yilmaz D. E., Kirschner K., Demirci H., Himmerkus N., Bachmann S., Mutig K, Immunosuppressive calcineurin inhibitor cyclosporine A induces proapoptotic endoplasmic reticulum stress in renal tubular cells, Journal of Biological Chemistry, 2022

Contribution: Duygu Elif Yilmaz is the sole first author. She designed, performed and analyzed the experiments. She prepared all figures (Figure 1-10, Supplemental Figure 1-9) and tables (Table 1-4). Dr. phil. Karin Kirschner generated knockout cells via CRISPR/Cas9 gene editing. Hasan Demirci performed the RT-PCR (Figure 4D-E) and immunoblotting (Figure 5E). Dr. med. Nina Himmerkus isolated and treated the rat proximal tubules. Prof. Dr. Sebastian Bachmann and PD Dr. med. Kerim Mutig conceived and designed the research, provided laboratory resources and funding.

---

Signature, date and stamp of first supervising university professor / lecturer

---

Signature of doctoral candidate

## Excerpt from Journal Summary List

Journal Data Filtered By: **Selected JCR Year: 2021** Selected Editions: SCIE,SSCI  
 Selected Categories: "**BIOCHEMISTRY and MOLECULAR BIOLOGY**" Selected  
 Category Scheme: WoS

**Gesamtanzahl: 296 Journale**

Rank	Full Journal Title	Total Cites	Journal Impact Factor	Eigenfaktor
1	NATURE MEDICINE	141,857	87.241	0.23255
2	CELL	362,236	66.850	0.53397
3	Molecular Cancer	32,250	41.444	0.03386
4	Signal Transduction and Targeted Therapy	11,026	38.104	0.01781
5	Annual Review of Biochemistry	25,139	27.258	0.01962
6	Molecular Plant	20,242	21.949	0.02339
7	MOLECULAR CELL	94,258	19.328	0.13937
8	NUCLEIC ACIDS RESEARCH	284,490	19.160	0.33755
9	NATURE STRUCTURAL & MOLECULAR BIOLOGY	33,999	18.361	0.04689
10	TRENDS IN MICROBIOLOGY	19,957	18.230	0.02015
11	CYTOKINE & GROWTH FACTOR REVIEWS	9,002	17.660	0.00625
12	MOLECULAR ASPECTS OF MEDICINE	8,986	16.337	0.00615
13	Nature Chemical Biology	31,125	16.174	0.04456
14	TRENDS IN MOLECULAR MEDICINE	14,585	15.272	0.01381
15	NATURAL PRODUCT REPORTS	14,564	15.111	0.01079
16	PROGRESS IN LIPID RESEARCH	7,982	14.673	0.00444
17	TRENDS IN BIOCHEMICAL SCIENCES	22,957	14.264	0.02170
18	EMBO JOURNAL	80,536	14.012	0.05438
19	MOLECULAR PSYCHIATRY	33,324	13.437	0.04914
20	Molecular Systems Biology	11,036	13.068	0.01483
21	EXPERIMENTAL AND MOLECULAR MEDICINE	12,199	12.153	0.01698

Rank	Full Journal Title	Total Cites	Journal Impact Factor	Eigenfaktor
22	PLANT CELL	67,319	12.085	0.02964
23	CELL DEATH AND DIFFERENTIATION	31,035	12.067	0.02639
24	BIOCHIMICA ET BIOPHYSICA ACTA-REVIEWS ON CANCER	8,255	11.414	0.00673
25	Cell Systems	8,047	11.091	0.03332
26	CURRENT BIOLOGY	85,124	10.900	0.10641
27	Redox Biology	20,557	10.787	0.02390
28	International Journal of Biological Sciences	14,100	10.750	0.01488
29	MATRIX BIOLOGY	9,415	10.447	0.00856
30	PLOS BIOLOGY	44,888	9.593	0.05920
31	Cell and Bioscience	4,564	9.584	0.00524
32	Science Signaling	17,426	9.517	0.02046
33	GENOME RESEARCH	51,169	9.438	0.05153
34	CELLULAR AND MOLECULAR LIFE SCIENCES	38,745	9.207	0.03204
35	Journal of Integrative Plant Biology	8,456	9.106	0.00730
36	EMBO REPORTS	21,705	9.071	0.02695
37	Cell Chemical Biology	6,651	9.039	0.01870
38	CURRENT OPINION IN CHEMICAL BIOLOGY	12,464	8.972	0.01277
39	MOLECULAR BIOLOGY AND EVOLUTION	67,311	8.800	0.07228
40	ONCOGENE	81,646	8.756	0.05014
41	CELLULAR & MOLECULAR BIOLOGY LETTERS	2,684	8.702	0.00250
42	CRITICAL REVIEWS IN BIOCHEMISTRY AND MOLECULAR BIOLOGY	5,108	8.697	0.00477
43	Molecular Ecology Resources	15,145	8.678	0.01553

Rank	Full Journal Title	Total Cites	Journal Impact Factor	Eigenfaktor
44	Plant Communications	743	8.625	0.00148
45	FREE RADICAL BIOLOGY AND MEDICINE	55,523	8.101	0.02824
46	INTERNATIONAL JOURNAL OF BIOLOGICAL MACROMOLECULES	112,372	8.025	0.09445
47	Biomedical Journal	2,388	7.892	0.00301
48	CURRENT OPINION IN STRUCTURAL BIOLOGY	13,407	7.786	0.01689
49	AMERICAN JOURNAL OF RESPIRATORY CELL AND MOLECULAR BIOLOGY	16,259	7.748	0.01386
50	Antioxidants	21,453	7.675	0.01946
51	EXPERT REVIEWS IN MOLECULAR MEDICINE	2,282	7.615	0.00062
52	Reviews of Physiology Biochemistry and Pharmacology	920	7.500	0.00043
53	ANTIOXIDANTS & REDOX SIGNALING	29,117	7.468	0.01390
54	Essays in Biochemistry	4,569	7.258	0.00691
55	Genes & Diseases	2,732	7.243	0.00322
56	Open Biology	5,227	7.124	0.00994
57	PROTEIN SCIENCE	18,673	6.993	0.02822
58	BIOMACROMOLECULES	46,963	6.978	0.02347
59	JOURNAL OF PHOTOCHEMISTRY AND PHOTOBIOLOGY B- BIOLOGY	18,610	6.814	0.01229
60	JOURNAL OF LIPID RESEARCH	29,128	6.676	0.01485
61	BIOCHIMICA ET BIOPHYSICA ACTA- MOLECULAR BASIS OF DISEASE	22,719	6.633	0.01820
62	MOLECULAR ECOLOGY	45,664	6.622	0.03311
63	AMYLOID-JOURNAL OF PROTEIN FOLDING DISORDERS	2,335	6.571	0.00312

Rank	Full Journal Title	Total Cites	Journal Impact Factor	Eigenfaktor
64	BIOFACTORS	5,614	6.438	0.00307
65	International Review of Cell and Molecular Biology	3,388	6.420	0.00314
66	MOLECULAR MEDICINE	7,039	6.376	0.00402
67	Food & Function	27,282	6.317	0.02290
68	Biochimica et Biophysica Acta-Genes Regulatory Mechanisms	8,926	6.304	0.00707
69	INTERNATIONAL JOURNAL OF MOLECULAR SCIENCES	211,517	6.208	0.24907
70	Computational and Structural Biotechnology Journal	6,436	6.155	0.00945
71	JOURNAL OF MOLECULAR BIOLOGY	66,672	6.151	0.03581
72	JOURNAL OF NUTRITIONAL BIOCHEMISTRY	15,277	6.117	0.00837
73	Frontiers in Molecular Biosciences	6,864	6.113	0.01068
74	BIOCONJUGATE CHEMISTRY	19,624	6.069	0.01508
75	Biomolecules	21,742	6.064	0.02602
76	GLYCOBIOLOGY	10,212	5.954	0.00650
77	STRUCTURE	17,734	5.871	0.01779
78	MACROMOLECULAR BIOSCIENCE	9,240	5.859	0.00565
79	FASEB JOURNAL	59,831	5.834	0.04452
80	ACS Chemical Neuroscience	12,168	5.780	0.01655
81	BIOELECTROCHEMISTRY	7,093	5.760	0.00463
82	JOURNAL OF ENZYME INHIBITION AND MEDICINAL CHEMISTRY	8,156	5.756	0.00580
83	Journal of Genetics and Genomics	3,129	5.723	0.00327
84	Acta Crystallographica Section D-Structural Biology	23,006	5.699	0.02041
85	REDOX REPORT	2,247	5.696	0.00082

Rank	Full Journal Title	Total Cites	Journal Impact Factor	Eigenfaktor
86	INTERNATIONAL JOURNAL OF BIOCHEMISTRY & CELL BIOLOGY	19,580	5.652	0.00820
87	RNA	16,041	5.636	0.01565
88	FEBS Journal	26,220	5.622	0.02110
89	JOURNAL OF LIPOSOME RESEARCH	1,990	5.586	0.00101
90	Metabolites	7,235	5.581	0.00987
91	APOPTOSIS	7,640	5.561	0.00338
92	Journal of Zhejiang University-SCIENCE B	4,436	5.552	0.00286
93	JOURNAL OF NEUROCHEMISTRY	40,901	5.546	0.01646
94	JOURNAL OF BIOLOGICAL CHEMISTRY	392,757	5.486	0.11856
95	Advances in Protein Chemistry and Structural Biology	1,457	5.447	0.00149
96	PROTEOMICS	15,944	5.393	0.00932
97	PLANT SCIENCE	22,434	5.363	0.01106
98	EUROPEAN JOURNAL OF HUMAN GENETICS	13,788	5.351	0.01710
99	BIOORGANIC CHEMISTRY	15,864	5.307	0.01521
100	JOURNAL OF BIOMOLECULAR STRUCTURE & DYNAMICS	12,828	5.235	0.01268
101	BIOCHIMICA ET BIOPHYSICA ACTA- MOLECULAR AND CELL BIOLOGY OF LIPIDS	13,646	5.228	0.00952
102	CHEMICO-BIOLOGICAL INTERACTIONS	17,307	5.168	0.00980
103	MOLECULAR CARCINOGENESIS	7,727	5.139	0.00622
104	HUMAN MOLECULAR GENETICS	47,419	5.121	0.03599
105	MedChemComm	5,715	5.121	0.00536
106	JOURNAL OF PHYSIOLOGY AND BIOCHEMISTRY	2,605	5.080	0.00192

# Printing copy(s) of the publication(s)

## JBC RESEARCH ARTICLE



# Immunosuppressive calcineurin inhibitor cyclosporine A induces proapoptotic endoplasmic reticulum stress in renal tubular cells

Received for publication, July 18, 2021, and in revised form, January 3, 2022. Published, Papers in Press, January 14, 2022.  
<https://doi.org/10.1016/j.jbc.2022.101589>

Duygu Elif Yilmaz<sup>1</sup>, Karin Kirschner<sup>2</sup>, Hasan Demirci<sup>1</sup>, Nina Himmerkus<sup>3</sup>, Sebastian Bachmann<sup>1</sup>, and Kerim Mutig<sup>2,4\*</sup>

From the <sup>1</sup>Institute of Functional Anatomy, and <sup>2</sup>Institute of Vegetative Physiology, Charité-Universitätsmedizin Berlin, Berlin, Germany; <sup>3</sup>Institute of Physiology, Christian-Albrecht-University Kiel, Kiel, Germany; <sup>4</sup>Department of Pharmacology, I.M. Sechenov First Moscow State Medical University of the Ministry of Healthcare of the Russian Federation (Sechenov University), Moscow, Russia

Edited by Ronald Wek

Current immunosuppressive strategies in organ transplantation rely on calcineurin inhibitors cyclosporine A (CsA) or tacrolimus (Tac). Both drugs are nephrotoxic, but CsA has been associated with greater renal damage than Tac. CsA inhibits calcineurin by forming complexes with cyclophilins, whose chaperone function is essential for proteostasis. We hypothesized that stronger toxicity of CsA may be related to suppression of cyclophilins with ensuing endoplasmic reticulum (ER) stress and unfolded protein response (UPR) in kidney epithelia. Effects of CsA and Tac (10  $\mu$ M for 6 h each) were compared in cultured human embryonic kidney 293 (HEK 293) cells, primary human renal proximal tubule (PT) cells, freshly isolated rat PTs, and knockout HEK 293 cell lines lacking the critical ER stress sensors, protein kinase RNA-like ER kinase or activating transcription factor 6 (ATF6). UPR was evaluated by detection of its key components. Compared with Tac treatment, CsA induced significantly stronger UPR in native cultured cells and isolated PTs. Evaluation of proapoptotic and antiapoptotic markers suggested an enhanced apoptotic rate in CsA-treated cells compared with Tac-treated cells as well. Similar to CsA treatment, knockdown of cyclophilin A or B by siRNA caused proapoptotic UPR, whereas application of the chemical chaperones tauroursodeoxycholic acid or 4-phenylbutyric acid alleviated CsA-induced UPR. Deletion of protein kinase RNA-like ER kinase or ATF6 blunted CsA-induced UPR as well. In summary, inhibition of cyclophilin chaperone function with ensuing ER stress and proapoptotic UPR aggravates CsA toxicity, whereas pharmacological modulation of UPR bears potential to alleviate renal side effects of CsA.

consisting of a catalytic subunit (CnA), a regulatory subunit (CnB), and calmodulin, which functions as a  $Ca^{2+}$ -dependent protein serine/threonine phosphatase. Alpha and beta isoforms of the catalytic subunit (CnA $\alpha$  and CnA $\beta$ ) fulfill distinct and nonredundant tasks in various tissues (1, 3). CnA $\beta$ -dependent dephosphorylation of nuclear factor of activated T-cell (NFAT) transcription factors is critical to T-lymphocyte activation and underlies the therapeutic action of CNI (4). Off-target effects of CNI include renal complications because of suppression of CnA $\alpha$  activity in kidney tissue (5, 6). A majority of organ-transplanted patients receiving CNI exhibit signs of kidney damage after several years of treatment (6). CNI-induced renal vasoconstriction, hyperactivity of the renin-angiotensin system (RAS), and dysregulation of major electrolyte transport systems cause hypertension and homeostasis disorders (6, 7). At the cellular level, CNIs have been shown to induce endoplasmic reticulum (ER) stress and trigger unfolded protein response (UPR), which in turn may promote apoptosis of kidney epithelia (8, 9).

Several retrospective studies suggested that CsA may be associated with stronger nephrotoxicity than Tac (10–14). Along the same line, a recent experimental study in cultured human cells demonstrated higher toxicity of CsA compared with Tac (15). The two CNIs inhibit Cn activity by forming complexes with distinct members of the immunophilin family: CsA binds to cyclophilins, whereas Tac interacts with 12 kDa FK506-binding protein (FKBP12). These individual interaction patterns may provide a reasonable explanation for distinct toxicity profiles of CsA *versus* Tac. Since the chaperone activity of cyclophilins is required for protein maturation, CsA may impair proteostasis (Fig. 1) (16, 17). Indeed, studies of CsA *versus* Tac in cell culture showed substantially stronger association of CsA with ER stress and UPR, but the role of cyclophilins herein remained to be elucidated (15, 18). UPR is a complex signal transduction pathway that is triggered by pathophysiological alterations of proteostasis leading to accumulation of misfolded protein (19, 20). Misfolded protein releases inositol-requiring protein 1 (IRE1 $\alpha$ ), protein kinase RNA-like ER kinase (PERK), and activating

Calcineurin (Cn) inhibitors (CNIs) are considered as the first-line immunosuppressive therapy in patients undergoing organ transplantation (1, 2). Two drugs of this class, cyclosporine A (CsA) and tacrolimus (FK506, Tac), have been widely integrated into clinical practice. Cn is a holoenzyme

\* For correspondence: Kerim Mutig, [kerim.mutig@charite.de](mailto:kerim.mutig@charite.de).



## Cyclosporine A induces ER stress in kidney epithelia

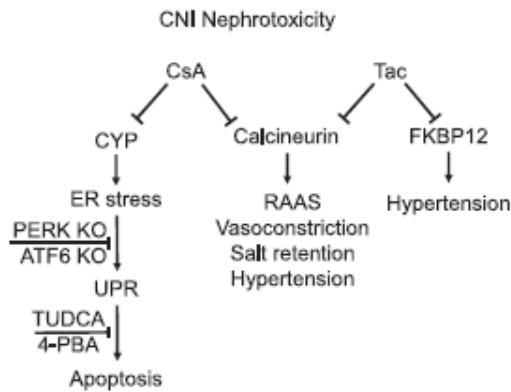


**Figure 1. Potential mechanisms mediating distinct nephrotoxicity of cyclosporine A (CsA) versus tacrolimus (Tac).** Schematic drawing illustrates common versus distinct pathogenetic mechanisms mediating nephrotoxic effects of CsA versus Tac. Both calcineurin inhibitors (CNIs) may lead to hyperactivity of renin-angiotensin-aldosterone system (RAAS), vasoconstriction, renal salt retention, and hypertension because of inhibition of the phosphatase activity of calcineurin (7, 54–56). In addition, CsA causes endoplasmic reticulum (ER) stress and proapoptotic unfolded protein response (UPR) because of suppression of chaperone function of cyclophilins (CYP; present study), whereas inhibition of FKBP12 by Tac may aggravate hypertension (57). Chemical chaperones (TUDCA or 4-PBA) alleviate the CsA-induced ER stress likely because of improved protein folding. Deletion of PERK (PERK KO) or ATF6 (ATF6 KO) blunted the CsA-induced proapoptotic UPR, suggesting that pharmacological modulation of these signaling pathways may improve cell survival. 4-PBA, 4-phenylbutyric acid; ATF6, activating transcription factor 6; TUDCA, tauroursodeoxycholic acid.

transcription factor 6 (ATF6) from their complexes with binding immunoglobulin protein (BiP) by competitive interactions with the latter. IRE1 $\alpha$ , PERK, and ATF6 serve as ER-stress sensors and initiate a number of adaptive reactions promoting cell survival. PERK phosphorylates and deactivates the eukaryotic translation initiation factor 2 $\alpha$ , thereby inhibiting protein translation. Parallel activation of IRE1 $\alpha$  and ATF6 stimulates autophagy and accelerates protein folding *via* several signaling pathways, such as transcription and splicing of X-box binding protein 1 (XBP1) (19). Failure of these adaptive mechanisms triggers the proapoptotic UPR branch *via* stimulation of the C/EBP homologous protein (CHOP), which is a transcription factor that induces expression of proapoptotic genes (9, 21, 22). Interestingly, Cn itself has been implicated in adaptive UPR signaling, enabling long-term cell survival upon ER stress (23). Therefore, Cn inhibition may impair the ability of kidney epithelia to compensate for metabolic stress. Pharmacological targeting of UPR using chemical chaperones, inhibitors of translation, or autophagy enhancers has been considered as an emerging strategy to delay progression of chronic kidney disorders (9). In this context, improved understanding of UPR-related molecular pathways affected by CNI may deliver new options for managing their nephrotoxicity.

The present study addresses mechanisms underlying distinct toxicity profiles of CsA versus Tac with a focus on ER stress and UPR. Based on comparative analysis of CsA and Tac in cultured human embryonic kidney 293 (HEK 293) cells, primary human renal proximal tubular (PT) epithelial cells

(HRPTEpCs), and freshly isolated rat PTs, we provide several lines of evidence in support of the hypothesis that the more pronounced toxic effects of CsA on proteostasis are rooted in the suppression of cyclophilin chaperone activity. Using genetic and pharmacological approaches, we show that targeting UPR bears therapeutic potential for alleviation of CsA nephrotoxicity.

## Results

### Establishing CNI treatment protocols

First, we aimed to define the optimal CNI concentrations and treatment duration to set up a protocol permitting comparative analysis of their effects on ER and UPR in human cervical cancer (HeLa) and human lung carcinoma (A549) cells after application of 10  $\mu$ M CsA for 6 h (15). Based on that protocol, we performed a dose–response analysis by treating native HEK 293 cells with increasing doses of CsA versus Tac (5–80  $\mu$ M each) for 6 h to evaluate the effects on cell viability using the 3-(4,5-dimethylthiazol-2-yl)-2,5-diphenyltetrazolium bromide (MTT) assay (24). A substantial decrease of cell viability below 50% was observed starting with 20  $\mu$ M CsA or 40  $\mu$ M Tac (Fig. 2A), which we defined as limitation precluding evaluation of ER stress and UPR because of the critical reduction of living cell mass. Since CsA has been reported to induce striking morphological changes such as cytoplasmic vacuolization (16, 25), we also compared effects of CsA versus Tac (10  $\mu$ M each) on cell morphology by light and electron microscopy. Ultrastructural analysis revealed no obvious morphological alterations after application of CsA or Tac for 6 h, whereas prolonged treatment for 24 h resulted in formation of cytoplasmic vacuoles in CsA-treated but not in Tac-treated cells (Fig. 2, B–G). Moreover, treatment of cells with CsA for 48 h resulted in a marked reduction of cell confluence compared with Tac or vehicle, as detected by light microscopy (Fig. S1). From these preliminary experiments, we concluded that the previously published treatment protocol for human cancer cells (10  $\mu$ M CsA versus 10  $\mu$ M Tac for 6 h) is applicable for our experimental settings (15), whereas increased CNI doses or treatment duration critically reduce the cell viability. Therefore, further experiments in HEK 293 cells, primary HRPTEpC, and microdissected rat PTs were performed using 10  $\mu$ M CsA versus 10  $\mu$ M Tac for 6 h.

To verify the equivalent efficacy of the chosen treatment protocols in terms of Cn inhibition, we evaluated phosphorylation of the established Cn substrate, NFAT (3). Immunoblotting using an antibody to phosphorylated NFAT showed comparable increases of phospho-NFAT levels in lysates from CsA-treated or Tac-treated HEK 293 cells suggesting that both CNIs attenuated Cn-dependent NFAT dephosphorylation to a comparable extent when applied at 10  $\mu$ M concentrations for 6 h (Fig. S2).

### CsA induces stronger ER stress and UPR than Tac

Next, we compared effects of CsA versus Tac on key UPR proteins using thapsigargin (Tg 0.1  $\mu$ M), an established

## Cyclosporine A induces ER stress in kidney epithelia

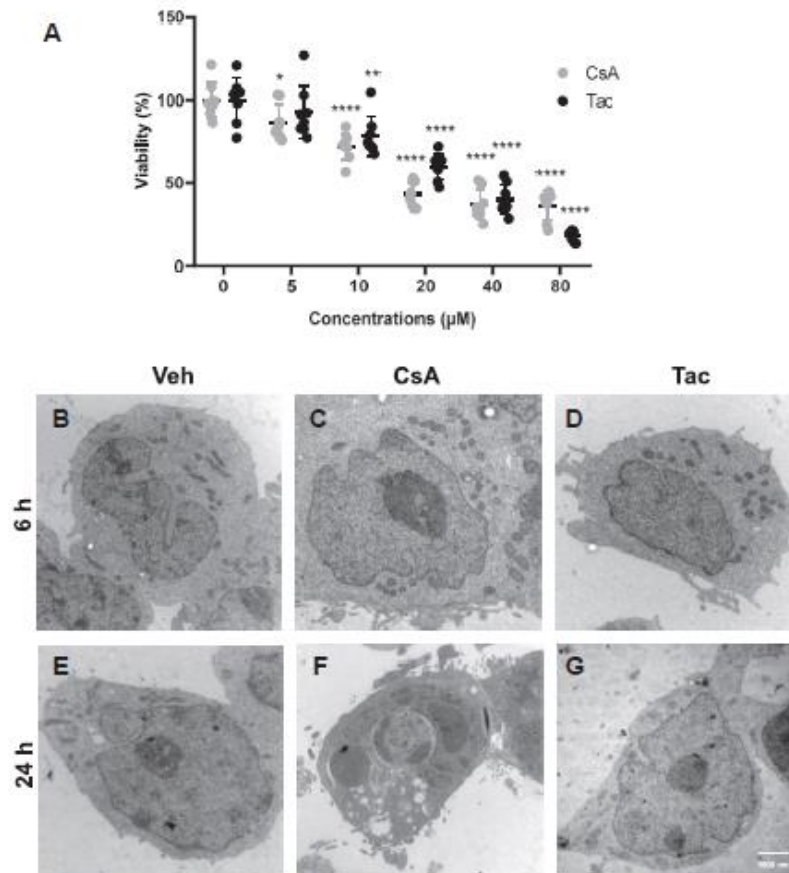


**Figure 2. Effects of cyclosporine A (CsA) and tacrolimus (Tac) on cell survival and morphology.** A, diagram shows results of viability assay using 3-(4,5-dimethylthiazol-2-yl)-2,5-diphenyltetrazolium bromide. HEK 293 cells were treated with increasing concentrations of CsA or Tac (5–80  $\mu\text{M}$ ) for 6 h. No or moderate effects on cell viability were observed with CsA or Tac doses of 5 or 10  $\mu\text{M}$ , whereas higher doses substantially decreased the cell viability. B–D, representative electron microscopic images of unmodified HEK 293 cells treated with vehicle (Veh), CsA (10  $\mu\text{M}$ ), or Tac (10  $\mu\text{M}$ ) for 6 h show largely preserved cell morphology at the applied doses and treatment duration. E–G, treatment of HEK 293 cells with CsA (10  $\mu\text{M}$  for 24 h) induced cytoplasmic vacuolization, whereas Tac (10  $\mu\text{M}$  for 24 h) produced no obvious morphological alterations compared with vehicle. N = three independent experiments. Data are the means  $\pm$  SD, \* $p$  < 0.05, \*\* $p$  < 0.01, \*\*\* $p$  < 0.001, \*\*\*\* $p$  < 0.0001. HEK 293, human embryonic kidney 293 cell line.

ER-stress and UPR inducer (26, 27), as positive control for these experiments. Compared with vehicle, CsA significantly increased levels of CHOP, spliced (s) XBP1, and phosphorylated (p) but not total IRE1 $\alpha$  as detected by immunoblotting (+227%,  $p$  < 0.001 for CHOP; +223%,  $p$  < 0.001 for sXBP1; and +230%,  $p$  < 0.01 for p-IRE1 $\alpha$ ; Fig. 3, A–E). Parallel quantitative PCR (qPCR) analysis revealed increased expression of the ER chaperone, BiP (+348%,  $p$  < 0.01), CHOP (+751%,  $p$  < 0.05), and sXBP1 (+2142%,  $p$  < 0.05) in response to CsA (Fig. S3). Similar changes were detected in lysates from Tg-treated cells, whereas Tac produced no significant effects on the tested UPR products (Figs. 3, A–E and S3). Next, we evaluated nuclear abundance of CHOP using immunofluorescence. Compared with vehicle, CsA and Tg induced significant increases of CHOP signal intensities in the 4',6'-diamidino-2-phenylindole (DAPI)-positive nuclear regions (CsA: +235%,  $p$  < 0.0001; Tg: +137%,  $p$  < 0.001),

whereas Tac did not alter the nuclear CHOP levels (Fig. S4, A–C). To follow up the downstream effects of CHOP activation, we evaluated the survival-promoting B-cell lymphoma protein-2 (BCL-2) as well as the proapoptotic products, BCL-2-associated X protein (Bax) and cleaved caspase-3 (cCas-3) (28). Immunoblotting analysis showed that CsA and Tg strongly decreased BCL-2 levels (CsA: –76%,  $p$  < 0.05; Tg: –58%,  $p$  < 0.01) and increased Bax abundance (CsA: +218%,  $p$  < 0.0001; Tg: +234%,  $p$  < 0.01), whereas Tac did not affect the BCL-2 abundance and only moderately increased the Bax levels (Tac: +168%,  $p$  < 0.05; Fig. 3, A and G). Immunofluorescence labeling of cCas-3 showed significant numerical increases of cCas-3-positive cells after CsA and Tg but not Tac treatments (Fig. S5, A–C). Together, these results demonstrate that, compared with Tac, CsA induces significantly stronger ER stress and proapoptotic UPR in cultured HEK 293 cells.

### Cyclosporine A induces ER stress in kidney epithelia

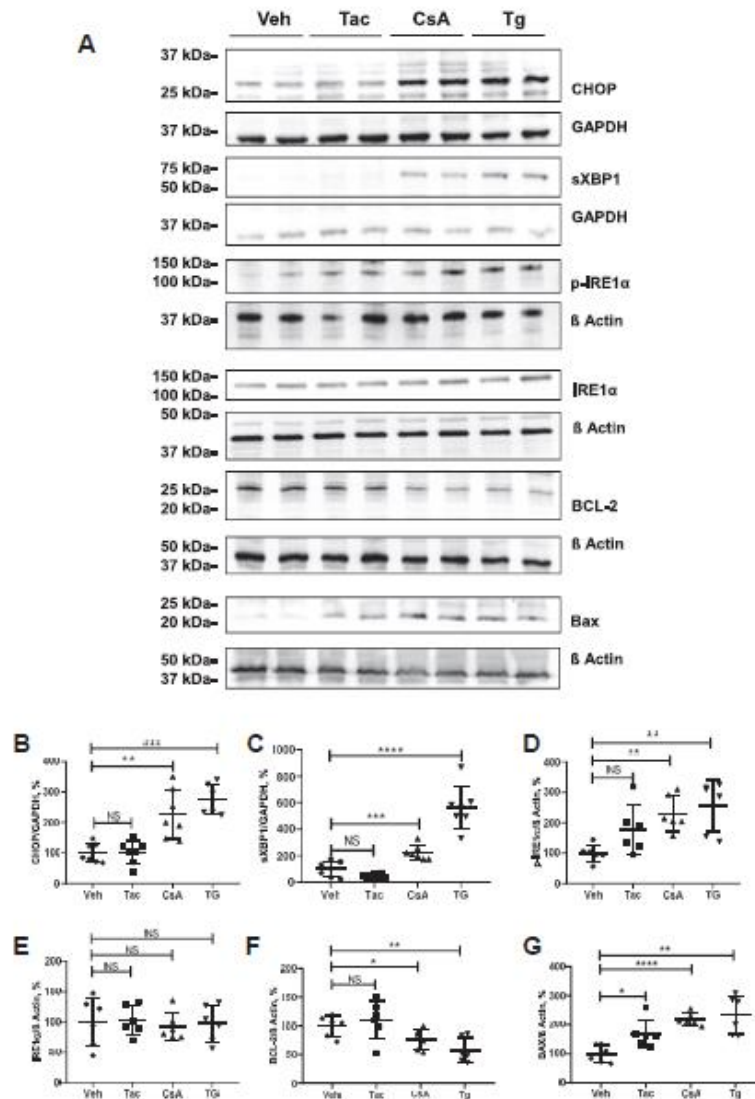


**Figure 3.** Effects of cyclosporine A (CsA), tacrolimus (Tac), and thapsigargin (Tg) on the key products of the unfolded protein response in HEK 293 cells. A, representative immunoblots showing signals for CHOP (approximately 27 kDa), spliced XBP1 (sXBP1; approximately 56 kDa), IRE1α and phosphorylated (p) IRE1α (approximately 110 kDa), BCL-2 (approximately 26 kDa), and Bax (approximately 20 kDa) in lysates from unmodified HEK 293 cells treated with vehicle (Veh), Tac (10 μM), CsA (10 μM), or Tg (0.1 μM) for 6 h. B–G, graphs showing densitometric evaluation of CHOP (B), sXBP1 (C), p-IRE1α (D), IRE1α (E), BCL-2 (F), and Bax (G). GAPDH or β-actin served as loading controls (approximately 37 and 42 kDa, respectively) and are shown below the respective immunoblots. N = three independent experiments with three technical replicates each. Data are the means ± SD, \* $p < 0.05$ , \*\* $p < 0.01$ , \*\*\* $p < 0.001$ , \*\*\*\* $p < 0.0001$ , NS, Bax, BCL-2-associated X protein; BCL-2, B-cell lymphoma protein-2; CHOP, C/EBP homologous protein; HEK 293, human embryonic kidney 293 cell line; IRE1, inositol-requiring protein 1; NS, not significant; XBP1, X-box binding protein 1.

#### CsA but not Tac induces ER stress and UPR in primary HRPTEpC and rat PTs

To corroborate the data obtained in HEK 293 cells in models with more differentiated kidney epithelial phenotype, we next treated HRPTEpCs and isolated rat PTs with either CNI or Tg. Similar to the results obtained in HEK 293 cells, CsA induced significantly stronger UPR compared with Tac in

HRPTEpCs, as detected by qPCR analysis of BiP (CsA: +233%,  $p < 0.0001$ ; Tac: +135%,  $p < 0.01$ ; and Tg: +1220%,  $p < 0.001$ ), sXBP1 (CsA: +288%,  $p < 0.0001$ ; Tac: +122%, not significant [ns]; and Tg: +1196,  $p < 0.001$ ), and CHOP (CsA: +278%,  $p < 0.01$ ; Tac: +113, ns; and Tg: +3589,  $p < 0.0001$ ; Fig. 4A), as well as by immunoblotting for sXBP1 (CsA: +188%,  $p < 0.01$ ; Tac: 100%, ns; and Tg: +309%,  $p < 0.0001$ ; Fig. 4, B and C).

### Cyclosporine A induces ER stress in kidney epithelia

Along the same line, expression levels of BiP and CHOP were significantly higher in isolated rat PTs treated with CsA (BiP: +234%,  $p < 0.05$ ; CHOP: +366%,  $p < 0.05$ ), than in the Tac group (BiP: +184%, ns; CHOP: +139%, ns; Fig. 4, D and E).

#### Knockdown of cyclophilins induces UPR

Since CsA but not Tac induced UPR, we assumed that this discrepancy may result from CsA-dependent suppression of cyclophilins rather than from Cn inhibition. Therefore, we separately suppressed cyclophilin A (CYPA) or cyclophilin B (CYPB) expression in HEK 293 cells using siRNA-mediated knockdown protocols. These protocols led to similar

decreases of CYPA or CYPB protein levels (-53% and -57%, respectively,  $p < 0.0001$ ; Fig. 5, A-D). Evaluation of CHOP abundance by immunoblotting revealed significantly increased levels in both CYPA-knockdown (CYPA-kd) cells (+247%,  $p < 0.0001$ ) and CYPB-knockdown (CYPB-kd) cells (+364%,  $p < 0.0001$ ; Fig. 5, E and F). In line with this, immunoblotting for cCas-3 showed increased immunoreactive signals in CYPA-kd cells (+284%,  $p < 0.001$ ) and CYPB-kd cells (+327%,  $p < 0.01$ ; Fig. 5, E and G). Notably, effects of CYPA-kd and CYPB-kd cells on CHOP and cCas-3 were largely comparable to effects of CsA in unmodified cells (Figs. 3, A and B and 5, E-G) suggesting a critical role of

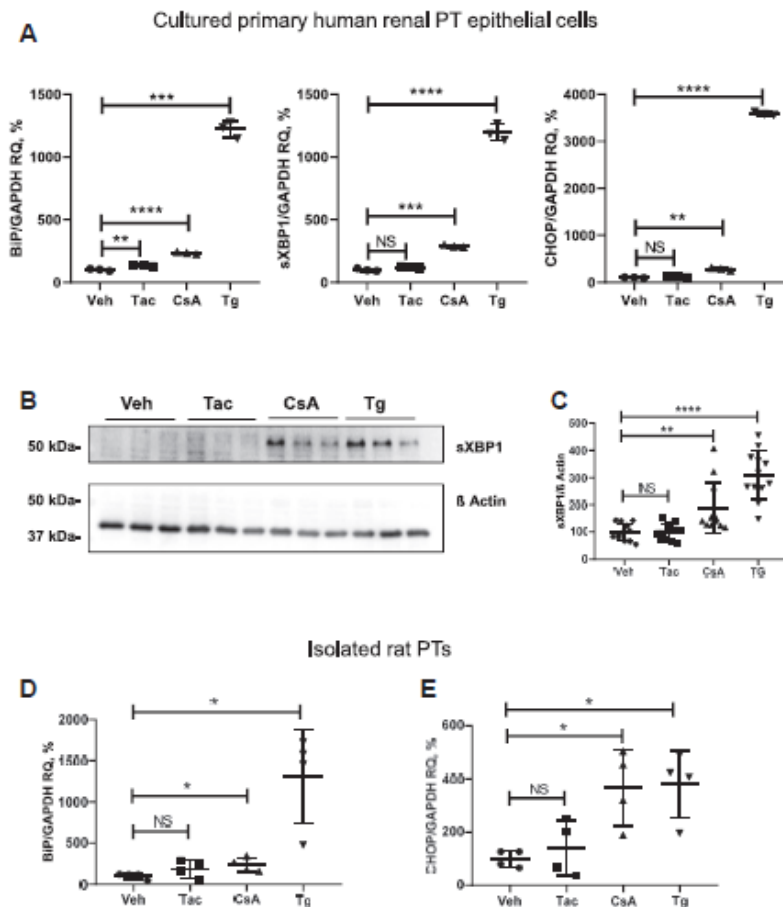


**Figure 4.** Effects of cyclosporine A (CsA), tacrolimus (Tac), and thapsigargin (Tg) on the key products of the unfolded protein response in HRPTEpC cells and isolated rat PTs, as detected by quantitative PCR and immunoblotting. **A**, graphs show mRNA levels of BiP, sXBP1, and CHOP in lysates from HRPTEpCs treated with vehicle, Tac (10  $\mu$ M), CsA (10  $\mu$ M), or Tg (0.1  $\mu$ M) for 6 h. Values obtained in the vehicle-treated cells were set at 100%; GAPDH expression levels were used for normalization of the data. **B**, representative immunoblot showing signals for spliced XBP1 (sXBP1; approximately 56 kDa) in lysates from HRPTEpCs treated with vehicle (Veh), Tac (10  $\mu$ M), CsA (10  $\mu$ M), or Tg (0.1  $\mu$ M) for 6 h.  $\beta$ -actin served as loading controls (approximately 42 kDa). **C**, densitometric evaluation of sXBP1 and signals normalized to loading control; N = three independent experiments with three biological replicates each. **D** and **E**, graphs show mRNA levels of BiP and CHOP in lysates from isolated rat PT cells treated with vehicle, Tac (10  $\mu$ M), CsA (10  $\mu$ M), or Tg (0.1  $\mu$ M) for 6 h. Values obtained in the vehicle-treated cells were set at 100%; GAPDH expression levels were used for normalization of the data. N = four independent experiments. Data are the means  $\pm$  SD, \* $p < 0.05$ , \*\* $p < 0.01$ , \*\*\* $p < 0.001$ , \*\*\*\* $p < 0.0001$ , NS, BiP, binding immunoglobulin protein; CHOP, C/EBP homologous protein; HRPTEpC, human renal proximal tubular epithelial cell; NS, not significant; PT, proximal tubule; sXBP1, spliced X-box binding protein 1.

## Cyclosporine A induces ER stress in kidney epithelia

suppressed cyclophilin activity in the CsA-induced ER stress and UPR.

### Chemical chaperones alleviate CsA-induced ER stress

Next, we tested the potential of the chemical chaperones, tauroursodeoxycholic acid (TUDCA; 300  $\mu$ M) or 4-phenylbutyric acid (4-PBA; 5  $\mu$ M), to alleviate the CsA-induced ER stress. The CsA-induced increases of CHOP

protein abundance were significantly blunted by concomitant application of TUDCA (from +625% [CsA] to +274% [CsA + TUDCA],  $p < 0.001$ ; Fig. 6A) or 4-PBA (from +712% [CsA] to +238% [CsA + 4-PBA],  $p < 0.0001$ ; Fig. 6B). Similarly, the CsA-induced increases of cCas-3-positive cells were blunted by both TUDCA and 4-PBA (from +697% [CsA] to +419% [CsA + TUDCA] or +388% [CsA + 4-PBA],  $p < 0.05$ ; Fig. 7, A–C), as detected by immunofluorescence.

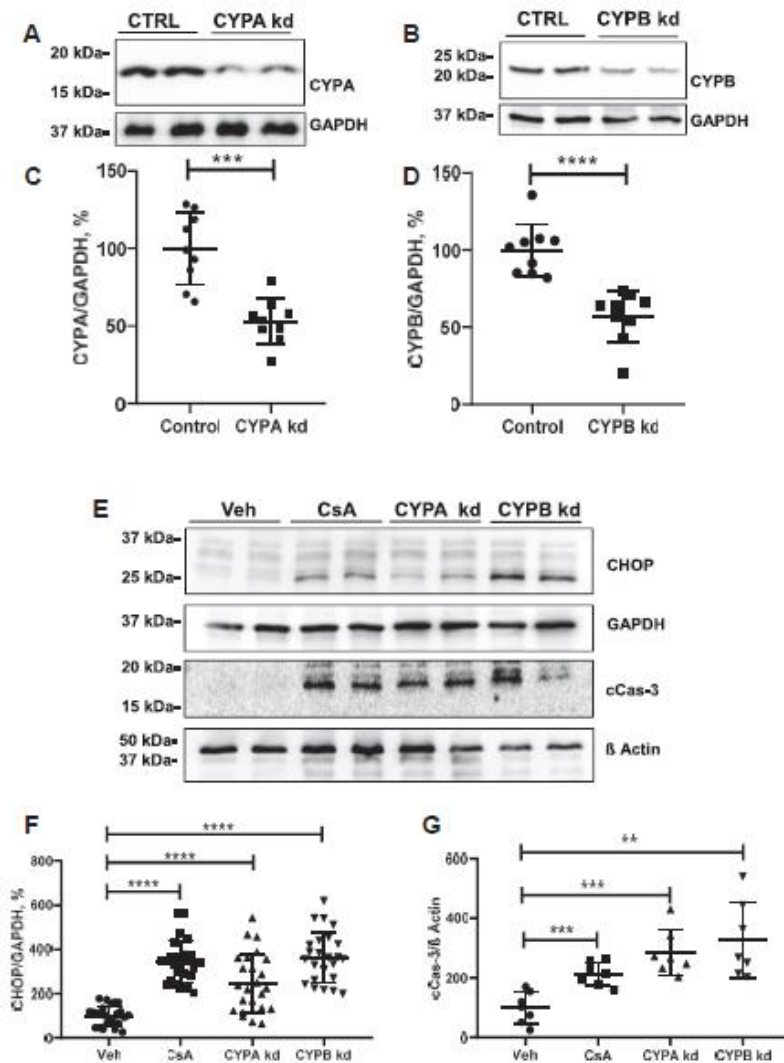


**Figure 5.** Effects of suppressed cyclophilin abundance on CHOP and cCas-3 expression in HEK 293 cells. A–D, representative immunoblots to verify siRNA-mediated knockdowns (kds) of cyclophilin A (CYPA, approximately 18 kDa; A) or cyclophilin B (CYPB, approximately 21 kDa; B) in HEK 293 cells; GAPDH detection serves as a loading control. Densitometric evaluation of signals is provided below the respective blots (C and D). E, representative immunoblots show significant increases of CHOP (approximately 27 kDa) and cCas-3 levels (approximately 19 kDa) in CYPA and CYPB kd cells as well as in normal cells treated with cyclosporine A (CsA; 10  $\mu$ M for 6 h) for positive control. GAPDH detection served as loading control (approximately 37 kDa). F and G, densitometric evaluation of CHOP and cCas-3 signals normalized to loading control. N = at least three independent experiments. Data are the means  $\pm$  SD, \* $p < 0.05$ , \*\* $p < 0.01$ , and \*\*\* $p < 0.001$ . cCas-3, cleaved caspase-3; CHOP, C/EBP homologous protein; HEK 293, human embryonic kidney 293 cell line.

### Cyclosporine A induces ER stress in kidney epithelia

#### Deletion of PERK or ATF6 attenuates the CsA-induced UPR

Next, we aimed at characterization of UPR pathways mediating the proapoptotic effects of CsA. To this end, we applied CRISPR/Cas9 gene editing for inactivation of critical ER-stress sensors and UPR initiators, IRE1 $\alpha$ , PERK, or ATF6, in HEK 293 cells. While we succeeded in generation of PERK-deficient or ATF6-deficient cell lines (Fig. S6), attempts to delete IRE1 $\alpha$  failed to produce viable cell colonies suggesting a critical role for this protein in cell metabolism. PERK-KO and ATF6-KO exerted no significant effects on CnA $\alpha$ , CnA $\beta$ , CYPA, CYPB, and FKBP12 protein levels except for a moderate increase of CYPA abundance in PERK-KO cells (+146%,  $p < 0.01$ ; Figs. S6–S8). These results suggest that deletion of PERK or ATF6 does not affect proteins mediating effects of CsA or Tac.

Since the absence of PERK or ATF6 may affect the proteostasis *per se*, we evaluated their downstream signaling components, namely CHOP and sXBP1. The baseline CHOP abundance was unaltered in PERK-KO cells but increased in ATF6-KO cells (+67%,  $p < 0.001$ ) as compared with control unmodified cells (Fig. 8A). Evaluation of sXBP1 revealed similar baseline levels in control, PERK-KO, and ATF6-KO cells (Fig. 8B). Hence, we concluded that ATF6 deficiency is associated with altered baseline proteostasis resulting in

activation of CHOP-inducing UPR branches such as PERK signaling (9).

Next, we treated PERK-KO and ATF6-KO cells with CsA, Tac, and Tg using the experimental protocols established for nonmodified control HEK 293 cells. PERK-KO cells showed significantly increased levels of CHOP (+165%,  $p \leq 0.001$ ) and sXBP1 (+245%,  $p \leq 0.0001$ ) in response to CsA, whereas levels of IRE1 $\alpha$  and p-IRE1 $\alpha$  were not affected by the treatment (Fig. 9, A–E). Tg increased sXBP1 and IRE1 $\alpha$  levels (+472%,  $p < 0.0001$ , +134%,  $p < 0.05$ , respectively), whereas Tac moderately reduced the sXBP1 abundance in PERK-KO cells (–54%,  $p < 0.05$ ; Fig. 9, A–E). ATF6-KO cells responded to CsA with significant increases of sXBP1 (+419%,  $p < 0.01$ ) and p-IRE1 $\alpha$  levels (+159,  $p < 0.05$ ), whereas CHOP and IRE1 $\alpha$  were not affected (Fig. 10, A–E). Tg increased the levels of sXBP1 (+902,  $p < 0.0001$ ) and p-IRE1 $\alpha$  (+145%,  $p < 0.001$ ), whereas Tac augmented the p-IRE1 $\alpha$  levels only (+129,  $p \leq 0.05$ ; Fig. 10, A–E), as detected by immunoblotting. Comparative statistical analysis of the effect strength showed that CsA-induced increases of CHOP and sXBP1 in PERK-KO and ATF6-KO cells were weaker than in unmodified cells (Table 1). These results suggest that induction of UPR by CsA is partially mediated by PERK-dependent and ATF6-dependent signaling pathways.

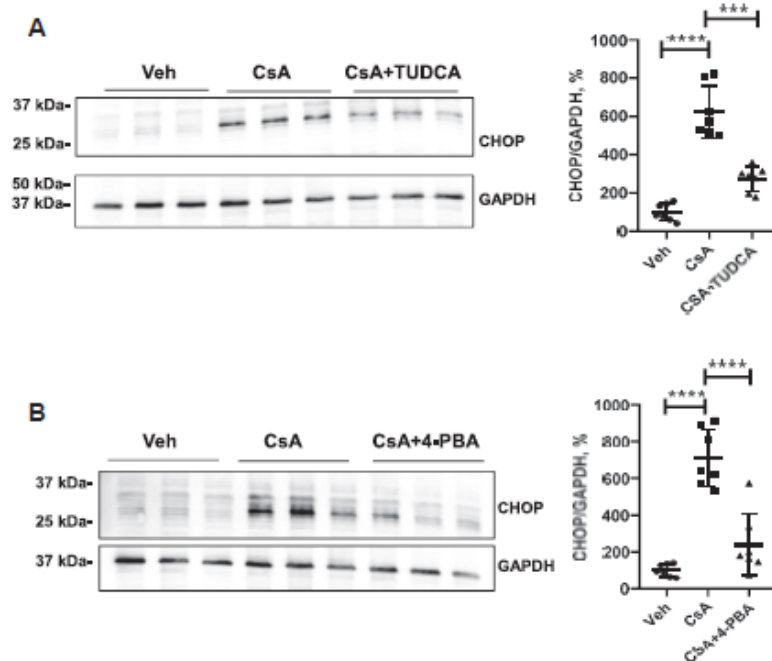


**Figure 6.** Effects of chemical chaperones (TUDCA or 4-PBA) on CHOP in cyclosporine A (CsA)-treated cells. A and B, representative immunoblots show CHOP abundance (approximately 27 kDa) in lysates from cells treated with vehicle (Veh), CsA, and CsA + TUDCA (A) or CsA + 4-PBA (B). GAPDH detection served as loading control (approximately 37 kDa). Densitometric evaluation of CHOP signals is shown on the right side of the respective immunoblots. N = three independent experiments. Data are the means  $\pm$  SD; \*\*\* $p < 0.001$ , \*\*\*\* $p < 0.0001$ . 4-PBA, 4-phenylbutyric acid; CHOP, C/EBP homologous protein; TUDCA, tauroursodeoxycholic acid.

### Cyclosporine A induces ER stress in kidney epithelia

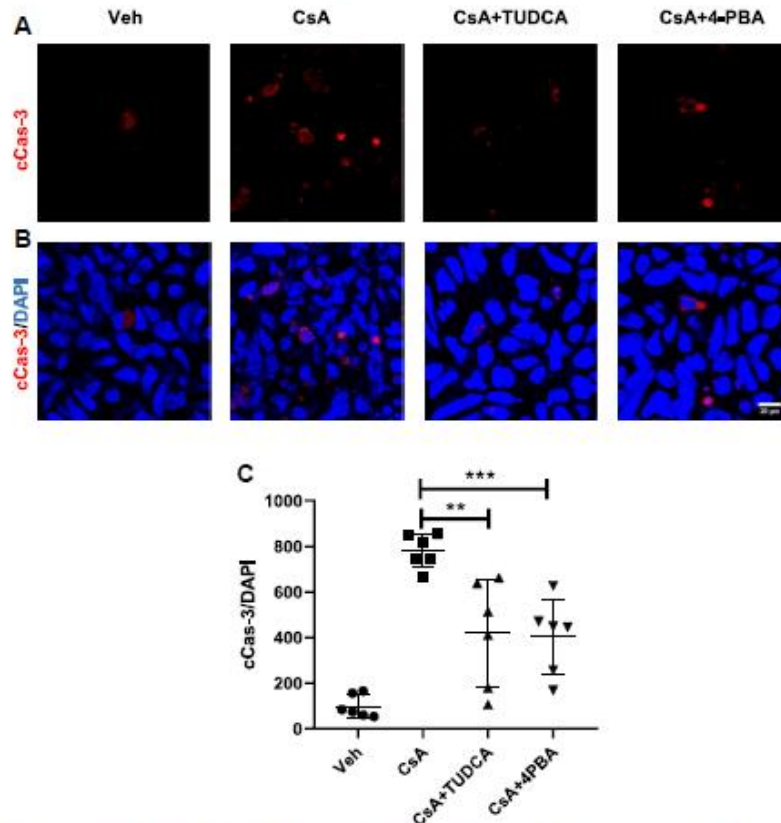


**Figure 7.** Effects of concomitant treatment of chemical chaperones (TUDCA or 4-PBA) on the abundance of cleaved caspase-3 (cCas-3) in HEK 293 cells. A, representative confocal microscopic images of cCas-3 (red signal; A) in unmodified HEK 293 cells treated with vehicle (Veh), CsA, and CsA + TUDCA or CsA + 4-PBA. Nuclei were counterstained with DAPI (blue signal; B). C, the graph shows numerical evaluation of cCas-3-positive cells normalized for total cell numbers in the analyzed regions. N = three independent experiments. Data are the means  $\pm$  SD. \*\* $p < 0.01$  and \*\*\* $p < 0.001$ . 4-PBA, 4-phenylbutyric acid; CsA, cyclosporine A; DAPI, 4',6-diamidino-2-phenylindole; HEK 293, human embryonic kidney 293 cell line; TUDCA, tauroursodeoxycholic acid.

### Discussion

Today, there is still considerable clinical demand for CsA in patients well adjusted on this drug or those requiring conversion from Tac to CsA for nonrenal side effects of Tac such as diabetes (29, 30). However, retrospective analysis of CNI nephrotoxicity suggested that Tac has more favorable pharmacological profile compared with CsA (6, 13, 14, 31). Cytotoxicity of CsA has been associated with impaired proteostasis and integrated stress response in cultured nonrenal human cells (15). In line with this, the present results obtained in cultured cells of renal origin and isolated rat PTs demonstrate that CsA stimulates multiple UPR pathways, as evident from enhanced levels of sXBP1, p-IRE1 $\alpha$ , and CHOP (8, 9, 32). Moreover, increased levels of CHOP, Bax, and cCas-3 along with decreased BCL-2 abundance in CsA-treated cells indicate failure of the adaptive UPR branches and switch to the proapoptotic mode (19). In contrast to CsA, Tac exerted only moderate or no effects on the UPR products in the present

study. These results were obtained not only in little-differentiated HEK 293 cells but also in more differentiated HRPTEpCs and dissected native rat PTs, which underlines their relevance in the pathophysiological context of CNI nephrotoxicity. Stronger cellular toxicity of CsA cannot be explained by different efficiency of CsA and Tac in terms of Cn inhibition, since our treatment protocols produced similar increases of NFAT phosphorylation levels. Therefore, we tested the possibility that toxic effects of CsA may be aggravated by the suppression of cyclophilins.

Cyclophilins assist in protein folding by catalysis of the *cis-trans* isomerization of proline imidic peptide bonds (17, 33). Since prolyl isomerization is an intrinsically slow process, its catalysis by cyclophilins may be considered as a rate-limiting step in protein folding (33, 34). Information on physiologic and pathophysiologic roles of different cyclophilin isoforms in the kidney is scarce and in part controversial. Earlier studies reported beneficial effects of pharmacologic

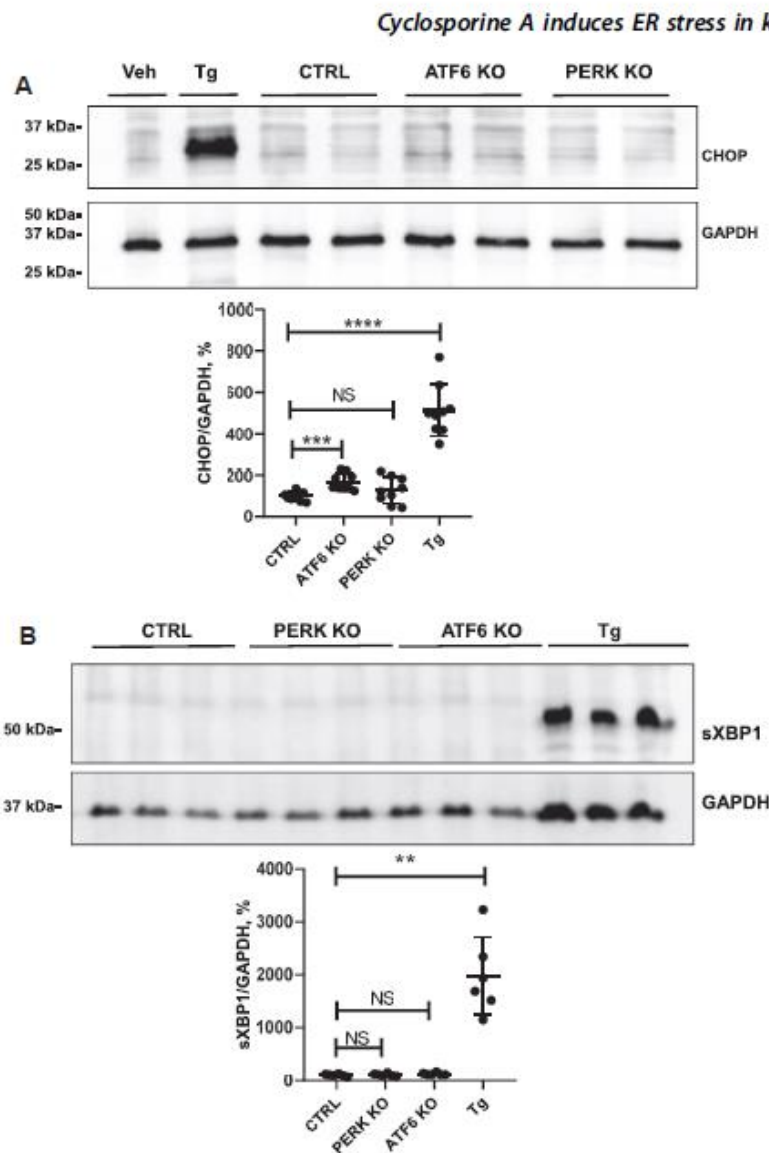


**Figure 8. Effects of inactivation of PERK and ATF6 on the unfolded protein response.** A, representative immunoblot showing baseline levels of CHOP (approximately 27 kDa). B, sXBP1 (approximately 56 kDa) in lysates from PERK-deficient and ATF6-deficient HEK 293 cells; both genes were inactivated using CRISPR/Cas9 gene editing strategy. The graphs showing densitometric evaluation of CHOP and sXBP1 signals are placed below the respective immunoblots. N = three independent experiments. Data are the means  $\pm$  SD. \*\* $p < 0.01$ , \*\*\* $p < 0.001$ , \*\*\*\* $p < 0.0001$ , NS, not significant; PERK, protein kinase RNA-like ER kinase; sXBP1, spliced X-box binding protein 1.

cyclophilin inhibition or genetic silencing of cyclophilin D in animal models of acute kidney injury or chronic kidney disorders, including CsA nephrotoxicity (35–37). In contrast, other studies documented protective effects of CYPA and CYPB in mouse models of CsA nephrotoxicity or RAS-induced kidney epithelial injury (38–40). It is tempting to speculate that interactions of CsA with CYPA or CYPB may

impair the proteostasis because of suppression of peptidyl-prolyl *cis-trans* isomerase activity, whereas CsA–cyclophilin D complexes appear to hamper the mitochondrial function (35, 38, 39, 41). Knockdown of CYPA or CYPB led to increased CHOP and cCas-3 levels in the present study, which supports a concept that CsA-induced suppression of cyclophilin-mediated chaperone function may cause ER stress

### Cyclosporine A induces ER stress in kidney epithelia

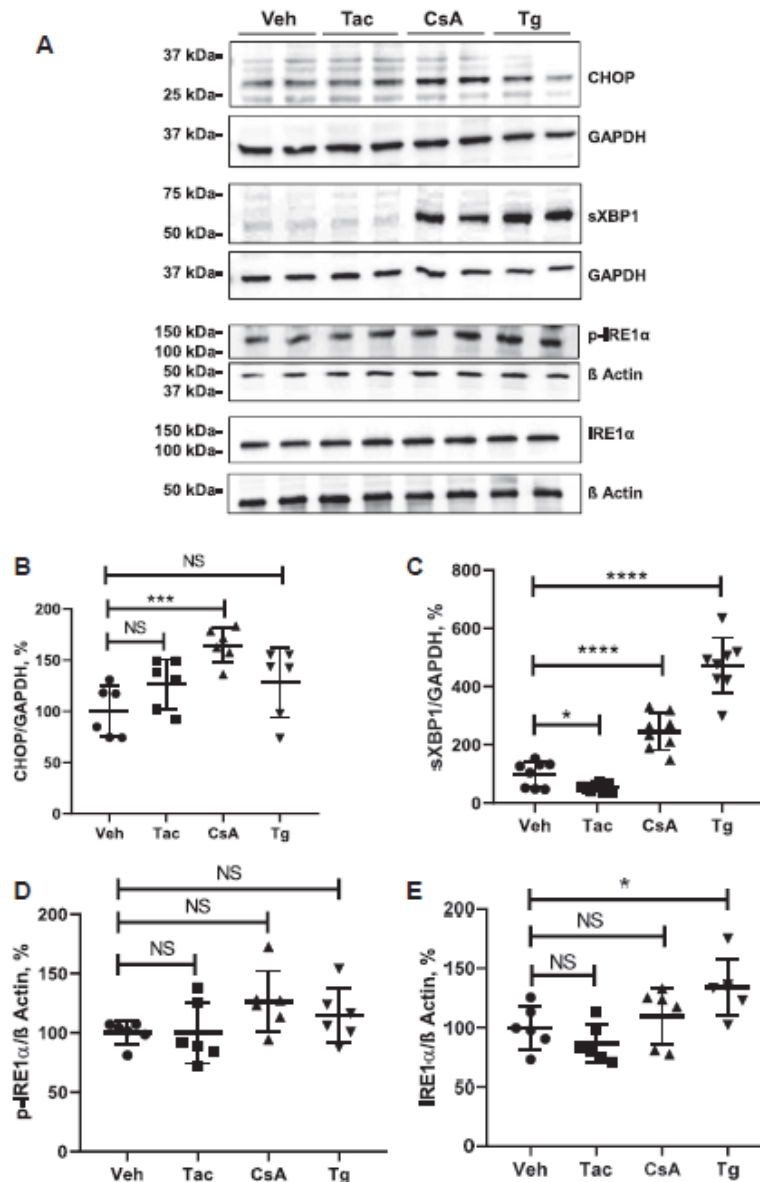


**Figure 9. Effects of cyclosporine A (CsA), tacrolimus (Tac), and thapsigargin (Tg) on key unfolded protein response products in PERK-deficient cells.** A, representative immunoblots showing signals for CHOP (approximately 27 kDa), spliced XBP1 (sXBP1; approximately 56 kDa), IRE1α and phosphorylated IRE1α (p-IRE1α) (approximately 110 kDa) in lysates from PERK-deficient HEK 293 cells treated with vehicle (Veh), Tac (10 μM), CsA (10 μM), or Tg (0.1 μM) for 6 h. B–D, graphs showing results of densitometric evaluation of CHOP (B), sXBP1 (C), p-IRE1α (D), and IRE1α (E). GAPDH or β-actin detection was used for loading control (approximately 37 and 42 kDa, respectively). N = three independent experiments. Data are the means ± SD. \**p* < 0.05, \*\*\**p* < 0.001, \*\*\*\**p* < 0.0001, NS, CHOP, C/EBP homologous protein; HEK 293, human embryonic kidney 293 cell line; IRE1α, inositol-requiring protein 1; PERK, protein kinase RNA-like ER kinase; NS, not significant; XBP1, X-box binding protein 1.

and proapoptotic UPR. According to their subcellular distribution, CYPA may be involved in folding and trafficking of cytosolic and membrane proteins, whereas CYPB may contribute to protein maturation and quality control in ER

(40, 42). The fact that knockdown of either cyclophilin isoform produced significant increases of CHOP and cCas-3 levels in the present study points to their nonredundant roles in proteostasis.

## Cyclosporine A induces ER stress in kidney epithelia

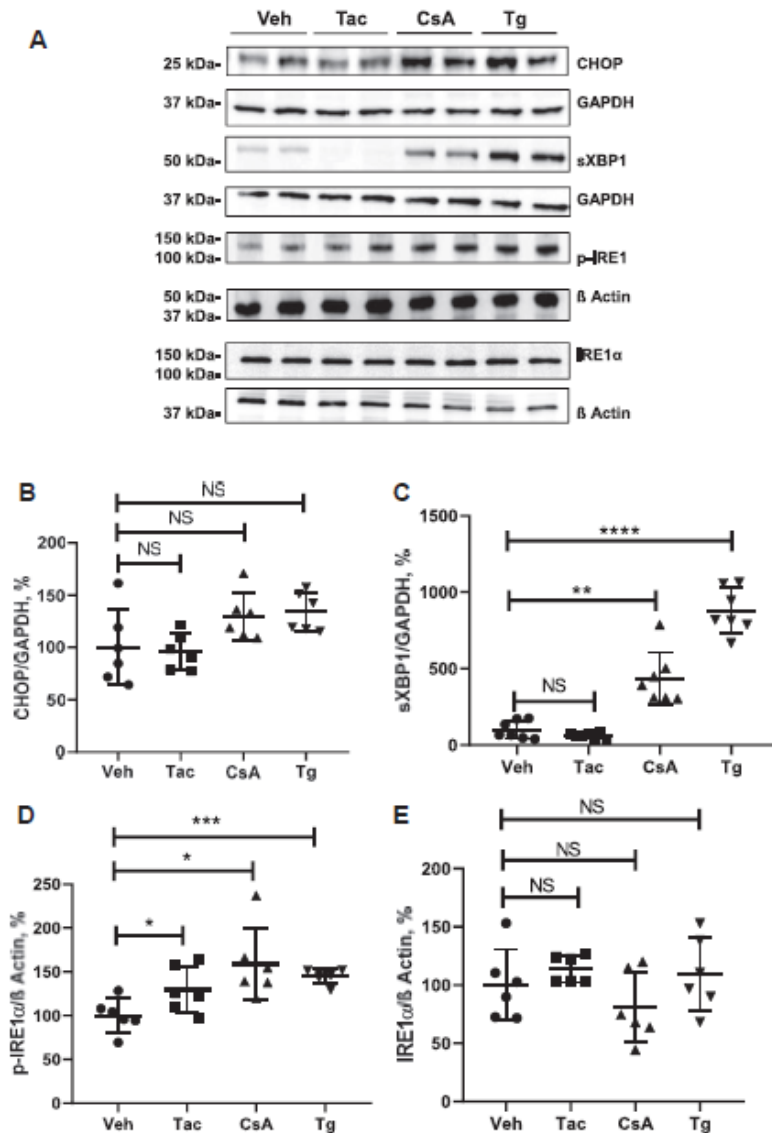


**Figure 10.** Effects of cyclosporine A (CsA), tacrolimus (Tac), and thapsigargin (Tg) on key unfolded protein response products in ATF6-deficient cells. A, representative immunoblots showing signals for CHOP (approximately 27 kDa), spliced XBP1 (sXBP1; approximately 56 kDa), IRE1 $\alpha$ , and phosphorylated IRE1 $\alpha$  (approximately 110 kDa) in lysates from ATF6-deficient HEK 293 cells treated with vehicle (Veh), Tac (10  $\mu$ M), CsA (10  $\mu$ M), or Tg (0.1  $\mu$ M) for 6 h. B–D, graphs showing results of densitometric evaluation of CHOP (B), sXBP1 (C), p-IRE1 $\alpha$  (D), and IRE1 $\alpha$  (E). GAPDH or  $\beta$ -actin detection was used for loading control (approximately 37 and 42 kDa, respectively). N = three independent experiments. Data are the means  $\pm$  SD. \* $p$  < 0.05, \*\* $p$  < 0.01, \*\*\* $p$  < 0.001, \*\*\*\* $p$  < 0.0001, NS, ATF6, activating transcription factor 6; CHOP, C/EBP homologous protein; HEK 293, human embryonic kidney 293 cell line; IRE1 $\alpha$ , inositol-requiring protein 1; NS, not significant; XBP1, X-box binding protein 1.

Since Tac produced only moderate effects on UPR signaling in the present study, we conclude that FKBP12 chaperone function is less important for intact proteostasis. Indeed, FKBP12 has been implicated in modulation of the cell cycle rather than in protein folding and proteostasis (43). However, administration of Tac *in vivo* may produce metabolic stress in

kidney epithelia indirectly, for example, because of RAS hyperactivity or constriction of renal arteries (7).

Targeting chaperone systems has been increasingly recognized as an emerging strategy for alleviation of kidney diseases (9). Previous studies in animal models suggest that ER stress contributes to progression of chronic kidney disorders to renal

## Cyclosporine A induces ER stress in kidney epithelia

**Table 1**

Comparative analysis of CsA effects on the indicated UPR products in PERK-KO and ATF6-KO HEK 293 cells versus unmodified HEK 293 cells (control)

HEK 293 cells	CHOP (%)	sXBP1 (%)	p-IRE1 $\alpha$ (%)
Control	+227	+223	+230
PERK-KO	+165 <sup>a</sup>	+245 NS	+126 NS
ATF6-KO	+130 NS	+419 <sup>b</sup>	+159 NS

<sup>a</sup>  $p < 0.05$ .

<sup>b</sup>  $p < 0.01$  for differences between effects of CsA in unmodified cells (control) and PERK-KO or ATF6-KO cells as calculated using Tukey's multiple comparisons test.

fibrosis, which can be retarded by use of chemical chaperones (9, 44). The present results indicate that stimulation of protein folding using TUDCA or 4-PBA may protect cells from CsA-induced ER stress, as reflected by blunted increases of CHOP and cCas-3 levels in HEK 293 cells treated with CsA and either chemical chaperone. While chemical chaperones improve protein folding in a nonselective way, characterization of specific UPR pathways affected by CsA may provide further options to prevent or reduce its cell toxicity. To address this issue, we intervened in early UPR events by inactivating either PERK or ATF6 using CRISPR/Cas9 gene editing in the HEK 293 cell model.

PERK and ATF6 sense ER stress and recruit distinct mechanisms to restore protein folding capacity (19). Inactivation of either PERK or ATF6 produced no effects on baseline abundance of sXBP1, whereas abundance of CHOP was moderately increased in ATF6-KO, which may reflect stimulated proapoptotic UPR (19, 45). Notably, our attempts to inactivate another ER-stress sensor, IRE1 $\alpha$ , produced no viable cell line suggesting that intact IRE1 $\alpha$  signaling is critical to cellular proteostasis and survival (32). Indeed, deletion of IRE1 $\alpha$  has been shown to impair protein folding, autophagy, and mitochondrial function in podocytes (46). In the present study, PERK-KO cells exhibited milder increases of CHOP and p-IRE1 $\alpha$  in response to CsA or Tg suggesting a blunted UPR. ATF6-KO cells showed blunted effects of CsA and Tg on CHOP and p-IRE1 $\alpha$  as well, whereas stimulation of sXBP1 was more pronounced in this cell line. Tac produced little or no effect on UPR in the KO lines, apart from decreased sXBP1 levels in PERK-KO and moderately increased p-IRE1 $\alpha$  levels in ATF6-KO cells. Although these results suggest that suppression of either PERK-mediated or ATF6-mediated signaling may interfere with the proapoptotic UPR branch and improve cell viability, further experiments including animal studies are mandatory to assess the individual impacts of these pathways in mediating the CsA toxicity.

In summary, the present comparative analysis of CsA versus Tac toxicity profiles suggests that the detrimental effects of CsA on proteostasis result from suppression of cyclophilins rather than Cn inhibition (Fig. 1). In addition, *in vivo* administration of CsA or Tac may indirectly cause or aggravate ER stress in kidney epithelia because of further local and systemic effects, such as sympathetic stimulation, rennin-angiotensin-aldosterone system hyperactivity, vasoconstriction and hypoxia of renal tissue, and imbalanced workload of kidney epithelia (7, 47, 48). Therefore, we consider pharmacologic

alleviation of ER stress using chemical chaperones or autophagy enhancers as an emerging therapeutic strategy to prevent or reduce CNI nephrotoxicity (8). In the clinical context, our data suggest that Tac possesses milder cytotoxicity compared with CsA and support the current trend of preferential Tac use in organ-transplanted patients (49).

## Experimental procedures

### Cell culture

HEK 293 cells were cultured in Eagle's minimum essential medium (Sigma-Aldrich) supplemented with 5% fetal bovine serum (Thermo Fisher Scientific) and 1% L-glutamine (Corning). Primary HRPTEpCs (catalog no.: 930-05A; Sigma-Aldrich) were cultured in RenaEpi Growth Medium (Sigma-Aldrich; supplemented with 5% fetal bovine serum) at 37 °C with atmospheric CO<sub>2</sub> concentration at 5% in a humidified incubator (Binder GmbH) (50). PERK-deficient and ATF6-deficient HEK 293 cell lines were generated using CRISPR/Cas9-mediated gene editing (51). In brief, oligonucleotides were designed (PERK: CACCGGGAAAATCTCTGACTACATA, AAACATATGTAGTCAGAGATTTCCG; ATF6: CACCGTGAATGGGGGAGCCGGCTG, AAACCAGCCGGCTCCCCATTTCAC) and cloned into pSpCas9(BB)-2A-GFP (catalog no.: PX458; Addgene) vector. After transfection, cells were sorted into 96-well plates using FACS Aria III (Becton Dickinson). Single-cell clones were expanded, and CRISPR/Cas9-mediated mutation was verified by Sanger sequencing of the respective genomic locus.

### Treatments

Cells were treated with CsA (Sigma-Aldrich) or Tac (FK-506 monohydrate; Sigma-Aldrich). Both drugs were dissolved in dimethyl sulfoxide (DMSO; Roth). Dose-response curves for CsA and Tac were established in native HEK 293 cells. Cell suspensions (100  $\mu$ l containing approximately 10<sup>6</sup> cells) were inoculated to a 96-well plate and incubated overnight at 37 °C with 5% CO<sub>2</sub>. Subsequently, cells were treated with CsA or Tac in concentrations of 0, 5, 10, 20, 40, and 80  $\mu$ M, respectively, for 6 h each. Cell viability was evaluated using MTT (BioFroxx GmbH). MTT (5 mg/ml) was dissolved in PBS, and the solution was filtered for sterilization (0.22  $\mu$ m; Whatman). Five microliters of the solution was added to each well at the end of the treatment. After ensuing incubation for 90 min at 37 °C, the medium was discarded, and precipitated formazan crystals were dissolved in 100  $\mu$ l DMSO and incubated with gentle agitation for further 15 min at 37 °C. Absorbance was measured at 560 nm in a microplate reader (Biochrom ASYS, Expert 96), and the values obtained in vehicle-treated cells were set at 100%. Based on the results of this assay, 10  $\mu$ M CsA and 10  $\mu$ M Tac doses were chosen for further experiments. To define the optimal treatment duration, cells were grown to 80% confluence, treated with CsA or Tac for 6, 24, or 48 h, and evaluated by light and electron microscopy. The 6 h duration showed the best results by viability assay as well as morphological estimation of cell survival and was therefore chosen for the main experimental protocol. To assess effects of CNI on

## Cyclosporine A induces ER stress in kidney epithelia

UPR, native HEK 293 cells, PERK-deficient (PERK-KO) or ATF6-deficient (ATF6-KO) cells were grown to 80% confluence and treated for 6 h with vehicle (DMSO), CsA (10  $\mu$ M), Tac (10  $\mu$ M), and Tg (Sigma-Aldrich; 0.1  $\mu$ M) serving as positive control. Effects of concomitant application of the chemical chaperones, 4-PBA (Abcam) or TUDCA (Calbiochem), were studied in native HEK 293 cells in the presence of CsA. Cells were then harvested and processed for qPCR or immunoblotting. Alternatively, cells were fixed for immunofluorescence or ultrastructural evaluation.

### Experiments in isolated rat PTs

Animal experiments were approved by the German Animal Welfare Regulation Authorities on the protection of animals used for scientific purpose (T0351/11). Adult male Wistar rats (7–9 weeks old) were sacrificed *via* intraperitoneal injection of 0.4 mg/kg body weight ketamine and 0.04 mg/kg body weight xylazine. Kidneys were removed immediately, and thin cortical slices were digested by collagenase II (2 mg/ml) in incubation solution (in millimolar: 140 NaCl, 0.4 KH<sub>2</sub>PO<sub>4</sub>, 1.6 K<sub>2</sub>HPO<sub>4</sub>, 1 MgSO<sub>4</sub>, 10 sodium acetate, 1  $\alpha$ -ketoglutarate, 1.3 calcium gluconate, 5 glycine, supplemented with 48 mg/l trypsin inhibitor, 25 mg/l DNase I, and pH 7.4) at 37 °C by continuous agitation (850 rpm) (52). PTs were sorted at 4 °C using a dissection microscope. Afterward, every sample was divided in four sets of around 20 to 40 PTs (Fig. S9A), which were then transferred into vials containing 10  $\mu$ M CsA, 10  $\mu$ M Tac, 0.1  $\mu$ M Tg, or 0.04% DMSO in 150  $\mu$ l of Dulbecco's modified Eagle's medium solution (low glucose; PAN Biotech) supplemented with 1% L-glutamine (PAA Laboratories; 200 mmol/l), and 1% penicillin/streptomycin (PAA Laboratories). After incubation for 6 h at 37 °C (8% CO<sub>2</sub>, open lid), PTs were harvested and snap-frozen for RNA isolation (Fig. S9B). For morphological control, some PTs were incubated on slides and stained with phalloidin-488 and DAPI after on-slide fixation with 4% paraformaldehyde in PBS (Fig. S9C).

### Immunofluorescence

HEK 293 cells were grown on coverslips to 80% confluence, treated, and fixed in 4% paraformaldehyde for 10 min.

Permeabilization of the cells was performed using 0.5% Triton X-100 (Merck) in Tris-buffered saline (TBS) for 30 min. Unspecific protein binding was blocked with 5% bovine serum albumin in TBS for 30 min at room temperature. Primary antibodies against CHOP or cCas-3 (both Cell Signaling Technology) were diluted in the blocking medium (1:500) and applied overnight at +4 °C in a humidified chamber. After washing steps, cells were incubated with Cy3-coupled secondary antibodies (1:250; Dianova) for 1 h at room temperature. Nuclei were counterstained with DAPI (Sigma-Aldrich), and the actin cytoskeleton was visualized using phalloidin (Alexa Fluor 488 phalloidin; Invitrogen), which was added to the secondary antibody solution. Coverslips were mounted (ProLong Glass Antifade Mountant; Invitrogen) on glass slides, and fluorescent signals were documented by confocal microscopy (LSM 5 Exciter; Carl Zeiss Microscopy GmbH). At least three independent experiments with five wells per treatment were quantified.

### Ultrastructural analysis

Cells were fixed in 2.5% glutaraldehyde buffered with 0.1 M sodium cacodylate buffer, harvested with a cell scraper, and processed for EPON embedding as described previously (53). Ultrathin sections were cut (70 nm thickness; Ultracut S ultramicrotome; Leica), contrasted in 5% alcoholic uranyl acetate and 1% lead citrate, and imaged using an EM 906 transmission electron microscope (Zeiss).

### Immunoblotting

Cells were harvested, dissolved in homogenization buffer (250 mM sucrose, 10 mM triethanolamine [AppliChem, Pan-Reac; ITW Reagents]), adjusted with a protease inhibitor cocktail (cOmplete; Roche), and sonicated five times for 1 s each. Cell debris was removed by centrifugation at 1000g at +4 °C for 10 min, and the supernatant was collected. Protein concentrations were measured using Micro BCA protein assay kit (Thermo Scientific).

Protein lysates (30  $\mu$ g per lane) were separated using SDS-PAGE (10% or 14%) and transferred to a nitrocellulose membrane (Macherey-Nagel). Membranes were then blocked

**Table 2**  
List of primary antibodies used for immunoblotting

Antibody	Company	Host & clonality	Dilution	Catalog number
ATF-6 (D4Z8V)	Cell Signaling Technology	Rabbit monoclonal	1:500, 5% BSA in PBS	65880
Bax	Abcam	Rabbit monoclonal	1:1000, 5% BSA in TBST	ab32503
BCL-2	Santa Cruz Biotechnology	Mouse, monoclonal	1:1000, 5% BSA in TBST	sc-7382
Calcineurin A $\beta$	Pineda Antikörper-Service	Rabbit	1:1000, 5% BSA in PBS	—
Calcineurin A $\alpha$	Pineda Antikörper-Service	Rabbit	1:1000, 5% BSA in PBS	—
CHOP (L63F7)	Cell Signaling Technology	Mouse, monoclonal	1:500, 5% BSA in TBST	2895
Cleaved caspase 3 (Asp175)	Cell Signaling Technology	Rabbit, polydonal	1:500, 5% BSA in TBS	9661
Cyclophilin A	Abcam	Rabbit, polydonal	1:1000, 5% BSA in PBS	ab41684
Cyclophilin B	Abcam	Rabbit, polydonal	1:1000, 5% BSA in PBS	ab41684
FKBP12	Abcam	Rabbit, polydonal	1:1000, 5% BSA in PBS	ab2918
GAPDH	Abcam	Rabbit, polydonal	1:2000, 5% BSA in TBS	ab181602
IRE1 $\alpha$	Cell Signaling Technology	Rabbit, monoclonal	1:1000, 5% BSA in TBST	3294
NFAT4/NF-ATc3 (phospho S165)	Abcam	Rabbit, polydonal	1:500, 5% BSA in TBST	ab59204
PERK	Cell Signaling Technology	Rabbit, monoclonal	1:1000, 5% BSA in PBS	C33E10
Phospho-IRE1 $\alpha$ (phospho S724)	Abcam	Rabbit, polydonal	1:1000, 5% BSA in TBST	ab48187
$\beta$ -actin	Sigma	Mouse, monoclonal	1:2000, 5% BSA in TBST	A2228
$\alpha$ XBP1	Abcam	Rabbit, monoclonal	1:1000, 5% BSA in PBS	ab220783

BSA, bovine serum albumin; TBST, Tris-buffered saline with Tween-20.

## Cyclosporine A induces ER stress in kidney epithelia

**Table 3**  
List of primers used for qPCR analysis

Gene	Species	Sequence (forward; reverse)
sXBP1	Human	CTGAGTCCGAATCAGGTGCAG; ATCCATGGGGAGATGTTCTGG
ATF4	Human	GTTCTCCAGCGACAAAGGCTA; ATCCTGCTTGTCTGTTGTTGG
CHOP	Human	AGAACCAGGAACGGAAACAGA; TCTCCTTCATGCGCTGCTTT
BiP	Human	TGTTCAAACAATTAACAGCAAACCTG; TTCTGCTGTATCCTCTTCACCACT
CHOP	Rat	AGAGTGGTCAGTGCGCAGC; CTCATTCTCCTGCTGCTTCTCC
BiP	Rat	TGGGTACA TTTGATCTGACTGGA; CTCAAA GGTGACTTCAATCTGGG

with 5% bovine serum albumin in TBS for 30 min at room temperature, followed by overnight primary antibody incubation at +4 °C. Antibodies used for immunoblotting are listed in Table 2. Signals were generated by incubation with the respective horseradish peroxidase–conjugated secondary antibodies (Dako; 1:2,000) for 1 h at room temperature, followed by incubation with Amersham ECL Western blotting detection reagent (GE Healthcare) and visualized in Intas ECL Chemocam Imager (Intas Science Imaging). Densitometric evaluation was performed using ImageJ software (National Institutes of Health).

### RNA extraction and real-time qPCR

Total RNA was isolated using RNeasy RNeasy Spin (Qiagen) according to the manufacturer's protocol. Reverse transcription was then performed with the help of Tetro Reverse Transcriptase kit (Bioline GmbH) using 1 µg total RNA. Specific primers used for evaluation of the expression of UPR-related genes are listed in Table 3 (27). Real-time qPCR was performed using HOT FIREPol EvaGreen qPCR Mix (Solis BioDyne) and 7500 Fast Real-Time PCR System (Applied Biosystems). Relative quantity of mRNA levels was normalized to endogenous GAPDH (forward: 5'-TGC ACC ACC AAC TGC TTA GC-3'; reverse: 5'-GGC ATG GAC TGT GGT CAT GAG-3') expression.

### siRNA-mediated knockdown

Specific CYPA and CYPB siRNA probes were generated by Ambion GmbH (Table 4). Transfection was performed at a cell confluence of 30% to 40% using INTERFERin (Polyplus-Transfection) according to the manufacturer's instructions.

### Statistical analysis

Results were analyzed by routine parametric statistics for normal distribution as assumed from the experimental design. Comparative analysis between two groups was performed by unpaired *t* test. Comparative evaluation of multiple groups was performed using one-way ANOVA followed by Tukey's multiple comparisons test. GraphPad Prism 8 (GraphPad Software

Inc) was used to analyze parameters. A probability level of *p* < 0.05 was accepted as significant.

### Data availability

All data are contained within the article.

**Supporting information**—This article contains supporting information.

**Acknowledgments**—We thank Anette Drobbe for secretarial help and Katja Dörfel for excellent technical assistance. This work received financial support from the Deutsche Forschungsgemeinschaft (grants MU2924/2-2, BA700/22-2, and SFB 1365-C04/-S01).

**Author contributions**—K. M. conceptualization; K. K., N. H., and K. M. methodology; D. E. Y. validation; D. E. Y. formal analysis; D. E. Y., H. D., and N. H. investigation; S. B. and K. M. resources; K. M. writing—original draft; S. B. writing—review & editing; D. E. Y. visualization; K. M. supervision; K. M. project administration; S. B. and K. M. funding acquisition.

**Conflict of interest**—K. M. and S. B. report that financial support was provided by Deutsche Forschungsgemeinschaft. All other authors declare that they have no conflicts of interest with the contents of this article.

**Abbreviations**—The abbreviations used are: 4-PBA, 4-phenylbutyric acid; ATF6, activating transcription factor 6; Bax, BCL-2-associated X protein; BCL-2, B-cell lymphoma protein-2; BiP, binding immunoglobulin protein; cCasp-3, deaved caspase-3; CHOP, C/EBP homologous protein; Cn, calcineurin; CNi, calcineurin inhibitor; CsA, cyclosporine A; CYPA, cyclophilin A; CYPB, cyclophilin B; CYPA-kd, CYPA-knockdown; CYPB-kd, CYPB-knockdown; DAPI, 4',6-diamidino-2-phenylindole; DMSO, dimethyl sulfoxide; ER, endoplasmic reticulum; FKBP12, 12 kDa FK506-binding protein; HEK 293, human embryonic kidney 293 cell line; HRPTEpC, human renal proximal tubular epithelial cell; IRE1α, inositol-requiring protein 1; MTT, 3-(4,5-dimethylthiazol-2-yl)-2,5-diphenyltetrazolium bromide; NFAT, nuclear factor of activated T-cell; ns, not significant; PERK, protein kinase RNA-like ER kinase; PT, proximal tubule; qPCR, quantitative PCR; RAS, renin–angiotensin system; sXBP1, spliced X-box binding protein 1; Tac, tacrolimus; TBS, Tris-buffered saline; Tg, thapsigargin; TUDCA, tauroursodeoxycholic acid; UPR, unfolded protein response; XBP1, X-box binding protein 1.

**Table 4**  
List of siRNA used for knockdown

siRNA	Sense	Antisense
CYPA	5'-AGGUCCCAAA GA CAGCAGAtt-3'	5'-UCUGCUGUCUUUGGG ACCUtg-3'
CYPB	5'-CCGUCAGAGUGU AUUUUGAtt-3'	5'-UCAAAA UACACCUUGA CGGtg-3'

### References

- Williams, C. R., and Gooch, J. L. (2012) Calcineurin inhibitors and immunosuppression - a tale of two isoforms. *Expert Rev. Mol. Med.* 14, e14

## Cyclosporine A induces ER stress in kidney epithelia

2. Casey, M. J., and Meier-Kriesche, H.-U. (2011) Calcineurin inhibitors in kidney transplantation: Friend or foe? *Curr. Opin. Nephrol. Hypertens.* **20**, 610–615
3. Ruzsák, F., and Mertz, P. (2000) Calcineurin: Form and function. *Physiol. Rev.* **80**, 1483–1521
4. Bueno, O. F., Brandt, E. B., Rothenberg, M. E., and Molkentin, J. D. (2002) Defective T cell development and function in calcineurin A beta-deficient mice. *Proc. Natl. Acad. Sci. U. S. A.* **99**, 9398–9403
5. Gooch, J. L., Roberts, B. R., Cobbs, S. L., and Tumlin, J. A. (2007) Loss of the alpha-isoform of calcineurin is sufficient to induce nephrotoxicity and altered expression of transforming growth factor-beta. *Transplantation* **83**, 439–447
6. Naesens, M., Kuypers, D. R. J., and Sarwal, M. (2009) Calcineurin inhibitor nephrotoxicity. *Clin. J. Am. Soc. Nephrol.* **4**, 481–508
7. Hoorntje, E. J., Walsh, S. B., McCormick, J. A., Zietse, R., Unwin, R. J., and Ellison, D. H. (2012) Pathogenesis of calcineurin inhibitor-induced hypertension. *J. Nephrol.* **25**, 269–275
8. Kitamura, M. (2010) Induction of the unfolded protein response by calcineurin inhibitors: A double-edged sword in renal transplantation. *Nephrol. Dial. Transplant.* **25**, 6–9
9. Cybulski, A. V. (2017) Endoplasmic reticulum stress, the unfolded protein response and autophagy in kidney diseases. *Nat. Rev. Nephrol.* **13**, 681–696
10. Ekberg, H., Tedesco-Silva, H., Demirbas, A., Vitko, S., Nashan, B., Gürkan, A., Margreiter, R., Hugo, C., Grinyó, J. M., Frei, U., Vanrenterghem, Y., Daloz, P., Halloran, P. F., and ELITE-Symphony Study (2007) Reduced exposure to calcineurin inhibitors in renal transplantation. *N. Engl. J. Med.* **357**, 2562–2575
11. Ekberg, H., Bernasconi, C., Tedesco-Silva, H., Vitko, S., Hugo, C., Demirbas, A., Acevedo, R. R., Grinyó, J., Frei, U., Vanrenterghem, Y., Daloz, P., and Halloran, P. (2009) Calcineurin inhibitor minimization in the symphony study: Observational results 3 years after transplantation. *Am. J. Transplant.* **9**, 1876–1885
12. Lucey, M. R., Abdelmalek, M. F., Gagliardi, R., Granger, D., Holt, C., Kam, L., Klintermalm, G., Langnas, A., Shetty, K., Tzakis, A., and Woodle, E. S. (2005) A comparison of tacrolimus and cyclosporine in liver transplantation: Effects on renal function and cardiovascular risk status. *Am. J. Transplant.* **5**, 1111–1119
13. Jurewicz, W. A. (2003) Tacrolimus versus ciclosporin immunosuppression: Long-term outcome in renal transplantation. *Nephrol. Dial. Transplant.* **18** Suppl 1, 7i–11i
14. Krämer, B. K., Montagnino, G., del Castillo, D., Margreiter, R., Sperschneider, H., Olbricht, C. J., Krüger, B., Ortuño, J., Köhler, H., Kunzendorf, U., Stummvoll, H.-K., Taberner, J. M., Mühlbacher, F., Rivero, M., and Arias, M. (2005) Efficacy and safety of tacrolimus compared with cyclosporin A microemulsion in renal transplantation: 2 year follow-up results. *Nephrol. Dial. Transplant.* **20**, 968–973
15. Fedele, A. O., Carraro, V., Xie, J., Averous, J., and Proud, C. G. (2020) Cyclosporin A but not FK506 activates the integrated stress response in human cells. *J. Biol. Chem.* **295**, 15134–15143
16. Ram, B. M., and Ramakrishna, G. (2014) Endoplasmic reticulum vacuolation and unfolded protein response leading to paraptosis like cell death in cyclosporine A treated cancer cervix cells is mediated by cyclophilin B inhibition. *Biochim. Biophys. Acta Mol. Cell Res.* **1843**, 2497–2512
17. Schönbrunner, E. R., Mayer, S., Trotschug, M., Fischer, G., Takahashi, N., and Schmid, F. X. (1991) Catalysis of protein folding by cyclophilins from different species. *J. Biol. Chem.* **266**, 3630–3635
18. Lamoureaux, E., Mestre, E., Essig, M., Sauvage, F. L., Marquet, P., and Gastinel, L. N. (2011) Quantitative proteomic analysis of cyclosporine-induced toxicity in a human kidney cell line and comparison with tacrolimus. *J. Proteomics* **75**, 677–694
19. Hetz, C. (2012) The unfolded protein response: Controlling cell fate decisions under ER stress and beyond. *Nat. Rev. Mol. Cell Biol.* **13**, 89–102
20. Walter, P., and Ron, D. (2011) The unfolded protein response: From stress pathway to homeostatic regulation. *Science* **334**, 1081–1086
21. Fougerey, S., Bouvier, N., Besune, P., Legendre, C., Anglicheau, D., Therivet, E., and Pallet, N. (2011) Metabolic stress promotes renal tubular inflammation by triggering the unfolded protein response. *Cell Death Dis.* **2**, e143
22. Urra, H., Dufey, E., Lisboa, F., Rojas-Rivera, D., and Hetz, C. (2013) When ER stress reaches a dead end. *Biochim. Biophys. Acta Mol. Cell Res.* **1833**, 3507–3517
23. Bonilla, M. (2002) Essential role of calcineurin in response to endoplasmic reticulum stress. *EMBO J.* **21**, 2343–2353
24. Mosmann, T. (1983) Rapid colorimetric assay for cellular growth and survival: Application to proliferation and cytotoxicity assays. *J. Immunol. Methods* **65**, 55–63
25. Lau, D. C., Wong, K. L., and Hwang, W. S. (1989) Cyclosporine toxicity on cultured rat microvascular endothelial cells. *Kidney Int.* **35**, 604–613
26. Madaro, L., Marrocco, V., Carnio, S., Sandri, M., and Bouché, M. (2013) Intracellular signaling in ER stress-induced autophagy in skeletal muscle cells. *FASEB J.* **27**, 1990–2000
27. Osłowski, C. M., and Urano, F. (2011) Measuring ER stress and the unfolded protein response using mammalian tissue culture system. *Methods Enzymol.* **490**, 71–92
28. Jelínek, M., Balušíková, K., Schmiedlová, M., Němcová-Fürstová, V., Šrámek, J., Stančíková, J., Zanardi, L., Ojima, L., and Kovář, J. (2015) The role of individual caspases in cell death induction by taxanes in breast cancer cells. *Cancer Cell Int.* **15**, 8
29. Wisning, K. M., Abramowicz, D., Weekers, L., Budde, K., Rath, T., Witzke, O., Broeders, N., Kianda, M., and Kuypers, D. R. J. (2018) Prospective randomized study of conversion from tacrolimus to cyclosporine A to improve glucose metabolism in patients with posttransplant diabetes mellitus after renal transplantation. *Am. J. Transplant.* **18**, 1726–1734
30. Rathi, M., Rajkumar, V., Rao, N., Sharma, A., Kumar, S., Ramachandran, R., Kumar, V., Kohli, H. S., Gupta, K. L., and Sakhuja V. (2015) Conversion from tacrolimus to cyclosporine in patients with new-onset diabetes after renal transplant: An open-label randomized prospective pilot study. *Transplant. Proc.* **47**, 1158–1161
31. Jiang, H., Sakuma, S., Fujii, Y., Akiyama, Y., Ogawa, T., Tamura, K., Kobayashi, M., and Fujitsu, T. (1999) Tacrolimus versus cyclosporin A: A comparative study on rat renal allograft survival. *Transpl. Int.* **12**, 92–99
32. Ali, M. M. U., Bagratuni, T., Davenport, E. L., Nowak, P. R., Silva-Santisteban, M. C., Hardcastle, A., McAndrews, C., Rowlands, M. G., Morgan, G. J., Aherne, W., Collins, L., Davies, F. E., and Pearl, L. H. (2011) Structure of the Ire1 autophosphorylation complex and implications for the unfolded protein response. *EMBO J.* **30**, 894–905
33. Lang, K., Schmid, F. X., and Fischer, G. (1987) Catalysis of protein folding by prolyl isomerase. *Nature* **329**, 268–270
34. Schmidpeter, P. A. M., and Schmid, F. X. (2015) Prolyl isomerization and its catalysis in protein folding and protein function. *J. Mol. Biol.* **427**, 1609–1631
35. Klawitter, J., Klawitter, J., Pennington, A., Kirkpatrick, B., Roda, G., Kotecha, N. C., Thurman, J. M., and Christians, U. (2019) Cyclophilin D knockout protects the mouse kidney against cyclosporin A-induced oxidative stress. *Am. J. Physiol. Renal Physiol.* **317**, F683–F694
36. Leong, K. G., Ozols, E., Kanellis, J., Badal, S. S., Liles, J. T., Nikolic-Paterson, D. J., and Ma, F. Y. (2020) Cyclophilin inhibition protects against experimental acute kidney injury and renal interstitial fibrosis. *Int. J. Mol. Sci.* **22**, 271
37. Hou, W., Leong, K. G., Ozols, E., Tesch, G. H., Nikolic-Paterson, D. J., and Ma, F. Y. (2018) Cyclophilin D promotes tubular cell damage and the development of interstitial fibrosis in the obstructed kidney. *Clin. Exp. Pharmacol. Physiol.* **45**, 250–260
38. Hong, F., Lee, J., Piao, Y. J., Jae, Y. K., Kim, Y.-J., Oh, C., Seo, J.-S., Yun, Y. S., Yang, C. W., Ha, J., and Kim, S. S. (2004) Transgenic mice overexpressing cyclophilin A are resistant to cyclosporin A-induced nephrotoxicity via peptidyl-prolyl cis-trans isomerase activity. *Biochem. Biophys. Res. Commun.* **316**, 1073–1080
39. Wang, B., Lin, L., Wang, H., Guo, H., Gu, Y., and Ding, W. (2016) Overexpressed cyclophilin B suppresses aldosterone-induced proximal tubular cell injury both *in vitro* and *in vivo*. *Oncotarget* **7**, 69309–69320
40. Bernasconi, R., Soldà, T., Galli, C., Pertel, T., Luban, J., and Molinari, M. (2010) Cyclosporine A-sensitive, cyclophilin B-dependent endoplasmic reticulum-associated degradation. *PLoS One* **5**, e13008

### Cyclosporine A induces ER stress in kidney epithelia

41. Lin, D.-T., and Lechleiter, J. D. (2002) Mitochondrial targeted cyclophilin D protects cells from cell death by peptidyl prolyl isomerization. *J. Biol. Chem.* 277, 31134–31141
42. Helekar, S. A., and Patrick, J. (1997) Peptidyl prolyl cis-trans isomerase activity of cyclophilin A in functional homo-oligomeric receptor expression. *Proc. Natl. Acad. Sci. U. S. A.* 94, 5432–5437
43. Aghdasi, B., Ye, K., Resnick, A., Huang, A., Ha, H. C., Guo, X., Dawson, T. M., Dawson, V. L., and Snyder, S. H. (2001) FKBP12, the 12-kDa FK506-binding protein, is a physiologic regulator of the cell cycle. *Proc. Natl. Acad. Sci. U. S. A.* 98, 2425–2430
44. Liu, S.-H., Yang, C.-C., Chan, D.-C., Wu, C.-T., Chen, L.-P., Huang, J.-W., Hung, K.-Y., and Chiang, C.-K. (2016) Chemical chaperon 4-phenylbutyrate protects against the endoplasmic reticulum stress-mediated renal fibrosis *in vivo* and *in vitro*. *Oncotarget* 7, 22116–22127
45. Yang, H., Niemeijer, M., van de Water, B., and Beltman, J. B. (2020) ATF6 is a critical determinant of CHOP dynamics during the unfolded protein response. *iScience* 23, 100860
46. Navarro-Betancourt, J. R., Papillon, J., Guillemette, J., Iwawaki, T., Chung, C.-F., and Cybulsky, A. V. (2020) Role of IRE1 $\alpha$  in podocyte proteostasis and mitochondrial health. *Cell Death Discov.* 6, 128
47. Hu, J., Xu, Y., Bachmann, S., and Mutig, K. (2020) Angiotensin II receptor blockade alleviates calcineurin inhibitor nephrotoxicity by restoring cyclooxygenase 2 expression in kidney cortex. *Acta Physiol. Oxf.* 232, e13612
48. Lyson, T., Ermel, L. D., Belshaw, P. J., Alberg, D. G., Schreiber, S. L., and Victor, R. G. (1993) Cyclosporine- and FK506-induced sympathetic activation correlates with calcineurin-mediated inhibition of T-cell signaling. *Circ. Res.* 73, 596–602
49. Vanrenterghem, Y. F. (1999) Which calcineurin inhibitor is preferred in renal transplantation: Tacrolimus or cyclosporine? *Curr. Opin. Nephrol. Hypertens.* 8, 669–674
50. Kawamura, N., Nimura, K., Nagano, H., Yamaguchi, S., Nonomura, N., and Kaneda, Y. (2015) CRISPR/Cas9-mediated gene knockout of NANOG and NANOGP8 decreases the malignant potential of prostate cancer cells. *Oncotarget* 6, 22361–22374
51. Ran, F. A., Hsu, P. D., Wright, J., Agarwala, V., Scott, D. A., and Zhang, F. (2013) Genome engineering using the CRISPR-Cas9 system. *Nat. Protoc.* 8, 2281–2308
52. Pohl, M., Kaminski, H., Castrop, H., Bader, M., Himmerkus, N., Bleich, M., Bachmann, S., and Theilig, F. (2010) Intrarenal renin angiotensin system revisited. *J. Biol. Chem.* 285, 41935–41946
53. Živanović, V., Seifert, S., Drescher, D., Schrade, P., Werner, S., Guttman, P., Szekeres, G. P., Bachmann, S., Schneider, G., Arenz, C., and Kneipp, J. (2019) Optical nanosensing of lipid accumulation due to enzyme inhibition in live cells. *ACS Nano* 13, 9363–9375
54. Lazelle, R. A., McCully, B. H., Terker, A. S., Himmerkus, N., Blankenstein, K. L., Mutig, K., Bleich, M., Bachmann, S., Yang, C.-L., and Ellison, D. H. (2016) Renal deletion of 12 kDa FK506-binding protein attenuates tacrolimus-induced hypertension. *J. Am. Soc. Nephrol.* 27, 1456–1464
55. Blankenstein, K. L., Borschewski, A., Labes, R., Paliage, A., Boldt, C., McCormick, J. A., Ellison, D. H., Bader, M., Bachmann, S., and Mutig, K. (2016) Calcineurin inhibitor cyclosporine A activates renal Na<sup>+</sup>(K)-Cl cotransporters via local and systemic mechanisms. *Am. J. Physiol. Renal Physiol.* 312, F489–F501
56. Borschewski, A., Himmerkus, N., Boldt, C., Blankenstein, K. L., McCormick, J. A., Lazelle, R., Willnow, T. E., Jankowski, V., Plain, A., Bleich, M., Ellison, D. H., Bachmann, S., and Mutig, K. (2016) Calcineurin and sorting-related receptor with A-type repeats interact to regulate the renal Na<sup>+</sup>-K<sup>+</sup>-2Cl<sup>-</sup> cotransporter. *J. Am. Soc. Nephrol.* 27, 107–119
57. Chiasson, V. L., Talreja, D., Young, K. J., Chatterjee, P., Baner-Berceli, A. K., and Mitchell, B. M. (2011) FK506 binding protein 12 deficiency in endothelial and hematopoietic cells decreases regulatory T cells and causes hypertension. *Hypertension* 57, 1167–1175

My *curriculum vitae* will not be published in the electronic version of my work due to data protection reasons.

My *curriculum vitae* will not be published in the electronic version of my work due to data protection reasons.

My *curriculum vitae* will not be published in the electronic version of my work due to data protection reasons.

My *curriculum vitae* will not be published in the electronic version of my work due to data protection reasons.

My *curriculum vitae* will not be published in the electronic version of my work due to data protection reasons.

## Publication list

1. Kriuchkova N., Breiderhoff T., Müller D., **Yilmaz D. E.**, Demirci H., Drewell H., Günzel D., Himmerkus N., Bleich M., Persson P. B., Mutig K. (2023) Furosemide rescues hypercalciuria in Familial Hypomagnesaemia with Hypercalciuria and Nephrocalcinosis model. *Acta Physiologica*, <https://doi.org/10.1111/apha.13927> (IF: 7.523)
2. Krappitz, M., Bhardwaj, R., Dong, K., Staudner, T., **Yilmaz, D. E.**, Pioppini, C., Westerberling, P., Ruemmele, D., Hollmann, T., Nguyen, T. A., Cai, Y., Gallagher, A.-R., Somlo, S., & Fedeles, S. (2022). XBP1 Activation Reduces Severity of Polycystic Kidney Disease due to a Nontruncating Polycystin-1 Mutation in Mice. *Journal of the American Society of Nephrology*, 34(1), 110–121. <https://doi.org/10.1681/ASN.2021091180> (IF: 14.978)
3. Oner, L., **Yilmaz, D. E.**, Demirci, H., Özbek, T., & Celik, S. Detection of aflatoxins in tomato and pepper pastes in Istanbul, Turkey. *European Journal of Science and Technology*, (35), 221-226. <https://doi.org/10.31590/ejosat.1074060> (IF: Not available)
4. **Yilmaz, D. E.**, Kirschner, K., Demirci, H., Himmerkus, N., Bachmann, S., & Mutig, K. (2022). Immunosuppressive calcineurin inhibitor cyclosporine A induces proapoptotic endoplasmic reticulum stress in renal tubular cells. *Journal of Biological Chemistry*, 298(3). <https://doi.org/10.1016/j.jbc.2022.101589> (IF: 5.486)
5. Kaya, S., **Yilmaz, D. E.**, Akmayan, I., Egri, O., Arasoglu, T., & Derman, S. (2022). Caffeic Acid Phenethyl Ester Loaded Electrospun Nanofibers for Wound Dressing Application. *Journal of Pharmaceutical Sciences*, 111(3), 734-742. <https://doi.org/10.1016/j.xphs.2021.09.041> (IF: 3.784)
6. Xu, Y., Hu, J., **Yilmaz, D. E.**, & Bachmann, S. (2021). Connexin43 is differentially distributed within renal vasculature and mediates profibrotic differentiation in medullary fibroblasts. *American Journal of Physiology-Renal Physiology*, 320(1), F17-F30. <https://doi.org/10.1152/ajprenal.00453.2020> (IF: 3.377)
7. **Yilmaz, D. E.**, & Sayar, N. A. (2015). Organic solvent stable lipase from *Cryptococcus diffluens* D44 isolated from petroleum sludge. *Journal of Molecular Catalysis B: Enzymatic*, 122, 72-79. <https://doi.org/10.1016/j.molcatb.2015.08.021> (IF: 2.381)

## Acknowledgments

My sincerest thanks go to my supervisor Prof. Dr. Sebastian Bachmann who gave me the opportunity to work in his laboratory, advised my dissertation and introduced me to new exciting scientific communities. I would also like to thank my second supervisor PD Dr. med. Kerim Mutig for his excellent mentoring and the joyful working environment he always managed to create. I would like to thank Dr. phil. Karin Kirschner and Dr. med. Nina Himmerkus for their contributions to my publication and Dr. Guy Yealland for his great help in proofreading.

I would like to thank my very dear colleagues Anette Drobbe, Katja Dörfel, Julia Shpak, Frauke Grams, Kerstin Riskowsky, Martin Thomson, MD/PhD Torsten Giesecke, Dr. med. Yan Xu, Dr. med. Junda Hu, Dr. Suncica Popovic and Dr. Natalia Kriuchkova for their support and friendship.

I would also like to sincerely thank my dearest friends Ilgin Isiltan, Ece Caglayan and Carolin Knappe. Their friendship is a treasure to me!

I would like to express my deepest gratitude to my dear family, my grandparents, mother and sister: nothing would be possible without their constant support and unconditional love. I would also like to thank the Türk family for making me feel at home in Berlin. Last but not least, I would like to thank to my dear husband, Hasan Demirci, for his priceless support that I feel in my every waking moment.